

Electronic Thesis and Dissertation Repository

8-21-2019 10:00 AM

Pyrolysis of Miscanthus and Products Characterization

Arshdeep Singh, *The University of Western University*

Supervisor: Dr. Franco Berruti, *The University of Western Ontario*

A thesis submitted in partial fulfillment of the requirements for the Master of Engineering Science degree in Chemical and Biochemical Engineering

© Arshdeep Singh 2019

Follow this and additional works at: <https://ir.lib.uwo.ca/etd>

 Part of the [Chemical Engineering Commons](#)

Recommended Citation

Singh, Arshdeep, "Pyrolysis of Miscanthus and Products Characterization" (2019). *Electronic Thesis and Dissertation Repository*. 6515.

<https://ir.lib.uwo.ca/etd/6515>

This Dissertation/Thesis is brought to you for free and open access by Scholarship@Western. It has been accepted for inclusion in Electronic Thesis and Dissertation Repository by an authorized administrator of Scholarship@Western. For more information, please contact wlsadmin@uwo.ca.

Abstract

Miscanthus, an invasive crop, has recently gained attention as an emerging energy crop because of certain features such as adaptability to lower temperature, efficient use of water and nutrients, low or no need of nitrogen fertilizers, high biomass yield, fast growing cycle and less intensive agricultural cultivation practices than other energy crops, such as corn.

The literature review is focused on the value-added applications and conversion of *Miscanthus* for bioenergy and biomaterial applications. The thermochemical conversion technologies reviewed in this chapter include pyrolysis, liquefaction, torrefaction and gasification, whereas biochemical conversion technologies include enzymatic saccharification and fermentation.

In this work, *Miscanthus* was selected as the feedstock for fast pyrolysis carried out in a mechanically fluidized bed reactor at three temperatures (400, 450 and 500°C) and three vapor residence times (1.4 s, 2.7 s and 5.2 s). *Miscanthus* was efficiently converted to energy-rich bio-oil and value-added biochar through fast pyrolysis. Fast pyrolysis performed at 450°C with 1.4 s of vapor residence time gave the highest yield of bio-oil (> 50 wt%). The biochar obtained at variable pyrolysis temperatures were also activated at 900°C for 1.5 h under CO₂ atmosphere to enhance its value as a potential adsorption agent for pollutants.

Several characterization techniques were used to study the bio-oils, biochars and activated biochars obtained from the pyrolysis of *Miscanthus*. The absorption of methylene blue as a model dye was done to evaluate the performance of activated biochar *versus* the biochar precursors. Both pyrolysis and physical activation complemented each other as new technologies for energy extraction and material synthesis from *Miscanthus*.

KEYWORDS

Miscanthus; pyrolysis; bio-oil; biochar; activated biochar; characterization

Summary

There are several environmental concerns relating to fossil fuels, increasing energy demands and pollution problems. In order to address these issues, alternative green fuels produced from biomass and wastes seem to be a sustainable option. In this study, *Miscanthus* was used as an energy crop to produce biofuels and bioproducts. *Miscanthus*, which is an invasive plant is considered energy crop due to some salient features such as adaptability to lower temperature, efficient use of water and nutrients, low or no need of nitrogen fertilizers, high biomass yield, fast growing cycle and less intensive agricultural cultivation practices than other energy crops. Thermochemical conversion technology such as pyrolysis was used to extract value out of this energy crop. Pyrolysis is a process in which thermal decomposition of biomass and organic wastes occurs in the absence of oxygen to produce condensable vapors (bio-oil), biochar and non-condensable gases. Pyrolysis can be slow, fast or intermediated depending upon the vapour residence time, heating rate and temperature used during the process. Maximum bio-oil yield from *Miscanthus* was obtained at higher heating rates and short residence times, whereas higher yields of biochar were obtained at longer residence times and short heating rates. The biochar was further activated at higher temperatures to produce activated biochar for use in environmental remediation. Various characterization techniques were used to study the bio-oils, biochars and activated biochars obtained from the fast pyrolysis of *Miscanthus*. The absorption of methylene blue as a model dye was done to evaluate the performance of activated biochar *versus* the biochar precursors. Both pyrolysis and physical activation complemented each other as new technologies for energy extraction and material synthesis from *Miscanthus*.

Co-authorship statement

Chapter 1 and Chapter 2

Article title: A review of thermochemical and biochemical conversion of <i>Miscanthus</i> to biofuels
Authors: Arshdeep Singh, Sonil Nanda and Franco Berruti
Article status: Unpublished
Contributions: Arshdeep Singh contributed in writing the manuscript. Sonil Nanda and Franco Berruti provided guidance to Arshdeep Singh in conducting the literature review on <i>Miscanthus</i> valorization to bioproducts.

Chapter 3 and Chapter 4

Article title: Studies on pyrolysis and activation of <i>Miscanthus</i> for value-added bio-oil and biochar production
Authors: Arshdeep Singh, Sonil Nanda, Jesus Fabricio Guayaquil-Sosa and Franco Berruti
Article status: Unpublished
Contributions: Arshdeep Singh performed all the pyrolysis experiments and wrote the thesis. Sonil Nanda and Franco Berruti designed the experimental plan. Arshdeep Singh analyzed the raw data with help of Sonil Nanda and prepared the tables and figures as well as structure the overall manuscript. Arshdeep Singh with the help from Sonil Nanda and Jesus Fabricio Guayaquil-Sosa performed experiments relating to the physical activation of biochar and absorption tests. Franco Berruti reviewed all the analyzed data and the entire manuscript.

Acknowledgement

I am very thankful to my supervisor Dr. Franco Berruti, for giving me this opportunity to work with him and his team at ICFAR (Institute for Chemicals and Fuels from Alternative Resources) in Western University. His support, vision, understanding, guidance and friendly mentorship on every step of my research was of great help.

I want to specially thank Dr. Sonil Nanda, Dr. Tahereh Sarchami, Dr. Fabricio Guayaquil Sosa and Mr. Tom Johnston for their support and efforts for this work. I am really thankful to Mr. Scott Abercrombie of Gildale Farms for providing raw Miscanthus for this research work.

Sardar Karnail Singh Brar (My grandfather), this work is for and because of you!

Thanks to my family and all friends to support me on every moment!

Table of Contents

Abstract	i
Summary.....	ii
Co-authorship statement.....	iii
Acknowledgement	iv
Table of Contents	v
List of Tables	viii
List of Figures	ix
List of appendices.....	x
CHAPTER 1	1
1. INTRODUCTION	1
CHAPTER 2	2
2. LITERATURE REVIEW.....	2
2.1 Cultivation of <i>Miscanthus</i>	8
2.2 Value-added Industrial applications of <i>Miscanthus</i>	11
2.3 Pre-treatment and bioconversion of <i>Miscanthus</i>	16
2.3.1 Pre-Treatment technologies.....	16
2.3.2 Bioethanol Production	17
2.4 Pyrolysis of <i>Miscanthus</i>	18
2.4.1 Bio-oil.....	20
2.4.2 Bio-Char.....	22
2.5 Torrefaction of <i>Miscanthus</i>	26
2.6 Liquefaction.....	27
2.7 Gasification.....	29
2.8 Knowledge gap in previous literature.....	30
2.9 Objective of research.....	30
CHAPTER 3	32

3. MATERIAL AND METHODS	32
3.1 Pyrolysis reactor: schematic and operation	32
3.2 Physical activation of biochar	34
3.3 Characterization of Biomass, bio-oil, bio-char and activated biochar.....	35
3.3.1 compositional analysis of biomass.....	35
3.3.2 Proximate and ultimate analysis	36
3.3.3. Karl Fischer titration.....	36
3.3.4. pH analysis.....	37
3.3.5. Thermogravimetric analysis.....	37
3.3.6. Fourier-Transform Infrared spectroscopy.....	37
3.3.7. Evolved gas analysis.....	37
3.3.8. Surface area and porosity analysis.....	38
3.3.9. Scanning electron microscopy-Energy-dispersive X-ray spectroscopy (SEM-EDX)	38
3.3.10. Methylene blue adsorption test.....	38
3.3.11 Gas chromatography-mass spectrometry (GC-MS) analysis of bio- oil.....	48
CHAPTER 4	41
4. Results and discussion	41
4.1 Product yields from pyrolysis and biochar activation.....	41
4.2 Compositional, proximate and ultimate analyse.....	48
4.3 Evolved gas analysis.....	52
4.4 thermogravimetric analysis.....	53
4.5 FT-IR analysis	58
4.6 Scanning electron microscopy.....	62
4.7 Porosity analysis.....	66
4.8 methylene adsorption.....	68
4.9 GC-MS of bio-oil.....	70

CHAPTER 5	75
5. Conclusion and recommendation.....	75
5.1 Conclusion.....	75
5.2 Recommendations for future study.....	76
Appendices.....	78
Reference	81
Curriculum Vitae.....	96

List of Tables

Table 2-1: Yields of solid, liquid and gaseous biofuels from <i>Miscanthus</i>	14
Table 4-1: Yields of solid, liquid and gaseous biofuels from <i>Miscanthus</i> in the previous studies.....	46
Table 4-2: Proximate analysis of <i>Miscanthus</i> -derived bio-chars and activated carbon generated from pyrolysis at 400-500°C for 2.7 s of vapor residence time and 1 h of run time and subsequent activation at 900°C for 1.5 h.....	49
Table 4-3: Ultimate analysis of <i>Miscanthus</i> -derived biochars and activated carbon generated from pyrolysis at 400-500°C for 2.7 s of vapor residence time and 1 h of run time and subsequent activation at 900°C for 1.5 h.....	51
Table 4-4: Ultimate analysis of <i>Miscanthus</i> -derived bio-oil generated from pyrolysis at 400-500°C for 2.7 s of vapor residence time and 1 h and 1.5 h of run times.....	52
Table 4-5: FT-IR assignment of bands identified in bio-oil, biochar and activated biochar generated from pyrolysis at 400-500°C for 2.7 s of vapor residence time and 1 h and 1.5 h of run times and subsequent activation at 900°C for 1.5 h.....	59
Table 4-6: BET porosity analysis of <i>Miscanthus</i> -derived biochars and activated carbon generated from pyrolysis at 400-500°C for 2.7 s of vapor residence time and 1 h of run time and subsequent activation at 900°C for 1.5 h.....	67
Table 4-7: Major components identified through GC-MS of the aqueous phase of <i>Miscanthus</i> -derived bio-oil at 450°C for 1.4 s of vapor residence time and 1.5 h of run time	72
Table 4-8: Major components identified through GC-MS of the organic phase of <i>Miscanthus</i> -derived bio-oil at 450°C for 1.4 s of vapor residence time and 1.5 h of run time	73

List of Figures

Fig. 2-1: Conversion of biomass to biofuels through thermochemical, hydrothermal and biochemical technology.....	7
Fig. 2-2: Uses of <i>Miscanthus</i> for biofuels and biomaterials production.....	12
Fig. 2-3: Distribution of components in pyrolysis of biomass.....	20
Fig. 3-1: Schematics of the mechanically fluidized bed reactor used for pyrolysis of <i>Miscanthus</i>	34
Fig. 3-2: Schematics of the physical activation reactor.....	35
Fig. 4-1: Effect of temperatures on the yield of pyrolysis products at different vapor residence times of (a) 1.4 s, (b) 2.7 s, and (c) 5.2 s for 1 h of run time.....	43
Fig. 4-2: Effect of vapor residence time on the yield of pyrolysis products at optimal temperature of 450°C for 1 h of run time.....	45
Fig. 4-3: Evolved gas analysis of <i>Miscanthus</i> using TG-IR analysis.....	54
Fig. 4-4: (a) TGA and (b) DTA of <i>Miscanthus</i> and its biochars generated from pyrolysis at 400-500°C with 2.7 s of vapor residence time for 1 h of run time.....	56
Fig. 4-5: TGA of <i>Miscanthus</i> -derived activated biochar generated from CO ₂ activation at 900°C.....	57
Fig. 4-6: FT-IR analysis of <i>Miscanthus</i> -derived (a) bio-oil, (b) biochar, and (c) activated biochar generated from pyrolysis at 400-500°C for 1 h of run time with 2.7 s of vapor residence time and subsequent CO ₂ activation at 900°C.....	62
Fig. 4-7: SEM analysis of <i>Miscanthus</i> and its biochars generated from pyrolysis at 400-500°C for 1 h of run time with 2.7 s of vapor residence time.....	63
Fig. 4-8: SEM-EDX analysis of <i>Miscanthus</i> and its biochars generated from pyrolysis at 400-500°C for 1 h of run time with 2.7 s of vapor residence time.....	64
Fig. 4-9: SEM-EDX analysis of activated biochars generated from <i>Miscanthus</i> biochars at 900°C for 1.5 h of run time with CO ₂ flow rate of 60 mL/min.....	65
Fig. 4-10: Methylene blue (MB) adsorption profiles for the reference commercial activated carbon (CAC) as well as <i>Miscanthus</i> -derived biochar and activated biochars generated from pyrolysis at 450-500°C and subsequent CO ₂ activation at 900°C.....	69

List of appendices

Appendix A: All data for pyrolysis experiments.....	78
Appendix B: Calculated Nitrogen gas flow rates.....	80

Chapter 1

1. INTRODUCTION

With the growth in the world population and the living standard of people improving, the per capita demand for energy is also enhanced. It is expected that the world's population will expand from the current 7.5 billion to 8 billion by 2030, which also indicates the rise in energy consumption up to 695 quadrillion British thermal units, i.e. 42% greater than the present scenario (Wu et al., 2010). The current consumption of gasoline and other liquid fossil fuels is also foreseen to escalate from 85.7 million barrels per day to 112.2 million barrels per day by 2035 (Nanda et al., 2014c). In addition, there are several environmental concerns such as the rise in fuel prices, increased greenhouse gas emissions, global warming and climate change (Petrou and Pappis, 2009). Alternative energy production mainly from renewable sources can not only address these environmental concerns, but also can help achieve the future demands. Among the renewable energy resources, such as solar, wind, tidal and geothermal, organic biomass is the only source that can provide biofuels for vehicles and engines. However, solar, wind, tidal and geothermal energy can provide electricity and heat.

Waste organic biomass in the form of lignocellulosic feedstocks (e.g. agricultural biomass, forestry residues, energy crops and invasive plants), food waste, animal manure and municipal solid waste are abundant resources that can be utilized for biofuel production (Nanda et al., 2015a). Biofuels have the tendency to meet the future energy challenges as they can be used directly as drop-in fuels or blended with fossil fuels to reduce their exploiting usage. Biofuels are also carbon neutral, which can offer the potential to reduce greenhouse gas emissions (Johnson, 2009). In contrast to the starch-based biofuel feedstocks (e.g. corn, potato, cassava, etc.), which are surrounded by the “food *versus* fuel” debate, lignocellulosic biomasses are suitable alternatives for biofuel production not only because they are inedible but also renewable, abundant and low-cost.

Generally, biofuels can be categorized into solid, liquid and gaseous fuels. Solid biofuels are the most traditional fuels in human history, examples of which include wood, pellets, sewage sludge, dung cakes and agricultural crop residues (straw, husk, corncobs, etc.). Liquid biofuels are produced through thermochemical and biochemical technologies, such as pyrolysis, liquefaction, transesterification and fermentation to produce commonly specific products like bio-oil, biodiesel, bioethanol and biobutanol (Naik et al., 2010; Nanda et al., 2014b). Gaseous biofuels are produced through thermochemical and biological technologies, such as gasification, dark- and photo-fermentation, and anaerobic digestion, resulting in synthesis gas, biohydrogen and biomethane (Nanda et al., 2017b). Combustible gaseous biofuels are used either directly or converted to liquid hydrocarbon fuels through Fischer-Tropsch synthesis or syngas fermentation (Ail and Dasappa, 2016; Kennes et al., 2016).

Dedicated energy crops, a group of lignocellulosic biomasses, include the plant species which are particularly cultivated for biofuel feedstock, such as alfalfa, bamboo, elephant grass, hybrid poplar, canary grass, switchgrass, timothy grass and *Miscanthus*. The annual availability of energy crops in Canada is up to 17.3 million ton, which have a potential to produce 4.7 billion liters of bioethanol per annum (Mabee and Saddler, 2010). Certain features, which makes a plant to be considered as an energy crops are as follows: (i) low cost, (ii) fast growth and short rotation harvesting, (iii) non-seasonal availability, (iv) high yield, (v) less intensive agricultural practices than other crops, including fertilizers and irrigation requirements, (vi) no competition with food crops for nutrients and sunlight, (vii) ability to grow on degraded lands, and (viii) resistance to extreme weather conditions (Nanda et al., 2016b).

Pyrolysis is a thermochemical conversion process in which the degradation of macromolecules in organic substrates occurs at higher temperatures (typically between 400 and 700°C) in the absence of the oxygen. Depending on the heating rate and vapor residence time, pyrolysis can be broadly classified into slow pyrolysis and fast pyrolysis. Slow pyrolysis is typically performed with a slow heating rate of 0.1-1°C/s for a longer vapor residence time of 10-100 min (Maschio et al., 1992). In contrast, fast pyrolysis requires a heating rate of 10-200°C/s and shorter vapor residence times of 30-1500 milliseconds

(Bridgwater, 1999). Slow pyrolysis is like carbonization because it results in higher biochar yields in contrast to fast pyrolysis, which leads to greater yields of bio-oil.

The bio-oil obtained from pyrolysis is usually oxygenated, which requires catalytic hydrotreating to upgrade its fuel properties like engine oils (Ruddy et al., 2014). Moreover, bio-oils are a storehouse of many platform chemicals, which originate from the thermal degradation of cellulose, hemicellulose and lignin. On the other hand, biochar is a solid co-product of pyrolysis made up of carbon and minerals, which has found application in energy production, agronomy and carbon sequestration. Biochar can be activated under an inert atmosphere (e.g. CO₂, N₂ or Ar) at higher temperatures (600-900°C) to produce activated carbon that has a typical surface area of 1500 m²/g (Azargohar and Dalai, 2006). The high carbon content, surface area and microporosity of activated biochar create many potential applications in manufacturing adsorbents, catalyst supports, fuel cells, supercapacitors, biocomposites and multifunctional carbon materials (e.g. carbon nanotubes, carbon nanohorns and templated porous carbon) (Nanda et al., 2016a). Last but not the least, the non-condensable gases obtained from biomass pyrolysis are a mixture of H₂, CO, CO₂, CH₄ and C₂₊ components (Nanda et al., 2014c).

Miscanthus, an invasive plant, native to East Asian countries, is predominantly found perennial in North America (Ontario's Invading Species Awareness Program, 2019). Initially considered as an invasive plant, *Miscanthus* is now referred to as an energy crop because of its rich lignocellulosic contents and fulfillment of the above-mentioned features of an ideal energy crop. Although *Miscanthus* is emerging as a promising energy crop, it is least explored for thermochemical conversion to produce value-added fuels and materials. Only a few researchers have reported on the pyrolysis of *Miscanthus* (Yorgun and Şimşek, 2008; Heo et al., 2010; Greenhalf et al., 2013; Du et al., 2014; Kim et al., 2014; Mimmo et al., 2014; Oginni et al., 2017; Wilk and Margdziaz, 2017; Pham et al., 2018). In addition to the limited literature on the pyrolysis of *Miscanthus*, the physicochemical characterization of its biochar and bio-oil largely remains unexplored. This paper aims to fill the gaps in the literature on the thermochemical valorization of *Miscanthus*. This paper discusses the fast pyrolysis of *Miscanthus* with focus on the effects of temperature (400-500°C) and residence

times (1.4, 2.7 and 5.2 s) on the yields and characteristics of the bio-oil and biochar products. Moreover, the physical activation of *Miscanthus*-derived biochar is investigated in an effort to increase its adsorption potential and, consequently, economical value.

CHAPTER 2

2. LITERATURE REVIEW

Waste plant biomass has been used as the traditional source for heating and cooking by the rural population worldwide. Owing to the renewable nature, low-cost, availability and abundancy, waste plant biomass and organic residues are considered for the production of biofuels that are carbon-neutral and generate low net greenhouse gas emissions (Nanda et al., 2013). However, for the sustainable production of bioenergy, it is important that the biomass is non-edible to prevent any food-versus-fuel controversy with no competition to food supply and arable lands (Nanda et al., 2015a). Lignocellulosic biomass is a collective group of non-edible plant residues containing cellulose, hemicellulose and lignin, examples of which include agricultural biomass, forestry residues, energy crops and invasive plants. Lignocellulosic biomass is also known as second-generation feedstock because it is not edible and it includes residues including wheat straw, corn cobs, rice husk, hybrid poplar, switchgrass, *Miscanthus*, etc.

Coal has been traditionally one of the most widely used fossil fuel resources since it has a carbon content from 75 to 90% (Jenkins et al., 1998). On the other hand, biomass consist of 50% carbon along with considerable amounts of oxygen, generating lower heating value than other fossil fuels. The combustion of the biomass is also hindered by the presence of the alkali and alkaline earth metals, which could form ash, resulting in corrosion, plugging, agglomeration, silicate melt-induced slagging and ash fusion in biomass-based power plants (Niu et al., 2016). Hence, suitable thermochemical and biochemical conversion technologies should be implemented to efficiently convert waste biomass to liquid and gaseous fuels (Fig. 2-1). Moreover, lignocellulosic biomass is more suitable for thermochemical conversion to produce alternate fuels than petrochemical resources, such as coal because of its high volatile components (Sims et al., 2006).

Miscanthus is one of the invasive plants, a genus of almost 20 perennial grass species, predominantly found in Asia and the pacific islands but invasive in most other geographical

regions. Most of the native species of *Miscanthus* are found in China, Korea, Japan, Taiwan and Philippines (Clark et al., 2014). *Miscanthus* has been recently targeted as a potential energy crop for biofuel production. As an energy crop, *Miscanthus* has many salient features, such as adaptability to lower temperature, low requirement of nutrient, efficient use of water and nutrients, low or no need of nitrogen fertilizers, high biomass yield, fast growing cycle and less intensive agricultural cultivation practices (Nanda et al., 2016b). Some of the common species of *Miscanthus* are *M. giganteus*, *M. sinensis*, *M. sacchariflorus*, *M. floridulus*, *M. fuscus*, *M. junceus*, *M. changii* etc.

Miscanthus shows better properties than switchgrass, another energy crop, in terms of tolerance to low temperatures, higher biomass yield, higher heating value and lower moisture content (Robbins et al., 2012). For instance, the typical biomass yield from *M. floridulus* (27.8-38 tons/ha/year) is much higher than that from switchgrass, *Panicum virgatum* L. (15 tons/ha/year) (Lee et al., 2015). In contrast, another invasive crop, giant reed (*Arundo donax*), has an even higher biomass yield and enhanced tolerance to draught than *Miscanthus* (Ge et al., 2016). However, *Miscanthus* has higher tolerance for the flooding pattern than giant reed. When compared with maize, *Miscanthus* can perform photosynthesis and grow at much lower temperatures (Dohleman et al., 2009).

Energy crops such as switchgrass (Yu et al., 2016), timothy grass (Nanda et al., 2016b), elephant grass (Fontoura et al., 2015), hybrid poplar (Shooshtarian et al., 2018), giant reed (Low et al., 2011), and microalgae (Su et al., 2017) have been investigated for second-generation biofuel production through thermochemical and biological conversion processes. However, there is limited literature available on the biorefining of *Miscanthus* for biofuel production. This chapter aims at reviewing the current knowledge on the potential of *Miscanthus* for the production of biofuels through thermochemical and biological conversion routes. This review summarizes the thermochemical conversion technologies (e.g. pyrolysis, gasification, liquefaction and torrefaction) and biological conversion technologies (enzymatic hydrolysis and fermentation) of *Miscanthus* to produce value added products, such as biofuels, bio-char, heat and power (Fig. 2-1).

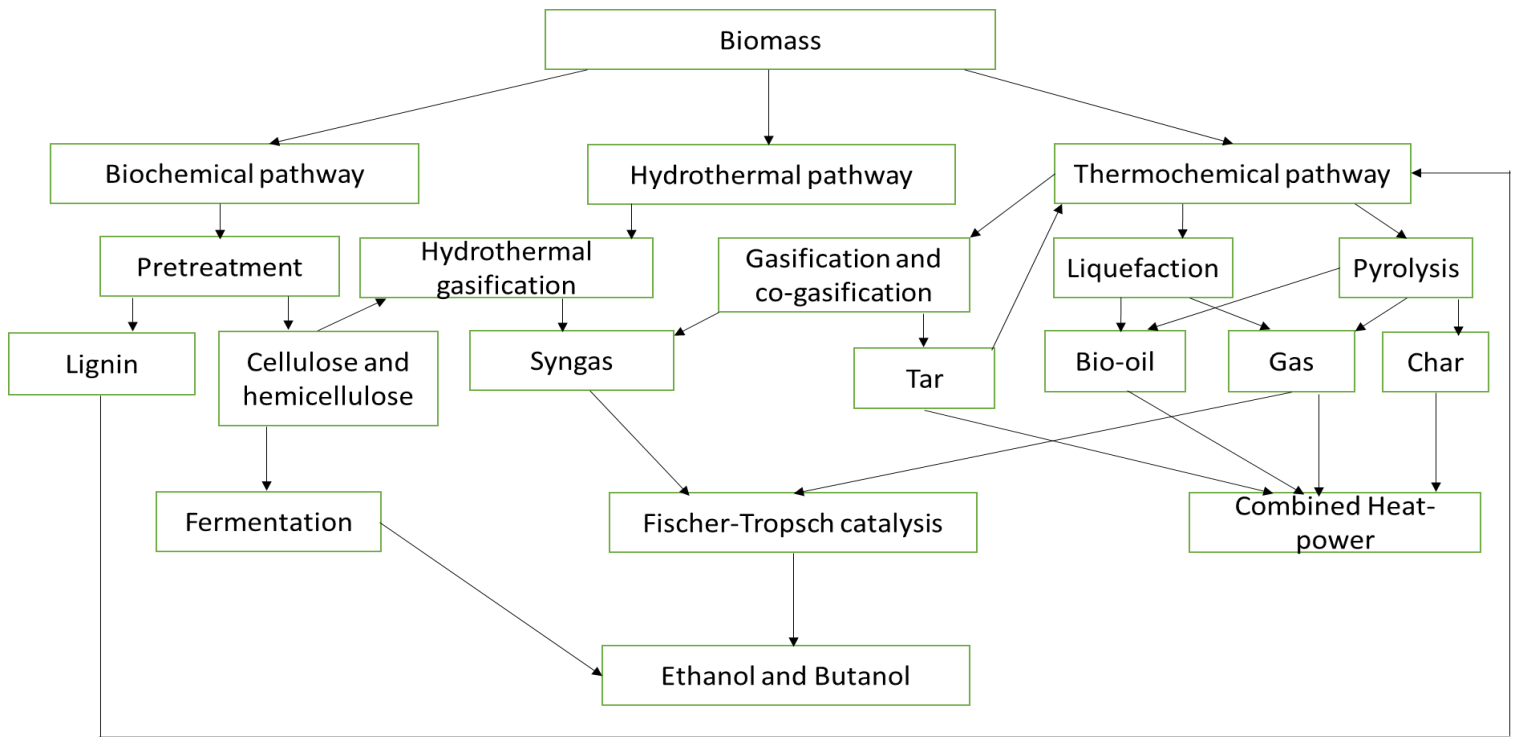


Fig. 2-1: Conversion of biomass to biofuels through thermochemical, hydrothermal and biochemical technology

2.1 Cultivation of *Miscanthus*

The annual biomass yields from *M. giganteus*, *M. floridulus* and *M. lutarioriparius* is found to be 14.8-33.5 (Germany), 27.8-38 (Taiwan) and 32 tons/ha (China), respectively. Higher yield of miscanthus in Taiwan could be due to the hot and humid climate. (Lee et al., 2015). *M. giganteus* is a sterile hybrid between *M. sinensis* and *M. sacchariflorus* which is beneficial in generating high biomass yields. Typically, mature *M. giganteus* can grow up to 3-4 m in height. Moreover, it is also resistant to the pests and diseases and has extraordinary tolerance to draught and cold temperatures (Lewandowski et al., 2003), making it a desirable energy crop (Yu et al., 2013). However, the disadvantage of culturing *M. giganteus* is that it does not produce any seed. Therefore, it can only be propagated through rhizome cutting (Bousiosa and Worrell, 2017). Typically, C4 plants can convert solar energy into carbohydrates in their biomass through photosynthesis with an efficiency 40% higher than C3 plants.

Plants can be classified based on the process of photosynthesis, i.e. light reaction and dark reaction. In light reaction, chlorophyll in the plants in the presence of sunlight (solar energy) synthesize energy-rich compounds such as adenosine triphosphate (ATP) and some co-enzymes, whereas in dark reactions, ATP and co-enzymes are converted to carbohydrates and CO₂. The dark reaction follows C3 and C4 cycles. The C3 plants use Calvin cycle (or C3 cycle) while C4 plants use Hatch-Slack pathway (or C4 cycle) for photosynthesis. The name C3 and C4 appears in these photosynthetic pathways because of the first stable carbon products, such as phosphoglyceric acid (a three-carbon compound) and oxaloacetic acid (a four-carbon compound), respectively.

The product quality and quantity mainly depend upon the composition of the raw material. The composition of *Miscanthus* genotype varies according to the harvesting season. The contents of hemicellulose and cellulose in *Miscanthus* in the summer harvest are higher than in the winter harvest. For instance, the yield of *M. giganteus* in Austria in autumn harvest was 17-30 tDW/ha compared to the winter harvest of 22 tDW/ha (Nsanganwimana et al., 2014). Similarly, biomass yield from *M. giganteus* in Germany during the autumn season (17-30 tDW/ha) was higher than in the winter season (10-20 tDW/ha). Likewise, the autumn

harvest from *M. giganteus* cultivated in Portugal was also higher (39 tDW/ha) than in the winter (26-30 tDW/ha). (Nsanganwimana et al., 2014).

In another study, *M. sinensis* genotype showed a significant difference in the production of biogas because of two different harvests, i.e. summer cut versus winter cut (Weijde et al., 2016). The biogas yield from *Miscanthus* from its summer harvest (539-591 mL/g dry matter) was found to be greater than its winter harvest (441-520 mL/g dry matter).

Fermentation and the ability to release sugars was also higher in the summer harvest than the winter harvest. An important parameter for combustion quality, i.e. ash content, was higher in the summer harvest (3.3%) than the winter harvest (1.5%). Therefore, a delay in the spring harvest benefits the combustion of *Miscanthus* due to the relatively lower K, Cl and N contents, which might be due to their lower accumulation from the soil during the winter season (Brosse et al., 2012).

Miscanthus can be cultivated for up to 25 years. It has two growth phases, namely building phase and adult phase. The biomass yield in the first year of cultivation is around 5.9 ton/ha, whereas in the second and third year of the growth, the biomass yield can be between 8 and 13 ton/ha (Arnoult et al., 2015). The canopy height and stem mass also increase rapidly within the first three years. The genotype variability is more evident in the initial 2-3 years. Temperature affects the biomass production in the first year of crop establishment. Low temperatures after the first winter of crop establishment decreases the biomass yield. For instance, *M. giganteus* and *M. sacchariflorus* died after the first winter when cultivated in Sweden and Denmark, whereas *M. sinensis* clones survived (Arnoult et al., 2015). Nitrogen application via fertilizer also impacts the biomass quality of *M. giganteus*. When the content of nitrogen was increased, the levels of cellulose, hemicellulose and lignin in the aboveground biomass decreased while ash concentration increased. The heating value of biomass is dependent upon the elemental composition (carbon, hydrogen and oxygen) and the variation in the content of cell wall composition and ash (Nanda et al., 2014a). Typically, on a dry basis, *Miscanthus* contains 47.1-49.7 wt% carbon, 5.38-5.92 wt% hydrogen and 41.4-44.6 wt% oxygen. The reported higher heating value of *M. giganteus* ranges between 17 and 20 MJ/kg (Brosse et al., 2012).

Miscanthus is a candidate energy crop within the lignocellulosic biomass family. As the name suggests, lignocellulosic biomass comprises of cellulose, hemicellulose and lignin. Cellulose, which is a repeating polysaccharide of β -D-glucopyranose units. Similarly, hemicellulose, which is a matrix polysaccharide containing pentose sugars, hexose sugars and sugar acids comprises 20-40 wt% of the *Miscanthus* biomass. Lignin, a three-dimensional phenyl propyl-based polymer, which binds cellulose and hemicellulose together provides structural rigidity and integrity to the biomass makes up 10-30 wt% of the *Miscanthus* mass on a dry basis (Brosse et al., 2012). The relative concentration of lignin acts as the determinant factor during the thermochemical and biochemical conversion of lignocellulosic biomass to biofuels. Since, lignin is insoluble in acids and enzymes, except for alkali, its presence creates hurdles for biological conversion of lignocellulosic biomass to alcohol-based biofuels. However, for thermochemical conversion, such as pyrolysis and hydrothermal liquefaction, the high content lignin results in bio-oil with better fuel properties (Hodgson et al., 2011).

The composition of *Miscanthus* depends upon different genotypes, harvest time, growth seasons, geographical locations and, if any, upon the type of fertilizers applied. *Miscanthus* also contains fatty acids, sterols and other aromatic compounds as the extractives (Brosse et al., 2012). These extractives are of high value in terms of precursors for industrial chemicals and materials. The polysaccharides in *Miscanthus* include α -cellulose, β -cellulose and γ -cellulose, whereas monosaccharides include xylose, arabinose and galactose (Villaverde et al., 2010). The compositions of cellulose in *M. giganteus*, *M. floridulus* and *M. lutarioriparius* are 33.9 wt%, 43.1 wt% and 43.9 wt% (Lee et al., 2015). Similarly, lignin contents in *M. giganteus*, *M. floridulus* and *M. lutarioriparius* were found to be 26.9 wt%, 22.3 wt% and 23.2 wt%. The composition of acid insoluble and acid soluble lignin in *Miscanthus* are 20.8 wt% and 0.9 wt%, respectively (Villaverde et al., 2010). The effect of biomass composition upon the higher heating value (HHV) also depends on the presence of lignin because lignin has nearly 30% higher calorific value than cellulose and hemicellulose together along with lower oxygen content (Nanda et al., 2015b).

2.2 Value-added industrial applications of *Miscanthus*

Some developing applications of *Miscanthus* in the chemical industries, pulp and paper making and biocomposite industries have also been reported (Fig. 2). Ethylene glycol is one of the bulk chemicals used worldwide with its consumption increasing over the years. Ethylene glycol is mostly used to produce polyester and polyesters resins and as a component for anti-freeze solvent and reductive agent. It is traditionally produced from the ethylene oxide, which is a petroleum base material. Water-soluble components in *Miscanthus* (5.3 wt%) are much lower than those of corn stalk (33.1 wt%) and ligneous woody biomass (15-25 wt%), which makes it a suitable raw material to produce ethylene glycol. Another factor which makes *Miscanthus* more attractive for ethylene glycol production is its lower lignin content than other lignocellulosic feedstocks. Moreover, lignin in herbaceous biomass is more easily decomposed than woody biomass-based lignin. The cellulose present in *Miscanthus* is being considered as a promising substrate for ethylene glycol production (Pang et al., 2014).

To produce paper and board from lignocellulosic biomass, many methods have been used to reduce the pretreatment and logistics cost. Pulp and paper industries at a global scale are now seeking for alternative feedstocks (i.e. agricultural biomass and invasive plants) to reduce the dependency for woody biomass. Invasive plants like *Miscanthus* have shown some promising attributes for use in pulp and paper industries. In China, *M. sacchariflorus* is being used for papermaking because of its fast-growth cycle, high biomass yield and easy pulping (Cappelletto et al., 2000). When compared with oat hull, pulp obtained from *Miscanthus* with sodium hydroxide treatment gave better yield, which could be used as a main component of low-grade paper and cardboard owing to satisfactory structural-dimensional characteristics (Budaeva et al., 2015). On the experiment basis, *Miscanthus* pulp also showed promising results with regards to the yield and strength than hybrid poplar pulp (Bousiosa et al., 2017). Refined *Miscanthus* soda pulp has abilities for use in packaging paper, which also reduces the amount of starch added to the paper for strength enhancement. In Netherlands, it is already used to produce the writing paper (Bousiosa et al., 2017).

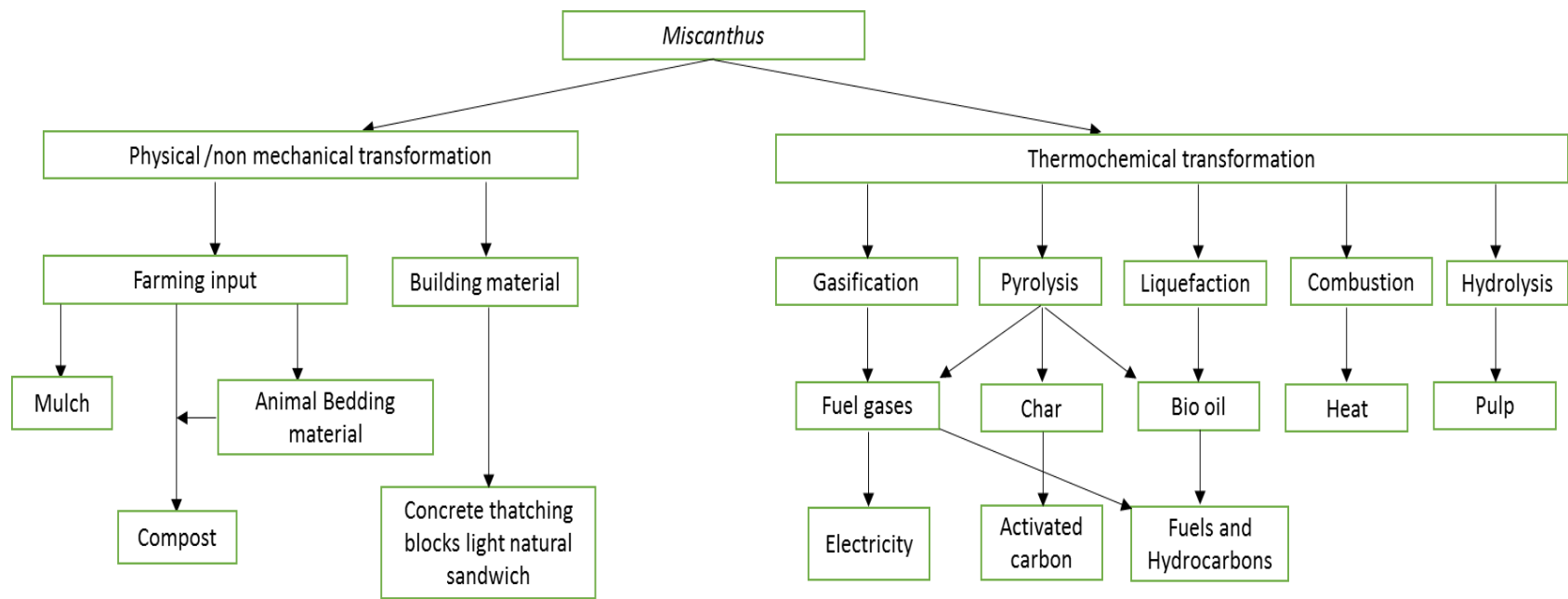


Fig. 2-2: Uses of *Miscanthus* for biofuels and biomaterials production

Nowadays, biopolymers are attracting global attention because of their biodegradable properties which is retained from their sustainable biomass precursors. However, due to lack of efficient technologies, the large-scale production of biopolymers is more costly than that of polymers derived from petroleum resources. To reduce the cost of biopolymers, filler or binder materials from lignocellulosic biomass are often used. Lignocellulosic polymers seem very effective because they can be added up to 49% as binders without affecting the quality of the biocomposite material. Adding fibres from *Miscanthus* into biopolymeric materials can improve their performance and decreases their cost (Johnson et al., 2005). However, it requires more research to be applied at an industrial level.

Two of the major components present in lignocellulosic biomass i.e. cellulose and hemicellulose are used to generate natural fibres and biopolymers for biocomposite applications. On the other hand, polymeric and aromatic lignin has many applications to be used to produce biofuels and platform chemicals. Many heterogeneous metal catalysts can be used to convert lignin into chemicals. Nickel is one of such heterogeneous metal catalysts that can cleave the C–O and C–C bonds of lignin. Different noble metals can also be used to depolymerize lignin, but their high cost restricts largescale applications (Kenneth et al., 2012).

In catalytic depolymerization of lignin, *Miscanthus* was milled to pass through a 40-mesh screen and reacted with Ni/C catalyst in methanol solvent at 225°C under H₂ pressure. (Luo et al., 2016). The liquid phase of lignin (279 mg/g) conversion contained aromatic products rich in phenolics, whereas the solid phase (612 mg/g) was composed of carbohydrates (glucan, xylan and arabinan). These depolymerized products can be further converted into the high-value chemicals. Despite the relatively lower content of lignin in *Miscanthus* (13 wt%) than hardwood (20-25 wt%), its higher conversion in *Miscanthus* was observed, which makes it a potential feedstock to produce phenolic compounds. Lewis acid catalysts were also used to convert the solid carbohydrate residues to furfurals and levulinic acid (Luo et al., 2016). Regardless, the major application of *Miscanthus* is realized in biofuel production. Table 1 summarizes the thermochemical and biochemical conversion processes involved in the conversion of *Miscanthus* to solid, liquid and gaseous biofuels.

Table 2-1: Yields of solid, liquid and gaseous biofuels from *Miscanthus*

Process	Process conditions	Product yield	References
Gasification	<p>Temperature: 639-726°C</p> <p>Biomass flow rate: 3.51-3.15 kg/h</p> <p>Air flow rate: 52.5-53 Ndm³/min</p> <p>Bed material loaded: 6.6 kg</p> <p>Equivalence ratio (ER): 0.234-0.264</p> <p>N₂: 5.5 kg/h</p> <p>Reactor type: Air-blown bubbling</p> <p>Fluidized-bed gasifier</p>	<p>For lowest ER (0.234) at 639°C:</p> <p>CO: 23.4 vol%</p> <p>H₂: 16.9 vol%</p> <p>CO₂: 42.5 vol%</p> <p>For highest ER (0.262) at 639°C:</p> <p>CO: 39.5 vol%</p> <p>CO₂: 33.3 vol%</p> <p>H₂: 17 vol%</p>	Xue et al. (2014)
Liquefaction	<p>Temperature: 220-280°C</p> <p>Feed: 10 g</p> <p>Heating rate: 15°C/min</p> <p>Liquifying agent: water/ethanol</p> <p>Catalysts: Formic acid, zinc chloride, trifluoroacetic acid and sodium carbonate</p> <p>Biomass/solvent ratio (w/w): 1:6, 1:8 and 1:10</p> <p>Water/ethanol ratio (v/v): 100:0, 90:10, 80:20, 70:30, 60:40 and 50:50</p>	<p>50% bio-oil yield at 280°C and 50% water/ethanol ratio. 280°C was considered as the optimal temperature</p>	Hafez et al. (2015)

	Reactor type: High-pressure Parr reactor with stirrer		
Torrefaction	Temperature: 250°C Run time: 30 min Feed: 130 g Heating rate: 10°C /min N ₂ flow rate: 40 L/h Reactor type: Electrically heated retort furnace	Mass yield: 73 wt% Energy yield: 80%	Wafiq et al. (2016)
Torrefaction	Temperature: 230-290°C Run time: 10-30 min Feed: 130 g Heating rate: 20°C/min N ₂ flow rate: 100 mL/min Reactor type: Horizontal furnace and tubular quartz reactor	Mass yield: 65.3-92.3 wt% Energy yield: 76.7-96%	Xue et al. (2014)
Fermentation	Pretreatment method: Dilute acid Temperature: 24°C Fermentation microorganism: <i>Candida shehatae</i>	Ethanol: 64-66%	Guo et al. (2008)
Fermentation	Pretreatment method: 0.73 wt% H ₂ SO ₄ blended with trifluoroacetic acid and maleic acid Temperature: 30°C Fermenting microorganism: <i>Saccharomyces cerevisiae</i>	Ethanol: 27-54%	Guo et al. (2012)
Fermentation	Pretreatment method: NaOH	Ethanol: 84.7%	Han et al. (2011)

	Fermenting microorganism: <i>Saccharomyces cerevisiae</i> Temperature: 32°C Time: 48 h		
--	---	--	--

2.3 Pretreatment and bioconversion of *Miscanthus*

2.3.1 Pre-treatment technologies

Lignocellulosic biomasses require pretreatment technologies involving chemical, physical and biological agents to depolymerize the cellulose-hemicellulose-lignin matrix and release the fermentable sugars for fermentation to alcoholic biofuels and chemicals (Nanda et al., 2014b). There are many pretreatment methods available, but some of promising ones include mechanical methods (grinding, milling and crushing of biomass), acid and alkali treatment, liquid hot water, organosolv, wet oxidation, ozonolysis, CO₂ explosion, steam explosion, ammonia fiber explosion (AFEX) and ionic liquids (Menon et al., 2012).

Liquid hot water has certain advantages over other widely used pretreatment technologies (e.g. acid/alkaline pretreatments, ozonolysis, ammonia fibre explosion, microwave etc.) concerning no chemical involvement, non-corrosiveness and lower production of intermediate components, such as furfural and 5-hydroxymethylfurfural (HMF). Liquid hot water is an environmental-friendly method and attractive process for the biomass pretreatment. A study by Li et al. (2013) indicated that water washing of *Miscanthus* resulted in approximately 75 w/w% of suspended solids, 18 w/w% of precipitated solids as well as 6 w/w% sand and salt.

Both furfural and HMF are sugar dehydration products obtained as intermediates of biomass pretreatment. Owing to their wide applications, these are considered among the top ten chemicals derived from bio-based materials (Yi et al., 2015). However, the presence of furfural and HMF in the biomass hydrolysate is inhibitory for the microorganisms to ferment monomeric sugars to alcohol-based biofuels, i.e. bioethanol or biobutanol (Nanda et al.,

2014b). Therefore, their recovery from the biomass hydrolysate is highly essential for bioconversion of biomass to bioethanol and biobutanol. Moreover, dilute sulphuric acid or alkaline pretreatment methods require solvent recovery and wastewater disposal, which are often difficult, expensive and energy-intensive.

Aqueous ammonia is also a good candidate for pretreatment because it shows higher lignin removal with 5% mixture of H₂O₂. Ammonia is a suitable pretreatment agent because it is volatile, easily regenerated and weakly reactive with carbohydrates (Yu et al., 2013). As *Miscanthus* has higher cellulose content than other invasive crops, extracting it in liquid solution is beneficial for bioconversion. When untreated *Miscanthus* was hydrolyzed it gave less than 5-10% glucan and xylan conversion. (Murnen et al., 2007). On the other hand, it has been shown that ammonia fibre explosion (AFEX) pretreatment significantly increases the enzymatic hydrolysis of *Miscanthus* and enhances the conversion between 30% and 90% depending on the pre-treatment parameters (Murnen et al., 2007).

2.3.2 Bioethanol production

The production of bioethanol from lignocellulosic biomass is a multistep process, which consist of physico-chemical pretreatment, enzymatic saccharification and microbial fermentation. In the first step, depolymerization of lignin is essential to break the cellulose-hemicellulose-lignin complex in the biomass. In the second step, degradation of structural polysaccharides into fermentable sugars is done via physico-chemical and enzymatic pretreatments. In the second step, monomeric sugars are fermented to bioethanol using suitable bacterial or fungal species. As mentioned earlier, pretreatment of lignocellulosic biomass followed by enzymatic saccharification can degrade the complex polysaccharides such as cellulose and hemicellulose into simple sugars such as glucose and xylose, which can be converted into bioethanol through fermentation. In biological conversion of biomass, pretreatment of lignin releases certain intermediate degradation compounds such as furfural, HMF and phenolics at moderate to high levels, which inhibit fermenting microorganisms (Hodgson et al., 2010). The neutralization of inhibitors in the fermentation medium (containing biomass hydrolysate and monomeric sugars) or the separation of inhibitory compounds through adsorption are essential for microbial fermentation.

Xylose containing liquor can be fermented using the yeast *Candida shehatae* because the common baker's yeast i.e. *Saccharomyces cerevisiae* lacks the natural ability to ferment C₅ sugars. Nevertheless, glucose, a widespread C₆ sugar present in *Miscanthus*, can efficiently be fermented to bioethanol using *S. cerevisiae*. By using *C. shehatae*, 64-66% yield of ethanol was obtained from the dilute acid-pretreated *Miscanthus* (Guo et al., 2008). However, the lower yield was due to the presence of inhibitors in the liquor. Similar yield was reported when the fermentation was carried out by *S. cerevisiae* when sulfuric acid and trifluoroacetic acid were used for pretreatment of biomass (Lee et al., 2015). On a theoretical basis, 70% yield can be obtained within 48 h of fermentation (Brosse et al., 2009).

On an economical basis, the production cost of ethanol fermentation from lignocellulosic biomass (second-generation feedstocks) is still higher than the starch or sugar-based feedstocks (first-generation feedstocks) (Nanda et al., 2015a). The main challenges are to have an efficient technology for biomass pretreatment to maximise fermentable sugar yields as well as simultaneous fermentation of xylose and glucose by a suitable yeast species (Lee et al., 2015). Although development of genetically engineered fungi is found to resolve the simultaneous fermentation of glucose and xylose at the laboratory scale, their stability, vitality and efficiency are still questionable when applied at the industrial level (Chandel et al., 2010).

2.4 Pyrolysis of *Miscanthus*

Pyrolysis is a process involving thermal decomposition of biomass and organic wastes in the absence of oxygen to produce condensable vapors (bio-oil), biochar and non-condensable gases (Fig. 3). The condensable vapors released from biomass pyrolysis can be quenched at different temperatures into several bio-oil fractions, whereas the solid residues are carbonized to form char. The gas products mostly arise from the carboxylic groups in the unbranched structure of saccharides in biomass. Usually the thermal cracking of hemicellulose releases CO₂ and water vapours. On the other hand, during pyrolysis, cellulose depolymerizes resulting in the cleavage of O–H and C–O groups, thus releasing CO and water vapors. The gaseous products from lignin include CH₄ and H₂, which mostly

arise from the branched polymer of aromatic rings and methoxy groups ($-O-CH_3$) (Osman et al., 2017). During pyrolysis, cellulose decomposes at temperatures in the range of 300-350°C, while hemicellulose degrades at 250-280°C and lignin cracks at 200- 500 °C (Jeguirim and Trouve, 2009; Correa et al., 2010). Therefore, at relatively low pyrolysis temperatures large amount of lignin remain uncarbonized, which results in less biochar yield (Oginnia, 2017).

Depending on the heating rate and vapor residence time, pyrolysis can be classified into slow, intermediate or fast pyrolysis. Moreover, pyrolysis process can be operated in both batch or continuous modes. In continuous process, the feeding of biomass and removal of biochar work continuously compared to the batch process. Batch process is mainly considered optimal for biochar production and requires less nitrogen and has abilities to accommodate longer residence times. In contrast, continuous processes requires more nitrogen to flush the vapors to the condensers rapid quenching resulting in bio-oil as the main product. Moreover, compared to batch pyrolysis processes, which are relatively easier to operate, continuous processes require maintenance, as they are prone to plugging by tar in the case of improper insulation of the reactor and tubings.

Fast pyrolysis of *Miscanthus* was carried out at 350-500°C at different residence times of 1.29-3.87 s (Kim et al., 2014). With the increase in pyrolysis temperature, it was noted that the yield of bio-oil decreased from 57.2 to 47.7 wt%, whereas this yield of gases increased from 20.9 to 35.5 wt%. Greenhalf et al. (2013) performed pyrolysis of *M. giganteus* at 490°C and obtained the yield of bio-oil and gases in the range of 41-51% and 22-35%, respectively. An increase in vapor residence time showed a decrease in bio-oil yield and increase in gas yield.

It was noted that the bio-oils obtained at longer residence times and higher temperatures had higher pH because of lower organic acids. The thermal cracking of organic acids at higher temperatures and longer residence times could further decompose into non-condensable gases. The energy conversion efficiency was lower in the case of *Miscanthus* bio-oil when

compared with softwood bio-oil, which was due to the presence of more inorganic components in *Miscanthus* (Kim et al., 2014).

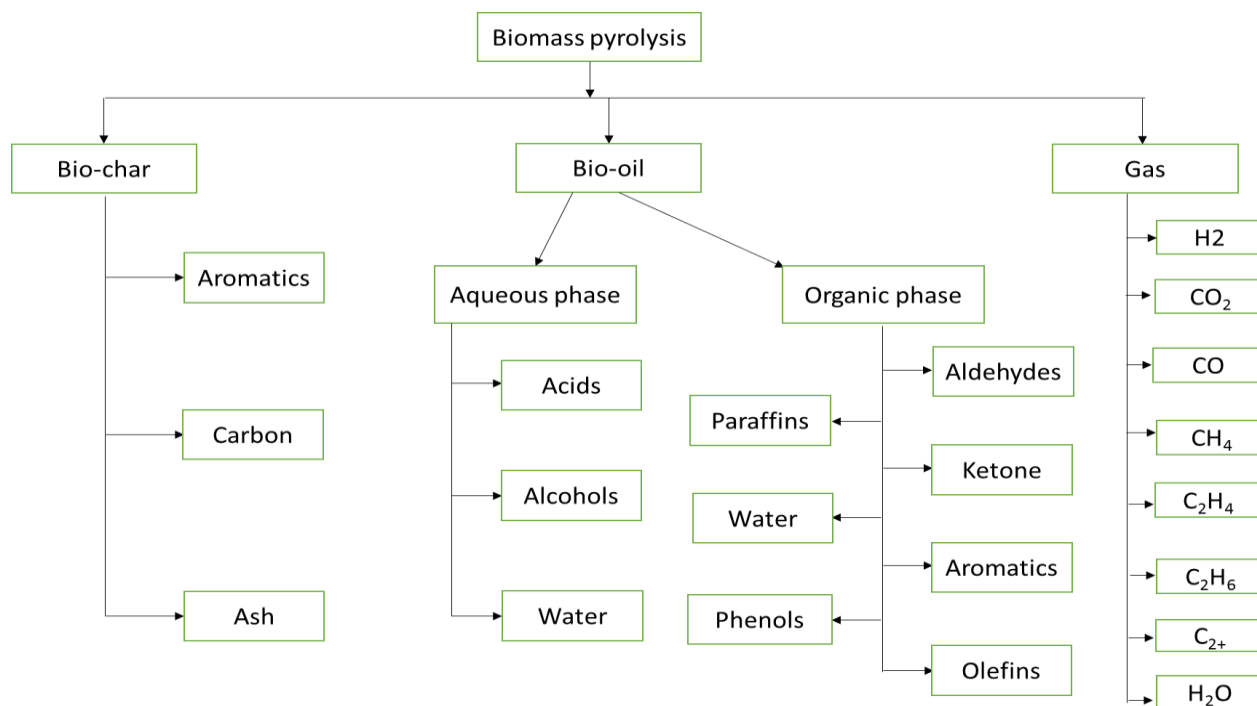


Fig. 2-3: Distribution of components in pyrolysis of biomass

2.4.1 Bio-oil

Bio-oil, a major product of biomass pyrolysis, is a mixture of oxygenated and aromatic compounds. When compared to petroleum-derived oil, bio-oil contains oxygenated compounds as opposed to hydrocarbons. Pyrolysis liquid is composed of both organic and aqueous fractions. These fractions are present due to the condensation process during biomass pyrolysis. While the aqueous fraction contains an acidic phase, the organic fraction consists of an oily phase (Nanda et al., 2014c). Bio-oil cannot be mixed with hydrocarbon liquids because it is composed of oxygenated compounds, which offer potential challenges for direct application.

Water content of bio-oil usually depends upon the moisture content of the biomass feedstock. Acidic pH of bio-oil along with its higher water content and oxygenation causes many issues relating to storage, polymerization and low calorific value. The acidic pH also

raises concerns for corrosivity. The high concentrations of oxygen, and the possible presence of nitrogen and sulfur of certain bio-oils, require upgrading such as hydrodeoxygenation, hydrodenitrogenation and hydrosulfurization to enhance fuel properties and direct use (Zacher et al., 2014). Bio-oil consists over 300 different compounds grouped under the classes of aldehydes, ketones, esters, ethers, alcohols, carboxylic acid, nitriles, carbohydrates and hydrocarbons (Czernik et al., 2004).

Pyrolysis temperature is the most important variable to produce bio-oil. In an experiment on the pyrolysis of *Miscanthus*, it was observed that by increasing the temperature from 350°C to 550°C, the biochar yield decreased from 32.4 wt% to 12.1 wt% (Heo et al., 2010). However, maximum bio-oil yield of 69.2 wt.% was observed at a temperature of 450°C while the yield decreased to 25 wt% at 550°C. This is because of the increased degree of primary tar produced in the pyrolysis vapors that crack to gases. In contrast, maximum yield of bio-oil of 53.9% in the case of hardwood was observed at 500°C, which can be due to the higher content of lignin compared to *Miscanthus* (Mohan et al., 2006). Higher temperatures lead to the breakdown of lignin, which slowly decomposes and results in biochar as the main product. The optimal temperature for *M. sinensis* was 450°C with higher oil yield of 65.2% and water content of 34.5%. A rapid increase in aromatic components in the bio-oil occurred at 550°C (Heo et al., 2010).

Bio-oil derived from the pyrolysis of *Miscanthus* at 1.9 s of residence time at 500°C (31.5 wt%) was higher than the bio-oil derived at 350°C (25.3 wt%) (Kim et al., 2014). The water content of bio-oils also influences its viscosity and flowability (Oginnia et al., 2017). The viscosity at 40°C of *Miscanthus*-derived bio-oil at 350°C (16.5 cSt) was relatively greater than 500°C (13.9 cSt) (Kim et al., 2014). The HHV of bio-oil generated from *Miscanthus* at 500°C (17.7 MJ/kg) was slightly greater than that at 350°C (16.6 MJ/kg). Residence time also has an impact on the quality of bio-oil. The water content of bio-oil produced from pyrolysis of *Miscanthus* at 400°C at 3.8 s (56.9 wt%) was much higher than that produced at 1.2 s (21.1 wt%) (Kim et al., 2014). However, the viscosity of bio-oil produced at 3.8 s (12.1 cSt) was lower than the bio-oil derived at 1.2 s (16.1 cSt).

Catalytic pyrolysis of *M. giganteus* with two different heating of 10°C/min and 50°C/min was studied at 550°C (Yorgun and Simsek, 2008). In the first case (10°C/min), pyrolysis conversion increased from 59.7 wt% to 79.9 wt%, but the solid yield decreased from 40.2 wt% to 23 wt% with the increase in the catalyst loading (activated alumina). In the second case (50°C/min), as the catalyst loading increased from 10 wt% to 100 wt% of the feedstock, pyrolysis conversion as well as solid, gaseous and liquid product yields were in the range of 65.2-79.4 wt%, 34.8-20.6 wt%, 16-31.7 wt% and 47.2-51 wt%, respectively. As the catalyst loading increased, the increase in the active sites also occurred, which enhanced the rate of polymerization, depolymerization and decarbonylation as well as hydrogen producing and consuming reactions increased. This is the reason for an increase in gaseous products, a decrease in solid product, and an increase in pyrolysis conversion. The maximum bio-oil yield was observed as 51 wt% with the heating rate of 50°C/min at 60 wt% catalyst loading (Yorgun and Simsek, 2008). In addition, the bio-oil produced in the presence of catalysts had higher degree of aromaticity than those produced during non-catalytic pyrolysis.

In an experiment on the pressurised pyrolysis of *Miscanthus* using a fixed-bed reactor at 550°C for 25 min with the heating rate of 13°C/min with 50 cm³/min flow of N₂, the yield of the bio-oil remained constant at approximately 35 wt% but increased in the case of the pressure above 16 bars. High yield of tar was observed in the pyrolysis experiments performed at atmospheric pressures. With the increase in the pressure during the reaction, an elevation in the carbon content was noted, which also increased the HHV of the liquid product. This can be due to the secondary decomposition reactions during which large amount of oxygen and hydrogen also are removed from the feedstock, thus retaining carbon in the tar or char. This confirms that pressure has an influence on the quality rather than the quantity of the product (Melligan et al., 2011).

2.4.2 Biochar

Biochar is the solid carbonaceous product of pyrolysis, which attracts widespread attention for its potential environmental and industrial applications. Biochar is a carbon-rich product obtained from the thermally decomposition of biomass in the oxygen-deprived conditions at the temperature range of 350-700°C (Kwapinski et al., 2010). Biochar can sequester carbon

in soil and helps to decrease the amount of net CO₂ emissions into the atmosphere. It can be used for agricultural applications, water purification, catalyst support, electronics and biomedicine (Budaia et al., 2017; Nanda et al., 2016a).

There are some evidences, which indicate that biochar not only increases the stability of carbon stocks in the soil, but also enhances the nutrient availability more than inorganic fertilizers. Biochar can enhance the soil quality than any other organic soil amendment. Biochar acts as a soil conditioner and organic fertilizer by providing soil organic carbon and improving microbial carbon metabolism and population dynamics (Kwapinski et al., 2010). The microbial response after the addition of biochar to the soil is mainly due to the available carbon and inorganic elements present in the biochar, which alter the soil pH in the relatively long term. It is also concluded that content of Gram-positive bacteria, Gram-negative bacteria, actinobacteria and fungi biomarkers has been increased in the biochar-modified soil (Lehmann et al., 2011). The large ratio of fungi/bacteria in the soil amended with biochar implies that fungi colonization is very important to break the structure of polyaromatics in the contaminated soils so that they will be available for other microbial groups for decomposition. (Kwapinski et al., 2010). Moreover, it has been noted that regardless the temperature of the biochar production, biochar application to highly acidic soils caused an increase in all phospholipid fatty acids by microorganisms. Biochar produced at lower temperature are more utilizable by microorganism (Kwapinski et al., 2010).

The type of feedstock influences the composition and surface area of the biochar. Biochar from crop residues and woody biochar have larger surface area when compared to the ones produced from other sources. Biochar generates oxygen-containing compounds when it undergoes oxidation in the soil, a few examples of which include carboxylic and lactonic acids and phenolic groups. The oxidation in biochar amended soils occurs thorough the microbial action, organic matter and solutes (Kim et al., 2017). The content of carbon availability instead of pH change is the main point to consider for determining the microbial utilization of biochar in acidic soils (Luo et al., 2017). In addition to sequester soil carbon, biochar also provides several advantages when it is applied to the soil like increasing the

crop yield. The contribution biochar to improving crop productivity is achieved through the retention of plant available nutrient in the rhizosphere, which results to increasing the soil pH, cation exchange capacity, water holding capacity, decrease in the greenhouse gas emissions and immobilization of toxic compounds such as heavy metals (Gronwald et al., 2016).

High yields of biochar are produced from pyrolysis at moderate temperatures and longer vapor residence time, especially the conditions optimal for slow pyrolysis. Temperature and heating rate are the most considerable factors in pyrolysis and carbonization, which can alter the yield and properties of the resulting biochar. Biochar from *Miscanthus* is found to have relatively large surface areas (50.9-51.1 m²/g) when produced at higher temperatures (e.g. 600°C) and longer residence times (e.g. 60 min) (Kwapinski et al., 2010). These properties are relevant for using biochar as the soil conditioner. The aromaticity of the biochar also determines its thermal stability in the soil at extreme environments (Budaia et al., 2017). The composition of feedstocks (i.e. contents of cellulose, hemicellulose, lignin, minerals and ash) also determine the chemical composition of biochar. The organic and inorganic components in the original precursor (biomass) act as catalysts during the pyrolysis and carbonization process to improve the quality of the biochar (Hodgson et al., 2016).

Dependant on pyrolysis temperature, the properties and yield of the biochar from *Miscanthus* varied to a large extent. The yield of biochar from *Miscanthus* reduced from 25.9-26.2 wt% at 500°C (for 10 min reaction time) to 19.8-20.2 wt% at 600°C (at 60 min reaction time) (Kwapinski et al., 2010). The surface area of *Miscanthus*-derived biochars also showed a rising trend with the increase in the temperature from 500°C (1.65-1.95 m²/g) to 600°C (50.9-51.1 m²/g). The HHV data showed little difference at variable temperatures of 400°C (29.4-30.3 MJ/kg), 500°C (29.9-30.7 MJ/kg) and 600°C (31.5-32.5 MJ/kg). As temperature plays a significant role for the biochar production and its properties, biochar produced at high temperature has high pH and more compact structure of polyaromatic compounds than biochar produced at lower temperature. It is suggested that the large surface area of biochar is useable for adsorption of pollutants from wastewater and retaining soluble carbon and nutrients, which is beneficial for soil applications (Luo et al., 2017).

In an assessment, *Miscanthus* cultivated on the contaminated land was found to accumulate more metals in the roots and rhizomes and less in shoots and stems compared to *Miscanthus* cultivated from uncontaminated land (Janus et al., 2017). Biochar produced from *Miscanthus* cultivated on the contaminated land were efficient for the removal of Cd, Pb and Zn from aqueous solutions. (Janus et al., 2017) Moreover, higher efficiency in the remove of impurities was found in case of biochar produced at higher pyrolysis temperatures. High desorption and low sorption of the biochar is also suitable for the treatment of wastewater (Janus et al., 2017).

In a study by Yang et al. (2017), biochar was produced from different feedstock (e.g. Masson pine wood, Chinese fir wood, Chinese fir bark, bamboo leaves, bamboo sawdust, *Miscanthus*, pecan shells and rice straw) through slow pyrolysis at 350°C and 500°C. Slow pyrolysis at 350°C showed the biochar yield trend as bamboo sawdust > pecan shells > *Miscanthus* > Masson pine wood > Chinese fir bark > rice straw > Chinese fir wood > bamboo leaves. However, at 500°C, the yields of all biochars decreased. The yields of biochar from the slow pyrolysis of all these feedstocks differed because of the variable composition of cellulose, hemicellulose and lignin, which have different thermal degradation kinetics. It has been proven in this study that the yield and thermal properties of biochar vastly affected by the composition of different feedstocks. The HHV of the biochars showed an increasing trend at 350°C but decreased at 500°C (Yang et al., 2017).

As opposed to the benefits of biochars, there is a negative influence due to the presence of polycyclic aromatic hydrocarbons (PAH), naturally generated during the pyrolysis process. Studies have shown that the total bioavailability of the PAHs is low in the biochar; hence, biochar can play the role of carbon sink rather than of organic pollutant (Hale et al., 2012; Mayer et al., 2016). The factors which affect the concentration of PAHs in biochar are temperature, feedstock composition and carrier gas. The levels of PAHs in the biochar usually increase with the rise in pyrolysis temperature. Aromatic hydrocarbons in the feedstocks depend upon the process parameters, which determine their fate in the biochar,

bio-oil or gases. High carrier gas flows result in decreasing the PAH concentration (Madej et al., 2016)

Like nitrogen and potassium, phosphorus is one of the essential elements for crop growth and yield. The impact of phosphorous can be seen in more tropical weathered soils where bioavailability of soil happens under natural conditions. The weathering of rocks releases essential elements for the growth of the crop at a slower rate (Trazzi et al., 2016). The surface area of biochar, volatile matter content and surface organic functional groups influence the phosphorus bioavailability in soils amended with biochar. It has been reported that biochar produced from wheat straw can affect phosphorous concentration depending on its quantity of amendment in the soil. It was noted that fast pyrolysis biochar decreased phosphorous fixation capacity in the soil (Trazzi et al., 2016). Increased temperature and residence time also increased the fixed carbon and surface area of *Miscanthus*-derived biochar, which resulted in higher phosphorus adsorption capacity than sugarcane bagasse biochar (Trazzi et al., 2016).

2.5 Torrefaction of *Miscanthus*

Torrefaction is most promising pretreatment process for biomass before pyrolysis. The physicochemical properties of torrefied biomass are like those of coal. Torrefaction is a process of moisture removal at low temperature, and hemicellulose decomposition is another key aspect of this process. By losing CO₂, moisture and other oxygen-containing compounds, the torrefied product demonstrates high energy density than the raw material. Furthermore, torrefaction helps to improve the grinding property of biomass, which helps to reduce the electric power consumption. Torrefaction decreases the content of oxygen and increases the carbon content due to loss of moisture, CO₂ and CO (Wafiq et al., 2016).

The impacts of pressure upon the yield of char from torrefaction of *Miscanthus* was studied at 250°C with a heating rate of 10°C/min, N₂ flow rate of 40 L/h for 30 min of reaction time. which indicated that at 1 bar, the char yield increased from 22 wt% to 29 wt% until 10 bar beyond which no further increase was observed with rising pressure. The biochar with torrefied *Miscanthus* showed similar trend of yield increase from 32 wt% to 42 wt% at 1-10

bar and no further increase at higher pressures (Wafiq et al., 2016). On the other hand, liquid product of pyrolysis decreased with the increase in pressure for torrefied *Miscanthus*, due to secondary pyrolysis reactions. The porosity of char was also studied for raw and torrefied *Miscanthus*, which showed that in case of raw *Miscanthus* the porosity decreased until 15 bars and increased at 30 bars. However, in the case of torrefied *Miscanthus*, the porosity decreased with increasing the pressure.

Raw *Miscanthus* also has some disadvantages like low bulk density, low energy density and non-uniform physical and chemical properties, which could lead to storage problem, lower thermal conversion and utilization. Torrefied *Miscanthus* also has high energy density and bulk density making it easier for transportation and storage. *Miscanthus* was torrefied at 270°C for a residence time of 30 min can achieve good properties like very low moisture and hemicellulose content, lower O/C ratio, porous structure, larger surface area and high alkali metal content, which is very optimal for pyrolysis or gasification (Xue et al., 2014). Furthermore, raw and torrefied *Miscanthus* were gasified at 850°C under N₂ and CO₂ atmosphere. During the torrefaction, the overall O/C ratio decreased, while the pore volume and surface area increased, which improved the gasification properties of torrefied *Miscanthus* compared to the raw *Miscanthus*. The penetration of CO₂ inside the porous particles improved, which positively affected gasification reactivity. Regardless, the composition of gas obtained from gasification depends upon the nature and composition of the feedstock.

2.6 Liquefaction

Thermochemical technologies to convert the biomass into liquid fuel products also include direct liquefaction and hydrothermal liquefaction. In hydrothermal liquefaction and hydrous pyrolysis, the use of water and catalyst are required for the conversion of biomass. There are some reactions which occurs during this process such as: (i) decomposition and reduction of cellulose, hemicellulose, lignin and lipids; (ii) hydrolysis of cellulose and hemicellulose to the simple sugars; (iii) hydrogenolysis in the presence of the hydrogen, (iv) reduction of amino acids; (v) reformation reactions; (vi) degradation of C–O and C–C bonds; and (vii) hydrogenation of functional groups (Balat, 2008). Drying of biomass is necessary for

pyrolysis, but not for hydrothermal liquefaction because the latter uses water as the aqueous medium. Catalyst requirement is very essential part of liquefaction. Alkali catalyst such as Na_2CO_3 and K_2CO_3 aid the liquefaction reactions (Nanda et al., 2014c).

Most typical temperature for liquefaction is between 300°C and 500°C . Over the years many improvements have been made to overcome technical problems associated with liquefaction. One of the improvements include application of subcritical water or supercritical water as the reaction medium for hydrothermal liquefaction (Kamio et al., 2006). Another iteration of hydrothermal liquefaction involves alcohol and water as the reaction medium. The advantage of such system is that the solvents can be evaporated, recycled and reused (Cheng et al., 2010). It is found that replacing 50% of water with alcohol during liquefaction increased bio-oil yield, whereas replacing water more than 50% can adversely affect the bio-oil yields (Cheng et al., 2010).

During the liquefaction of *Miscanthus*, it has been noted that by increasing the temperature from 220°C to 280°C , the quantity of residues decreased while the liquid yields increased. According to the value of oil yield, residue content and heating value, 15 min liquefaction time was efficient for *Miscanthus* liquefaction without any catalyst. The reaction temperature (280°C) and water/ethanol ratio (50%) were two most effective parameters for this process. The optimal results obtained in the case of *Miscanthus* liquefaction was 52% yield of bio-oil having a heating value of 25 MJ/kg when the biomass-to-solvent ratio used was 1:8 with ZnCl_2 as the catalyst (Hafez et al., 2015).

A comparison between pyrochar and hydrochar obtained from slow pyrolysis and hydrothermal carbonization was made. For pyrochar from *M. giganteus*, a Pyreg reactor was used at 750°C for 0.75 h, and for hydrochar mixture of 1 kg of dry *Miscanthus* with 10 kg of water in tubular reactor was used at 200°C and 2 MPa for 11 h (Gronwald et al., 2016). Hydrochar is produced from hydrothermal carbonization, which is usually performed at low temperatures ($180\text{-}300^\circ\text{C}$) in the presence of water under high pressures (2.0-2.5 MPa) for several hours. The hydrochar was found to have low surface area, low degree of carbonization and less aromatic carbon compared with pyrochar. Moreover, hydrochar had a

higher ratio of H/C (1.01) than O/C (0.31) from pyrochar (Gronwald et al., 2016). Compared to hydrochar, the application of pyrochar in the soil can retain the carbon for longer period. On the other hand, hydrochar applied directly to the soil showed performance with slow release of fertilizer. Low stability of hydrochar and higher proportion of the functional groups provide additional benefits for carbon sequestration (Gronwald et al., 2016).

2.7 Gasification

Gasification operates in the presence of a limited supply of oxygen to produce syngas, which mainly contains H₂ and CO along with other products such as CO₂, CH₄ and C₂₊. During gasification, carbon conversion is the key feature, which is used to determine the gasification efficiency (Nguyen et al., 2015). Biomass gasification is emerging as the one of the clean technologies to produce biofuels and decrease the dependence on fossil fuels. Because of the high reactivity of the biomass char, gasification is gaining widespread interest for energy production. The reactivity of biochar depends upon three basic properties that is chemical structure, porosity and inorganic constituents. *Miscanthus* has been proved as an appropriate biomass for gasification because of its higher volatility and low ash content (Karampinis et al., 2012).

The gasification of *Miscanthus* char was investigated above 800°C specifically in the presence of steam, and the complete burn out of *Miscanthus* was detected at the 1000°C in the blended (air/oxygen) ambience as well as 1050°C for the steam medium (Jayaraman et al., 2015). This shows that the amount of oxygen affects the reaction rate and temperature. With regards to H₂ gas evolution during the whole process from pyrolysis to gasification of *Miscanthus*, it was observed that it started at 350°C with the highest concentration at 950°C, and then decreased similarly to the CO content. It was also observed that the H₂ yield decreased when the gasification medium changed from pure steam to steam enriched with oxygen and air (Jayaraman et al., 2015).

The bubbling fluidized bed is the simplest and most cost-effective method for biomass gasification. Such reactors are flexible to gasify a wide variety of biomass because of high heat transfer and uniform temperature distribution. However, the disadvantage of such reactors is the risk of bed agglomeration because of the presence of sintering ash and high alkali metals in the biomass which might also affect the reactor material (corrosion) at high temperatures and catalyze or retard the reaction. During *Miscanthus* gasification, agglomeration was observed at low temperature due to the presence of high silica, potassium and sodium content (Xue et al., 2014). It was reported that in the case of gasification of *M. giganteus*, the quality of product gas deteriorated with the rise in temperature from 645°C to 726°C using optimal equivalence ratio of 0.26 and air flow rate of 53 Ndm³/min. Among all the gases, CO yield decreased from 39.5 to 33.4 vol% but the concentration of CO₂ increased from 33.3 to 36.8 vol%. The yields of H₂ and hydrocarbons did not show any deviation at higher temperature (700-726°C) in comparison with 645°C (Xue et al., 2014).

2.8 Knowledge gap in the literature

Based on the literature review, the following gaps have been identified:

1. Lack of a comprehensive characterization of *Miscanthus* biomass and of its derived continuous pyrolysis products.
2. Need for a systematic investigation of the effects of process parameters, such as temperature and vapor residence time for the continuous pyrolysis of a well characterized *Miscanthus* biomass feedstock on the quality of the derived products.
3. Need to enhance the value of the derived biochar produced at different temperatures through activation and comparative characterization of the performance of activated biochar as adsorbent.

2.9 Objectives of the research

The main objective of this study is to add new knowledge on the thermochemical conversion of *Miscanthus* as an energy crop through pyrolysis to produce bio-oil, biochar and gases. The following are the sub-objectives of this work:

1. Investigation of the process parameters (i.e. temperature and vapour residence time) for the continuous pyrolysis of *Miscanthus* and their effects on the bio-oil yields.

2. Physical activation of *Miscanthus* biochar to enhance its value by producing activated biochar for purposed adsorption applications.
- 3.
4. Physicochemical characterization of *Miscanthus* biomass and its derived bio-oil and biochar and activated biochar.

CHAPTER 3

3. Material and methods

3. 1 Pyrolysis reactor: Schematics and operation

A mechanically fluidized bed reactor located at the Institute for Chemicals and Fuels from Alternative Resources (ICFAR) at Western University, London, Ontario, Canada was used for the pyrolysis of *Miscanthus* biomass (Fig. 3-1). The dimensions of the reactor are 58.42 cm long, 7.62 cm I.D. The reactor, its assembly lines and condensers are made of stainless steel SS316. The reactor is electronically heated using four band heaters covering the entire reactor body with proper insulation to minimize heat losses. The heaters are individually controlled by digital temperature controllers, and the temperature inside the reactor is monitored using Type-K thermocouples (McMaster-Carr, Aurora, USA). Nitrogen gas was used as the fluidizing medium and to create an inert atmosphere during the reaction.

Nitrogen was fed through two inlet ports, one installed at the bottom of the reactor and one through the hopper (auger feeder). The flow rate of the nitrogen gas was regulated by the digital gas flow meters (Omega FMA-A2317, Norwalk, CT, USA) A fine mesh filter (< 10 μm) (McMaster-Carr, Aurora, USA) was used to separate the fine char particles from the hot vapors exiting the reactor and retain them in the bed. A series of four condensers was used to fractionally condense the vapors at different temperatures. The four condensers arranged in the series were named as condenser 1 (maintained in a hot oil bath at 110°C), condenser 2 (an electrostatic precipitator, ESP maintained at 70-80°C), condenser 3 and condenser 4 (both condensers immersed in ice cold water at temperatures always < 15°C). In the bio-oil condensing system, condenser 1 3 and 4 are cyclonic condensers. Condenser 1 was immersed under hot oil bath heated by electronic heater and controlled by a digital controller. Condenser 3 and 4 were immersed under chilled water. Condenser 2 is an electrostatic precipitator that charged droplets escaping from the condenser and collected them in an electric field (Mohammad et al., 2015) Condenser 1, 3 and 4 are 60 cm long with 5 cm I.D., whereas condenser 2 is 38 cm long with 6.5 cm I.D. Finally, the non-condensable gases exited condenser 4 through a column filter packed with Fiberfrax[®] (Unifrax, Tonawanda, USA).

Miscanthus biomass used in this study was obtained from Gildale Farms (courtesy of Mr. Scott Abercrombie) in St. Marys, Ontario, Canada. The powdered *Miscanthus* biomass (particle size < 2 mm) was fed using the auger feeder located on side of the reactor. A stirrer controlled by a motor was used to uniformly mix the biomass inside the reactor at 30 rpm. The speed of the motor was regulated by using a Penta KB Drive KBMD 240D multi-drive motor control (KB Electronics Inc., Coral Springs, USA). A mechanical motor, at a fixed speed, controlled the feeder to maintain the constant flow of biomass into the reactor during all experiments. The biomass feeding rate was maintained at 8-9 g/min and the biomass was fed into the reactor through the auger feeder only when the reactor temperatures had reached the desired temperature set points. The effect of pyrolysis temperature was studied by operating the bed at three different temperatures 400, 450 and 500°C. The effect of vapor residence time was studied by varying the flow of N₂ gas. Three different vapor residence times studied were 1.4 s, 2.7 s and 5.2 s. The run time is referred to as the reaction time during which the biomass was constantly fed through the hopper (feeder) during the pyrolysis experiments. After determining the optimal temperature with maximum bio-oil yields with a standard run time of 1 h, the run time of 1.5 h was used to validate the material balances and further investigate the impacts of vapor residence times (1.4-5.2 s) at the constant temperature.

After the completion of each pyrolysis experiment, the yield of bio-oil, biochar and gas (by difference) were measured. The bio-oils fractions separately collected from each condenser were stored in clean glass jars under freezing conditions to prevent degradation by polymerization until further characterization. On the other hand, the biochars were stored in plastic bags for characterization and physical activation experiments. All the experiments were performed in duplicates and the results are hereby presented as average measurements. The biochar samples collected at 400, 450 and 500°C are represented as BC-400, BC-450 and BC-500, whereas the bio-oil samples collected at the above-mentioned temperatures are denoted as BL-400, BL-450 and BL-500.

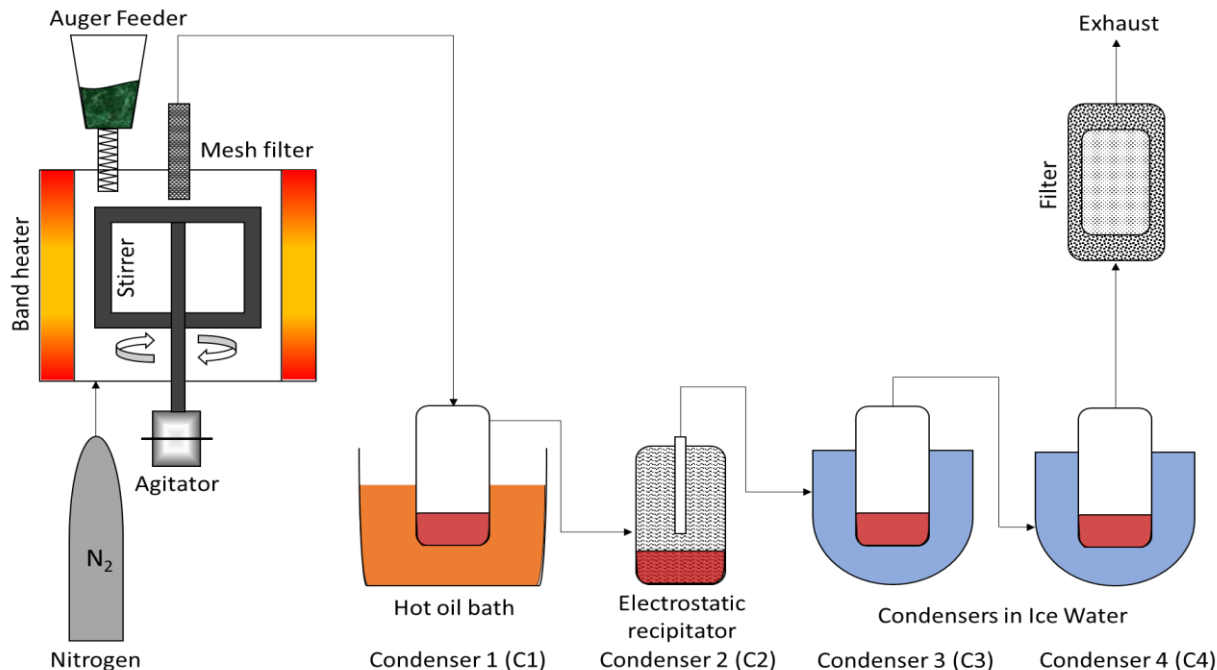


Fig. 3-1: Schematics of the mechanically fluidized bed reactor used for pyrolysis of *Miscanthus*

3. 2 Physical activation of biochar

Samples of the biochars obtained from the pyrolysis of *Miscanthus* biomass at 400-500°C for 1.5 h of run time with 5.2 s of vapor residence time were physically activated using CO₂ as the activation medium. The CO₂ activation was performed at 900°C for 1.5 h of holding time with 60 mL/min of CO₂ flow rate using a SS316 tubular reactor (100 cm long and 5 cm O.D.). (Yang et al. 2010; Chen et al; 2016) The activation reactor was heated using a 240 volts electric tube furnace (Lindberg/Blue M, Ashville, USA) with an in-built temperature control system. The temperature inside the activation reaction was monitored using a Type-K thermocouple (McMaster-Carr, Aurora, Colorado, USA). The activation of biochar was performed in batch mode with 150 g of biochar per batch. The schematics of the activation reactor is presented in **Fig.3-2**. The activated biochar samples collected from the precursor biochars (originally generated from *Miscanthus* pyrolysis at 400, 450 and 500°C) are represented as AB-400, AB-450 and AB-500.

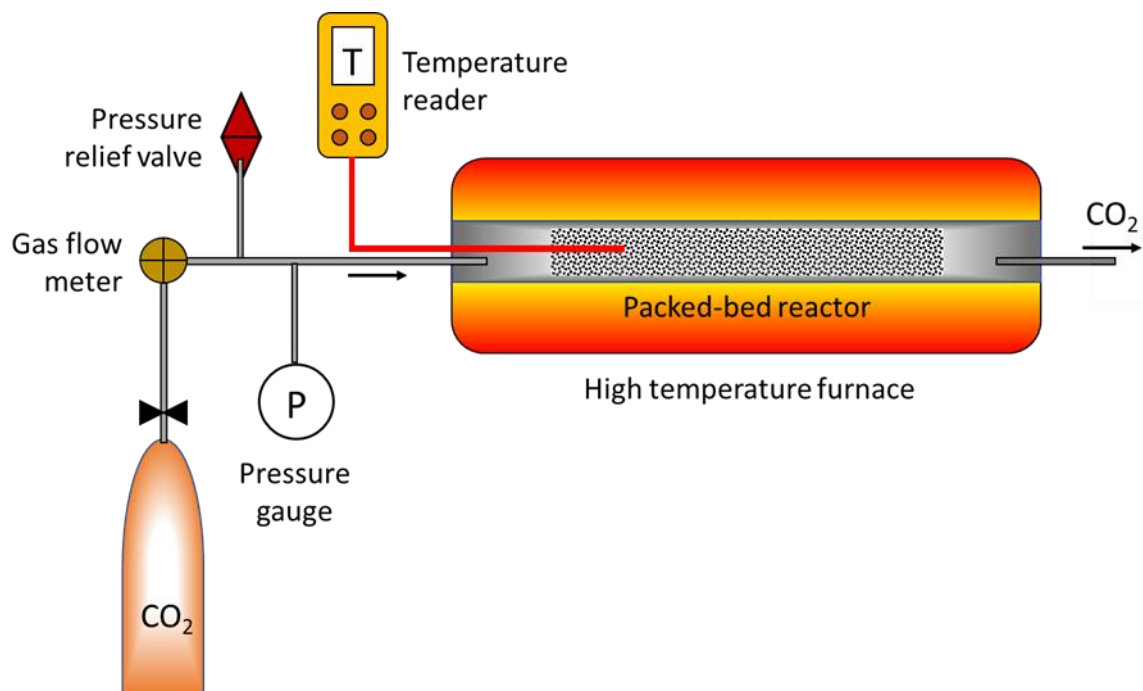


Fig. 3-2: Schematics of the physical activation reactor

3.3 Characterization of biomass, bio-oil, biochar and activated biochar

3.3.1. Compositional analysis of biomass

The biochemical composition (cellulose and hemicellulose) of *Miscanthus* biomass was determined using the standard NREL method (Sluiter et al., 2008). According to the two-step acid hydrolysis protocol, *Miscanthus* was hydrolyzed for 1 h at 30°C with 72% of H₂SO₄ followed by second hydrolysis for 1 h at 121°C with 4% H₂SO₄. After hydrolysis, the hydrolysate was separated by filtration from the solid residue. The hydrolysates were filtered using 0.2 µm filters and analyzed in a Hewlett Packard Series 1100 model HPLC (high pressure liquid chromatography) using an Aminex HPX 87H ion-exclusion column (BioRad, Hercules, USA). The column temperature was maintained at 55°C and the mobile phase used was 5 mM H₂SO₄ at a flow rate of 0.6 mL/min. The degraded carbohydrates in the biomass hydrolysate were determined from the composition of glucan and cellobiose (cellulose) as well as xylan and arabinan (hemicellulose). The concentration of acid-soluble

lignin in the hydrolysate was determined through spectroscopic analysis using an Evolution 201/220 UV-Vis spectrophotometer (ThermoFischer Scientific, Mississauga, Canada) with absorbance at 320 nm.

3.3.2. Proximate and ultimate analysis

The proximate analysis of *Miscanthus* biomass and biochars was performed to determine moisture, ash, volatile matter and fixed carbon contents. Moisture content in biomass was determined using a METTLER TOLEDO HB43-S moisture analyzer (Mississauga, Canada). Standard ASTM methods were followed to determine the ash (ASTM E1755-01, 2007) and volatile matter (ASTM D3175-11, 2011). According to the ASTM procedures, 1 g of *Miscanthus* biomass or biochar was placed in a clean and dry ceramic crucible and placed in a muffle furnace at $575\pm 10^\circ\text{C}$ for 4 h (for ash content) and $950\pm 10^\circ\text{C}$ for 7 min (for volatile matters). The difference in the initial and final weights of the samples was used to determine the ash and volatiles. Fixed carbon in the biomass and biochar was estimated by the difference of moisture, ash and volatile matter.

The ultimate analysis of *Miscanthus* and its derived bio-oils, biochars and activated biochars was performed using a ThermoScientific FlashEA 1112 Series CHNSO elemental analyzer (ThermoFischer Scientific, Mississauga, Canada) to measure the concentrations of organic elements such as carbon, hydrogen, sulfur, nitrogen and oxygen. The higher heating value (HHV) of *Miscanthus* and its bio-oil and biochar were calculated using an IKA C2000 oxygen bomb calorimeter (IKA Works, Inc., Wilmington, USA).

3.3.3. Karl Fischer titration

The water content in the bio-oil samples generated from the pyrolysis of *Miscanthus* was calculated through Karl Fischer titration using a METTLER TOLEDO V20 Volumetric KF Titrator (METTLER TOLEDO, Mississauga, Canada). The samples were titrated using HYDRANAL™ Composite 5 and methanol-chloroform (3:1 vol/vol) mixture as the solvent, as suggested in ASTM D95 (ASTM D95-13, 2018).

3.3.4. pH analysis

For pH analysis, the biochar samples were soaked in deionized water in the ratio of 1:5 biochar/water for 24 h with intermittent agitation (Song and Guo, 2012). The slurry was filtered, and the pH was measured using an Oakton pHTestr® 10 Waterproof BNC Pocket pH Tester (Cole-Parmer, Montreal, Canada).

3.3.5. Thermogravimetric analysis

Thermogravimetric analysis (TGA) and differential thermogravimetric analysis (DTA) were performed for *Miscanthus*, biochar and activated biochar using a PerkinElmer Pyris 1 thermogravimetric analyzer (Waltham, USA). Approximately 10 mg of sample were heated from room temperature to 700°C at a heating rate of 10°C/min under N₂ flow rate of 30 mL/min to understand its devolatilization behavior of the samples.

3.3.6. Fourier-Transform Infrared spectroscopy

Fourier transform infrared (FT-IR) spectroscopy was performed for *Miscanthus*, biochar, activated biochar and bio-oil with Frontier FT-IR Spectrometer (PerkinElmer, Waltham, USA) to detect the organic functional groups. Each spectrum averaged 32 scans with a resolution of 4 cm⁻¹ and collected in the range of 600 to 3600 cm⁻¹.

3.3.7. Evolved gas analysis

The evolved gas analysis (EGA) was carried out through the thermogravimetric analysis combined with infrared spectrometry (TG-IR) using a TL8000 Balanced Flow FT-IR EGA system. The TG-IR analysis was conducted for understanding the pattern of gas evolution from *Miscanthus* biomass during devolatilization from 400-4000 cm⁻¹. The TL8000 system consisted of five components, namely gas flow cell, gas transfer line, controller module, vacuum pump and SealINK DIO-16 relay-box. The gases produced during the TGA analysis with the increasing temperature were scanned by the FT-IR spectrophotometer.

3.3.8. Surface area and porosity analysis

The surface area, pore size distribution and total pore volume of *Miscanthus*-derived biochars and activated biochars were analyzed using Brunauer-Emmett-Teller (BET) analysis. The analysis was performed using Nova 1200e Surface Area & Pore Size Analyzer (Quantachrome Instruments, Anton Paar QuantaTec Inc., Florida, USA). Liquid nitrogen at -196°C was used for used for adsorption studies. Degassing was done at 250°C for 3 h.

3.3.9. Scanning electron microscopy-Energy-dispersive X-ray spectroscopy (SEM-EDX)

The surface morphology of *Miscanthus* biomass and its derived biochar and activated biochars was studied using scanning electron microscopy coupled to an energy-dispersive X-ray spectroscopy (SEM-EDX). The analysis was performed using a Hitachi SU3500 Scanning Electron Microscope (Hitachi, Krefeld, Germany) combined with an Oxford AZtec X-Max50 SDD energy dispersive X-ray (EDX) detector (Oxford Instruments, High Wycombe, UK). EDX is a semi-quantitative technique that can detect elements with a minimum detection limit of approximately 0.5 wt%. The imaging was done using back-scattering electron mode at 10 kV accelerating voltage. The samples were coated with thin layer of gold to minimize charging artifacts.

3.3.10. Methylene blue adsorption test

The adsorption performance of biochars and activated biochars was investigated by comparing it with that of commercial activated carbon using the adsorption of methylene blue (MB) as a target model molecule. A commercial activated carbon CAC (GC 12×40AW) originally made in Indonesia was procured from General Carbon Corp. (Paterson, USA) for use as a reference adsorbent material. The CAC (GC 12×40AW) is a granular acid washed activated carbon made from bituminous coal and reported to be ideal for liquid phase adsorption of organics components. The CAC (GC 12×40AW) had a specific area of $900\text{ m}^2/\text{g}$ with 8 wt% ash, 3 wt% moisture, density of $0.47\text{-}0.53\text{ g/cm}^3$ and pH of 6-7 (General Carbon Corporation, 2019). Methylene blue was purchased in analytical purity from Sigma-Aldrich (Oakville, Canada) and used without further purification.

Methylene blue solutions were prepared with distilled water and stored in amber colored flasks to prevent photodegradation.

The adsorption experiments were carried out under ambient conditions by using stirred flasks. Batch experiments were performed in a set of 250 mL conical flasks that contained a definite volume of fixed initial concentrations of methylene blue solution. The flasks were kept on a stirrer plate shaker at a speed of 500 rpm without any heat treatment. For predetermined time intervals, the sample solutions were filtered after attaining equilibrium conditions using 0.2 μm disposable syringe filters (VWR International LLC, Mississauga, Canada) to filter out the fine char particles. The adsorbate concentrations in the initial, during adsorption and final aqueous solutions were measured by using an UV-Vis spectrophotometer (ThermoFischer Scientific, Mississauga, Canada) at 668 nm. The equilibrium adsorption experiments were completed by adding a fixed amount of activated carbon into 100 mL of 250 mg/L (ppm) initial concentration of methylene blue. The aqueous samples were taken at desired time intervals and their concentrations were determined. The amount of methylene blue adsorption at equilibrium was calculated by using Eq. (1).

$$q_e = (C_o - C_e) V/W \quad \text{Eq. (1)}$$

where, C_o and C_e (mg/L) are the initial and equilibrium concentrations of methylene blue, respectively, V (L) is the volume of the solution, and W (g) is the mass of adsorbents used. The uptake of methylene blue at time t i.e. q_t (mg/g) was calculated using Eq. (2), where C_t is the concentration of methylene blue at a particular time interval. All experimental data were the average of triplicate determinations and the relative errors were less than 4%.

$$q_t = (C_o - C_t) V/W \quad \text{Eq. (2)}$$

3.3.11 Gas chromatography-mass spectrometry (GC-MS) analysis of bio-oil

GC-MS analysis was carried out to identify compounds in the bio-oil produced from the pyrolysis of *Miscanthus*. The preparation of samples for the GC/MS analysis is mentioned as follows. 2-propanol and bio-oil were mixed at 10:1 vol/vol to extract the chemical compounds. Anhydrous Na₂SO₄ was used to extract the water-containing compounds in the bio-oil. The GC-MS system consisted of a Shimadzu GCMS-QP2010 quadrupole mass spectrometer (Columbia, Maryland, USA) equipped with a capillary column (DB-5MS; 30 m × 0.25 mm ID and 0.25 μm thickness). Electron ionization was used with an ion source temperature of 200°C and the interface temperature of 250°C. During electron ionization, the instrument was used in scan mode initially to confirm the identity of the compounds. The injector temperature in the GC was 200°C. An AOC-20S auto sampler with a 10 μL syringe was used to inject 1 μL of the samples at a rate of 10 μL/s. The carrier gas was ultrapure helium at a constant flow of 1.5 mL/min. At a constant heating rate of 10°C/min, the oven temperature in the GC was programmed as follows: initial temperature of 40°C (held for 10 min) rising to 200°C (held for 10 min) and rising to 300°C (held for 30 min) with a total run time of 75 min. This temperature program was selected to provide adequate separation of most of the compounds of interest. All the compounds were identified by means of the National Institute of Standards and Technology (NIST05 and NIST05s) mass spectral data library.

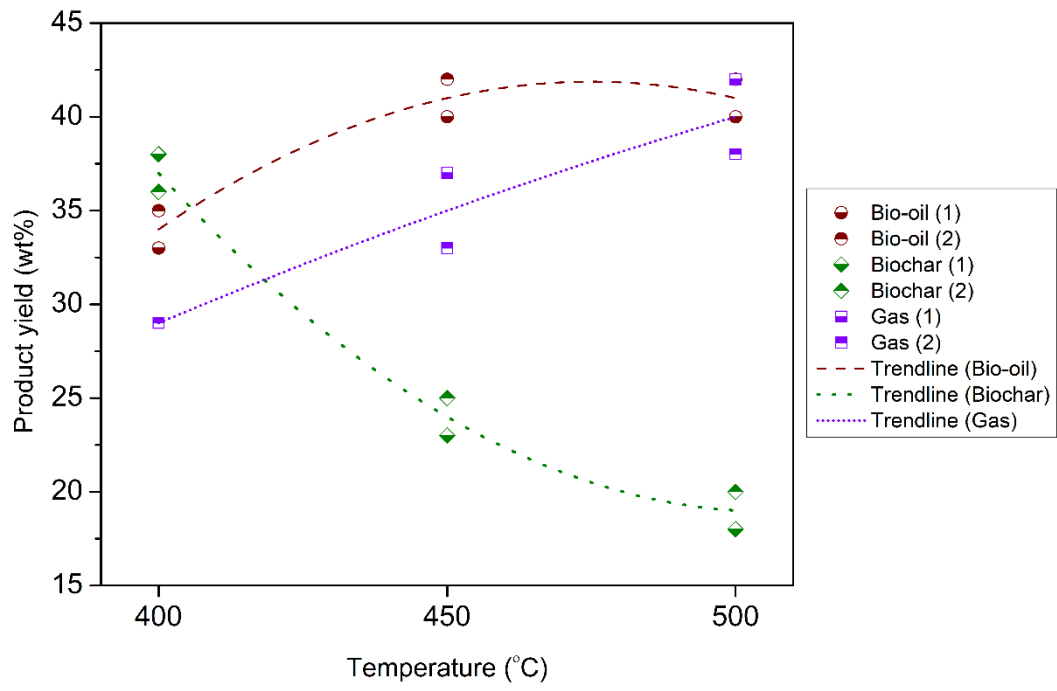
CHAPTER 4

4. RESULTS AND DISCUSSION

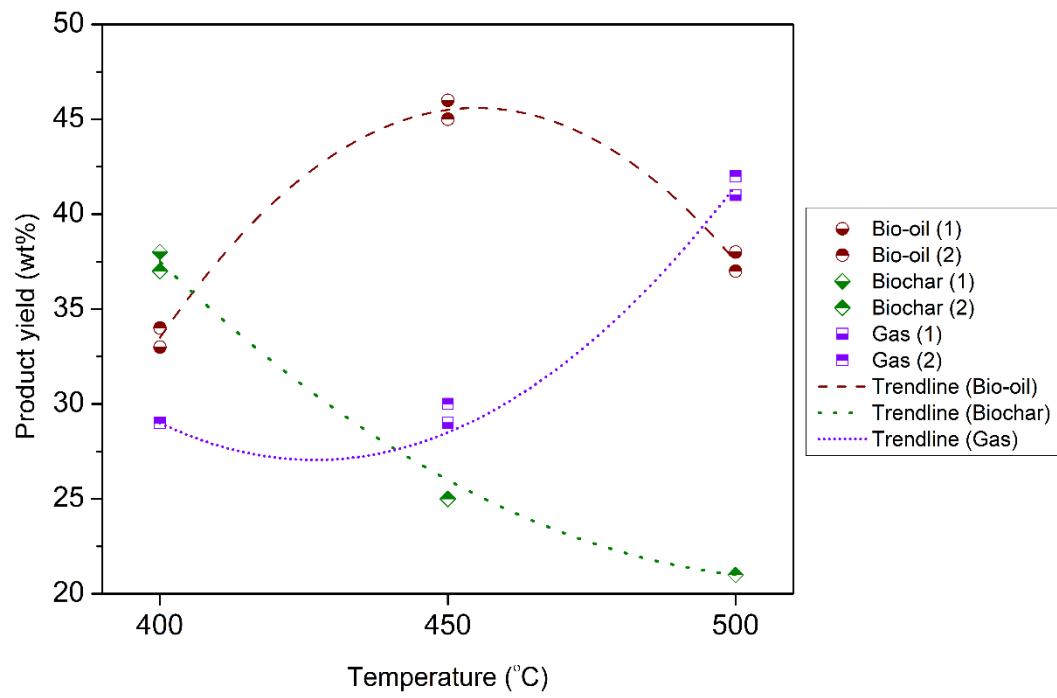
4.1 Product yields from pyrolysis and biochar activation

Miscanthus was pyrolyzed in a mechanically fluidized bed reactor at a feeding rate of 8-9 g/min to investigate the effect of temperature (400-500°C) and vapor residence time (1.4, 2.7 and 5.2 s) for a standard run time of 1 h. The trends of pyrolysis product yields are shown in **Fig. 4-1**. Average data obtained after replicate experiments were considered for discussion in the thesis although all data points have been displayed in the graphs (designated as (1) and (2)) for reference and uncertainty check. Regardless of the vapor residence time, it was seen that with a rise in temperature, the biochar yield decreased. In contrast, the yield of bio-oil increased from 400°C until 450°C and then decreased as the amount of gas production increased. In the case of 1.4 s vapor residence time, the yield of bio-oil increased from 34 wt% at 400°C up to 41 wt% and stayed constant at 450 and 500°C (**Fig. 4-1a**). The bio-oil yield increased from 34 wt% at 400°C up to 46 wt% at 450°C and then decreased to 38 wt% at 500°C with 2.7 s of vapor residence time (**Fig. 4-1b**). Similarly, pyrolysis at 5.2 s of vapor residence time, gave bio-oil yield of 29 wt% at 400°C, 37 wt% at 450°C and 35 wt% at 500°C (**Fig. 4-1c**). The optimal temperature and vapor residence time for generating maximum bio-oil yield of 46 wt% were found to be 450°C and 2.7 s, respectively.

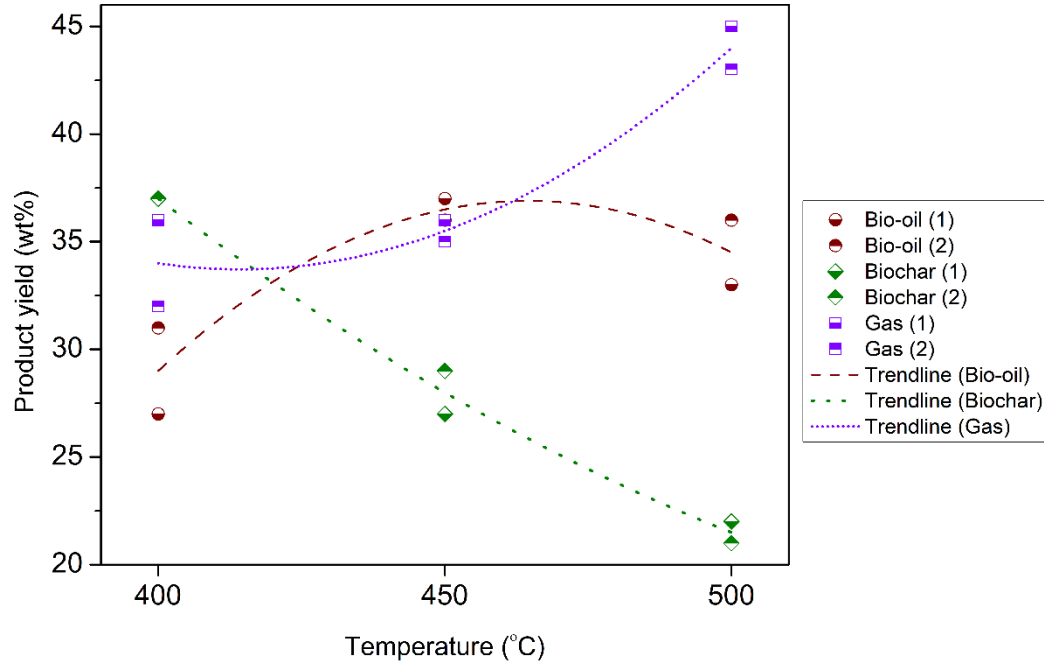
The yield of biochar was noted to be highest at 400°C (37-38 wt%) and gradually decreased with the rise in temperature up to 500°C (19-22 wt%). Among all the vapor residence times tested, maximum the biochar yield of 38 wt% was obtained from pyrolysis at 2.7 s of vapor residence time (**Fig. 4-1b**). On the other hand, the yield of gas products gradually increased as the temperature increased from 400°C (29-34 wt%) to 500°C (40-44 wt%). At the optimal temperature for gas 500°C, the highest gas yields of 44 wt% was achieved from the pyrolysis of *Miscanthus* at 5.2 s of vapor residence time while the lowest yield was obtained at 1.4 s of vapor residence time.



(a)



(b)



(c)

Fig. 4-1: Effect of temperatures on the yield of pyrolysis products at different vapor residence times of (a) 1.4 s, (b) 2.7 s, and (c) 5.2 s for 1 h of run time

Greenhalf et al. (2013) showed that bio-oil yield of 41.2-51.2 wt% was obtained at 490°C for *Miscanthus giganteus*. Heo et al. (2010) performed the pyrolysis of *Miscanthus sinensis var. purpurascens* using a bench-scale fluidized bed reactor in the temperature range of 350-550°C and concluded that 450°C was optimal for maximum bio-oil yield of 69.2 wt%. They suggested that 450°C was optimal for highest bio-oil yield from *Miscanthus* pyrolysis because it corresponded to the completion of the thermal composition of cellulose and hemicellulose in the biomass. In this present study, it was also concluded that 450°C was the best temperature among those tested for maximizing the bio-oil yield. TGA analysis showed the complete degradation of cellulose and hemicellulose up to 350°C after that degradation of lignin occurred which mainly produced char. However, Heo et al. (2010) got 69.2 wt% of bio-oil content but failed to specify the vapour residence time as well as the amount of aqueous and organic phases of the bio-oil.

After determining 450°C as the temperature for maximizing bio-oil yields, the run time was extended from the initial standard test time of 1 h to 1.5 h. As identified that the material losses during the products collection may have negatively affected the material balance. As such, It was decided to extend the run time to 1.5 hours (the maximum allowed by the capacity of the equipment) to ensure the production of more products collected in the individual condensers and, correspondingly lower relative material losses during their recovery. The improved material balances showed more correctly higher yields. The yield of biochar increased as the vapor residence time increased from 1.4 s (25 wt%) to 5.2 s (31 wt%). Theoretically, biochar yield is favored at longer residence times due to polymerization reactions and secondary cracking of vapors while bio-oil yield is promoted at short residence times (Bridgewater, 2012). On the other hand, the bio-oil yield increased up to a maximum of 59 wt% at a short residence time of 1.4 s (**Fig. 4-2**). In contrast, the gas yields were highest at longer vapor residence time 5.2 s (29 wt%) compared to that of the lower vapor residence time of 1.4 s (16 wt%).

In a similar study by Kim et al. (2014), fast pyrolysis of *Miscanthus sacchariflorus* was conducted in the temperature range of 350-500°C with vapor residence time of 1.9 s. It was reported that with the increase in temperature from 350 to 500°C, the yield of bio-oil and biochar yield decreased from 57.2 to 47.7 wt% and 22.0 to 17.1 wt%, respectively but the gas yield increased from 22 wt% to 35.5 wt%. Kim et al. (2014) also reported increase in the water content in bio-oil from 22.3 wt% to 31.5 wt% and failed to specify the organic and aqueous part of the bio-oil. In this study, maximum bio-oil yield was noted to be 58.9 wt% at 350°C with vapor residence time of 1.9 s, which did not align with our study. We concluded 450°C as the best temperature. This difference could be attributed to the presence of inorganic content (higher amount of potassium) in *Miscanthus*. Kim et al. (2014) indicated that higher amount of potassium can make the biomass to degrade at relatively lower temperatures. Moreover, Choi et al. (2019) fast pyrolysis of *Miscanthus sacchariflorus* in fluidized bed reactor reported higher bio-oil yield 51.9 wt% at 500°C but failed to specify the vapour residence time and run time (Choi et al. 2019)

In this work, lower vapor residence times than 1.4 s was not achieved due to some practical limitations of the equipment because of the higher nitrogen gas velocity in the bed, which could create excessive pressure drop through hot filter as well plugging of filter, thereby increasing the reactor pressure. Progressively, it could lead to a more difficult product condensation if excessively diluted gas/vapor product streams with inert nitrogen is used. Longer vapor residence time in the reactor tends to increase the secondary cracking reaction of primary degradation products, which results to minimizing bio-oil and biochar yields while maximizing gas yields (Mohanty et al., 2013). Higher temperatures enhance the primary degradation of biomass while restraining the secondary cracking reactions, which helps to increase the bio-oil yield. Longer vapor residence time with lower condensation rate as well as intermediate temperature can help the formation of heavy molecular weight compound, such as tar and biochar (Nanda et al., 2016a).

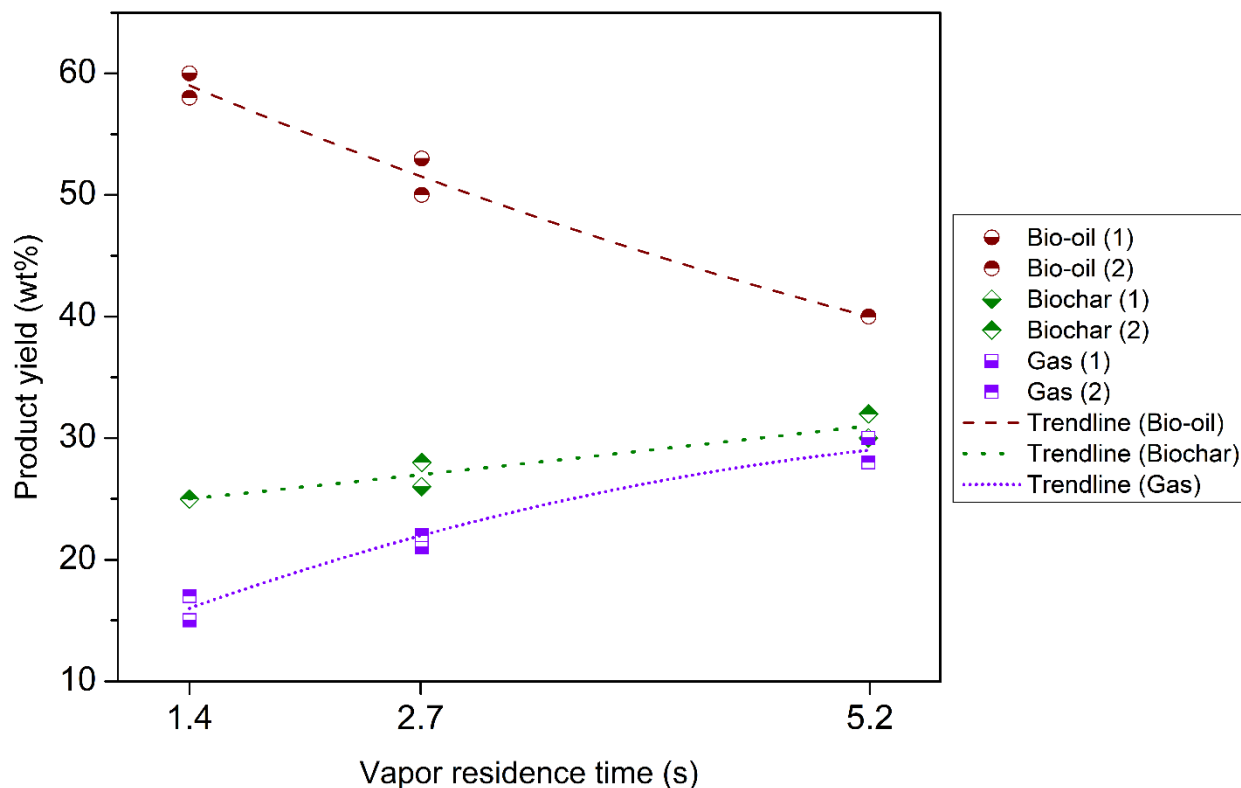


Fig. 4-2: Effect of vapor residence time on the yield of pyrolysis products at optimal temperature of 450°C for 1.5 h of run time

Table 4-1: Yields of solid, liquid and gaseous biofuels from *Miscanthus* in the previous studies

Process	Process conditions	Product yield	References
Slow pyrolysis	Temperature: 500°C Reaction time: 30 min Feed amount: 400 g Heating rate: 7°C/min N ₂ flow rate: 2 L/min Reactor type: Fixed-bed batch reactor	Bio-oil: 45-51 wt% Biochar: 30 wt% Gas: 20-25 wt%	Oginni et al. (2017)
Fast pyrolysis	Temperature: 350-550°C Feeding rate: 2.5 g/min N ₂ flow rate: 3.0 and 4.0 L/min Reactor type: Fluidized-bed reactor	Bio-oil: 25-69 wt% Biochar: 15-30 wt% Gas: 5-55 wt%	Heo et al. (2010)
Fast pyrolysis	Temperature: 350-500°C Feeding rate: 150 g/h Residence time: 1.29 s, 1.93 s and 3.87 s Run time: 1 h N ₂ flow rate: 3.0 and 4.0 L/min Reactor type: Fluidized-bed reactor	Bio-oil: 47.7-57.2 wt% Biochar: 17.1-22 wt% Gas: 20.9-35.5 wt%	Kim et al. (2014)
Fast Pyrolysis	Temperature: 400-550 °C Feeding rate: 200 g/h Reactor type: fluidized bed reactor N ₂ flow rate: Not reported Run time: Not reported	Bio-oil: 43- 51.9 wt% Biochar: 35-21 wt% Gas: 20-29 wt%	Choi et al. (2019)

In order to potentially increase their value, the biochars obtained from the pyrolysis of *Miscanthus* at 400, 450 and 500°C were physically activated at 900°C with a CO₂ flow rate of 60 mL/min for 1.5 h. Activation is expected to increase the specific surface area of the material and, correspondingly, its successful application in adsorption processes. Because of CO₂ activation, some weight losses were noticed in the activated biochar. When compared with the initial weight of biochars, approximately, 40%, 33% and 27% weight losses were measured in the activated biochars, i.e. AB-400, AB-450 and AB-500, respectively. Maximum weight loss in AB-400 was attributed to the thermal degradation during activation of higher amount of volatile matter and partially unreacted lignocellulose in *Miscanthus* biochar produced at 400°C (Yang et al., 2010). The lowest magnitude of weight loss in AB-500 was due to its biochar precursor i.e. BC-500 which already had relatively lower amounts of volatile matter.

In our study, fractional condensation of the pyrolysis vapors was performed using four condensers (named as C1-C4), maintained at different selected temperatures. The first two condensers (C1 and C2) operated at 110°C and 70°C, respectively, whereas the other two condensers (C3 and C4) operated at temperatures below 15°C. The condensers C1 collected fractions of dry organic phase while C2 produced an equivalent combination of organic and aqueous phase. Finally, C3 and C4 produced mostly aqueous phase. The two phases of the pyrolysis liquid collected from all the condensers were separated using centrifugation into an aqueous (water, solvents and organic acids) and organic phase (bio-oil). After separation of two distinct phases from all the condensers produced at 450°C, run time 1.5 h with 1.4 s of vapor residence time (with maximum bio-oil yield), the mass fractions of organic bio-oil and aqueous phases were 35 and 65 wt%, respectively. The bio-oil fraction recovered from the pyrolysis oil was used for further characterization studies.

The organic fraction of pyrolysis liquid is considered as the “dry” bio-oil, which may have the best fuel properties, whereas the aqueous fraction may offer alternative industrial values for the extraction of fine chemicals (e.g. organic acids, phenolics, ethers, esters, aldehydes, ketones, etc.). The aqueous fraction of bio-oil is helpful for enhancing its fluidity and atomization during burning. However, it also tends to decrease the heating value and flame

temperature of the bio-oil. The water in bio-oil occurs as the free and bound water during vapor condensation and through the dehydration reactions of carbohydrates or lignin during pyrolysis (Kim et al., 2014).

4.2 Compositional, proximate and ultimate analyses

The biochemical composition of *Miscanthus* was determined using the standard NREL protocol involving dilute H₂SO₄ hydrolysis followed by determination of sugars and lignin by HPLC and UV-Vis spectrophotometer. *Miscanthus* biomass used in this study was composed of 44.8% cellulose, 27.1% hemicellulose and 23.1 % of lignin. Kim et al. (2014) reported 72.1 wt% holocellulose (cellulose and hemicellulose), 24.9 wt% lignin and 4.6 wt% ash in *Miscanthus sacchariflorus*. On a dry matter basis, a typical lignocellulosic biomass is made up of 30-60% cellulose, 20-40% hemicellulose and 15-20% lignin (Nanda et al., 2013). Lignocellulose is a prominent component of plants, which provides them structural integrity in the roots, stalks and leaves. The plant cell walls are mainly composed of cellulose, hemicellulose, lignin, pectin and glycosylated proteins, each of which has dedicated physiological functions. Cellulose is the repeating structure of β -D glucopyranose and mostly comprises of glucose polymer linked by β -1,4 glycosidic linkages (Nanda et al., 2014c). Hemicellulose contains pentose and hexose sugars and sugar acids, which is relatively easily hydrolysable. In contrast, lignin is a cross-linked phenylpropane polymer, which holds cellulose and hemicellulose together providing rigidity and integrity to plant cells (Brosse et al., 2012). The composition of cellulose, hemicellulose and lignin in the biomass determines the quality and quantity of the fuel and chemical products by thermochemical and biochemical conversion technologies (Hodgson et al., 2010).

The proximate analysis of *Miscanthus* biomass, biochar and activated biochar is shown in **Table 4-2**. *Miscanthus* contained 7.45 wt% moisture, 5.67 wt% ash, 80.8 wt% volatile matter and 6.08 wt% fixed carbon. The content of ash was found to increase in the biochars produced at high temperatures. In addition, the activated biochars produced from respective biochar precursors also showed higher ash contents. Ash content of biochar increases with rise in temperature (Azargohar et al., 2013). Ash is composed of several inorganic elements of biomass, which includes diverse species of silicates, carbonates, sulfates and phosphates

(Vassilev et al, 2010). With the increase in temperature, the moisture and volatile matter in biochars and activated biochars gradually decreased mainly due to the dehydration and devolatilization reactions (Azargohar et al., 2014). While the moisture is released through dehydration of hydroxyl groups, the volatile matter is liberated in the form of light hydrocarbons, tars, as well as condensable and non-condensable gases (Vassilev et al, 2010). The concentration of fixed carbon also amplifies in the biochars and activated biochar produced at higher temperatures. In the case of biochars and activated carbon, highest levels of fixed carbon was measured in BC-500 (63.8 wt%) and AC-500 (80.1 wt%), respectively. With the dramatic loss of moisture and volatile matter during CO₂ activation at 900°C, the activated biochars showed highest levels of fixed carbon (76.9-80.1 wt%).

Table 4-2: Proximate analysis of *Miscanthus*-derived biochars and activated carbon generated from pyrolysis at 400-500°C for 2.7 s of vapor residence time and 1 h of run time and subsequent activation at 900°C for 1.5 h

Sample	Moisture (wt%)	Ash (wt%)	Volatile matter (wt%)	Fixed carbon (wt%)
<i>Miscanthus</i>	7.45	5.67	80.8	6.08
BC-400	1.93	6.14	49.7	42.3
BC-450	1.84	8.36	38.7	51.1
BC-500	1.79	8.67	25.7	63.8
AB-400	1.91	8.78	12.4	76.9
AB-450	1.82	9.14	10.1	78.9
AB-500	1.78	10.64	7.5	80.1

The compositions of CHNSO in *Miscanthus* biomass, biochars and activated biochars are shown in **Table 4-3**. *Miscanthus* contained 45.7 wt% C, 5.8 wt% H, 0.44 wt% N, 0.15 wt% S and 42.2 wt% O. The carbon content increased drastically from 68.4 wt% in BC-400 up to 72.2 wt% in BC-500. Similarly, the carbon content in AB-500 (83.4 wt%) was dramatically greater than AB-400 (72.9 wt%). In contrast, hydrogen and oxygen contents reduced in their composition in biochars and activated biochars due to dehydration (moisture loss) and devolatilization (removal of volatiles) at higher temperatures. Regardless, greater amount of

carbon in the activated biochars, especially at 500°C, i.e. AB-500 suggest improved carbonization and aromatization.

In a study on slow pyrolysis of *Miscanthus giganteus*, Wilk and Margdziaz (2017) showed that with the increase in residence time and temperature, the carbon content in biochar as well as its HHV increased. The experiments were performed in a quartz tubular reactor at 350-500°C with 0.5-1.5 h of residence time. Mimmo et al. (2014) performed the pyrolysis of *Miscanthus* at temperatures ranging from 350°C to 450°C with a residence time of 15 min. A decrease in biochar yield was observed with an increase in temperature. Moreover, in the biochars produced at higher temperature, the contents of O and H decreased, while those of N and C increased. The pH of biochar also increased with the increase in the temperature. The analysis of calorific value or HHV is essential for energy analysis. After complete combustion, the energy produced per unit mass or volume of the fuel can be defined as its HHV, which also includes the energy present in the water vapors in the exhaust gas (Yang et al., 2017). The HHV of *Miscanthus* biomass was estimated to be 17.4 MJ/kg (**Table 4-3**). The heating value of biomass is totally dependent upon the elemental and biochemical composition of the plant cell wall as well as the ash content. The reported higher heating value of *M. giganteus* is between 17 and 20 MJ/kg (Brosse et al., 2012). The effect of the biomass composition upon the HHV also depends to the presence of lignin because lignin has less oxygen content and more heating value (23.3-25.6 MJ/kg), which is 30% greater than holocellulose (Novaes et al., 2010).

With the increase in temperature, the HHV of biochars (24-28.2 MJ/kg) and its activation counterparts (27.4-28.8 MJ/kg) also increased. The samples BC-500 and AB-500 were found to exhibit maximum HHVs of 28.2 MJ/kg and 28.8 MJ/kg, respectively (**Table 4-3**). Yang et al. (2017) also reported the same trend in a study on the pyrolysis of *Miscanthus* where the HHV of biochar produced at 500°C was greater than that at 350°C. This was due to the carbonization of the volatile components essential for higher HHV in high-temperature biochars. In another study, Kwapinski et al. (2010) reported an increase in the HHV from 29.4-30.3 MJ/kg to 31.5-32.5 MJ/kg for *Miscanthus* biochar when temperature soared from 400°C to 600°C.

As the pyrolysis and activation temperature increased, the pH values of biochar and activated biochar increased from 7.2 to 7.9 and 8.4 to 9.7, respectively (**Table 4-3**). Among the biochars and their respective activated biochars, BC-500 (7.9) and AB-500 (9.7) revealed the highest pH values. The variation in pH values could be related to the ash content. As it can be seen that the ash contents in the biochars and activated biochars increase with the rise in temperature, which is due to the intensification of alkali metals, especially Na, Mg, P, K and Ca (Mohanty et al., 2013; Azargohar et al., 2014). The increase in the pH values with temperature is also attributed to the separation of inherent alkali salts from the organic matrix present in the raw feed (Janus et al., 2017). These alkali metals induce alkalinity to the biochars, thus raising their pH values. Biochar with high pH values can be applied to the acidic soils for neutralizing and reducing soil acidity. The pH of the activated biochar is also effective to decide its ionic strength, which influences the absorption capacity of organic particles on its surface (Nanda et al., 2016a). Pyrolysis at lower temperatures results in the production of organic acids and phenolics from the thermal cracking of cellulose and hemicellulose, which lower the pH of biochar and bio-oil (Cao and Harris, 2010).

Table 4-3: Ultimate analysis of *Miscanthus*-derived biochars and activated carbon generated from pyrolysis at 400-500°C for 2.7 s of vapor residence time and 1 h of run time and subsequent activation at 900°C for 1.5 h

Analysis	<i>Miscanthus</i>	BC-400	BC-450	BC-500	AB-400	AB-450	AB-500
C (wt%)	45.7	68.4	72.2	77.5	72.9	78.3	83.4
H (wt%)	5.8	4.65	4.1	3.71	4.53	3.98	3.54
N (wt%)	0.44	0.58	0.71	0.83	0.62	0.73	0.97
S (wt%)	0.15	0.17	0.15	0.14	0.16	0.16	0.15
O (wt%)	42.2	20.1	14.5	9.15	13.0	7.7	1.3
High heating value (MJ/kg)	17.4	24.0	24.6	28.2	27.4	28.4	28.8
pH value	-	7.2	7.4	7.9	8.4	8.9	9.7

Note: The percentage of O was calculated as the difference of C, H, N, S and ash.

Table 4-4 summarizes the ultimate composition of bio-oils produced at the optimal vapor residence of 2.7 s that gave higher bio-oil yields. The carbon content in the bio-oils elevated

with the pyrolysis temperature i.e. BL-400 (47.6 wt%), BL-450 (51.9 wt%) and BL-500 (54.8 wt%). On the other hand, bio-oil produced at 450°C at 1.5 h of reaction time contained highest levels of carbon (63.2 wt%) and hydrogen (9.6 wt%). The HHV for bio-oils produced at two different run times (1 h and 1.5 h) did not show any major variation. Among the bio-oils produced with 1 h of run time, the HHV of BL-500 (27.4 MJ/kg) was greater than that of BL-400 (26.5 MJ/kg). Some important factors, which influence the HHV of bio-oils, are its C, H and O composition as well as moisture content (Oginni et al., 2017). BL-500 (1 h run time) and BL-450 (1.5 h run time) revealed superior HHVs of 27.4 and 27.6 MJ/kg as well as low levels of moisture contents of 0.18 and 0.05 wt% as determined through Karl Fischer titration. Wang and Lee (2018) reported water content of 55.6% in the bio-oil produced from fast pyrolysis of *Miscanthus* at 450°C. Kim et al. (2014) also observed higher moisture content in *Miscanthus*-derived bio-oils produced at 500°C than that of 350°C.

Table 4-4: Ultimate analysis of *Miscanthus*-derived bio-oil generated from pyrolysis at 400-500°C for 2.7 s of vapor residence time and 1 h and 1.5 h of run times

Analysis	BL-400 (1 h)	BL-450 (1 h)	BL-500 (1 h)	BL-450 (1.5 h)
C (wt%)	47.6	51.9	54.8	63.2
H (wt%)	5.2	6.7	5.3	9.6
N (wt%)	1.2	1.4	1.3	1.7
S (wt%)	0	0	0	0
O (wt%)	46	40	38.6	25.5
High heating value (MJ/kg)	26.5	26.7	27.4	27.6
Moisture content (wt%)	0.72	0.62	0.18	0.05

Note: The percentage of O was calculated as the difference of C, H, N and S.

4.3 Evolved gas analysis

The evolved gas analysis was performed to study the different gases and volatile matters released during the controlled pyrolysis of *Miscanthus* in a coupled TG-IR device as shown in **Fig. 4-3**. This analysis helped to understand the fundamental volatile species and the variety of evolved gas in the energetic pattern. The evolved volatiles and gases from five different temperatures (150, 250, 350, 450 and 550°C) using TGA analysis were

qualitatively identified at particular wave numbers using the coupled infrared spectrometer. Between the absorbance band of 3400 and 4000 cm^{-1} , fewer small molecular gaseous products were released such as H_2O , CO , CO_2 and CH_4 (Gu et al., 2014). It is interesting to note that these gases started to evolve at temperatures above 350°C. The bands between 2800 and 3500 cm^{-1} showed the presence of CH_4 , which occurred at higher temperatures (450°C and 550°C). CH_4 is formed because of secondary reactions such as methanation and hydrogenation, which occur at higher temperatures and longer reaction time (Nanda et al., 2017a).

As shown in **Fig. 4-3**, the occurrence of CO and CO_2 in the gas products at 350-550°C is indicated in the absorbance band of 2000-2200 cm^{-1} and 2200-2400 cm^{-1} , respectively (Gu et al., 2013). The absorbance bands between 600 and 800 cm^{-1} in the TG-IR spectra of 350-550°C was also ascribed to the release of CO_2 . The presence of volatile organic species, particularly carbonyl ($\text{C}=\text{O}$) components of acids, aldehydes, ketones and esters were also evident at 1600-1800 cm^{-1} (Biagini et al., 2006). The release of volatiles was only seen in the TG-IR spectra at 350°C and its absence at higher temperatures indicate improved thermal cracking, dehydration and devolatilization. Moreover, the bands between 1300 and 1600 cm^{-1} are assigned to $\text{C}-\text{O}-\text{C}$ stretching vibrations by aldehyde, ketones and furans, whereas the bands between 1000 and 1150 cm^{-1} are due to the release of hydroxyls, phenols and alcohols (Gu et al., 2013). The hydroxyls, phenols and alcohols are found to be liberating from *Miscanthus* even at lower temperatures of 150°C. From the TG-IR analysis, CO_2 can be considered as one of the primary gas products of pyrolysis, whereas CH_4 as one of the secondary gas products.

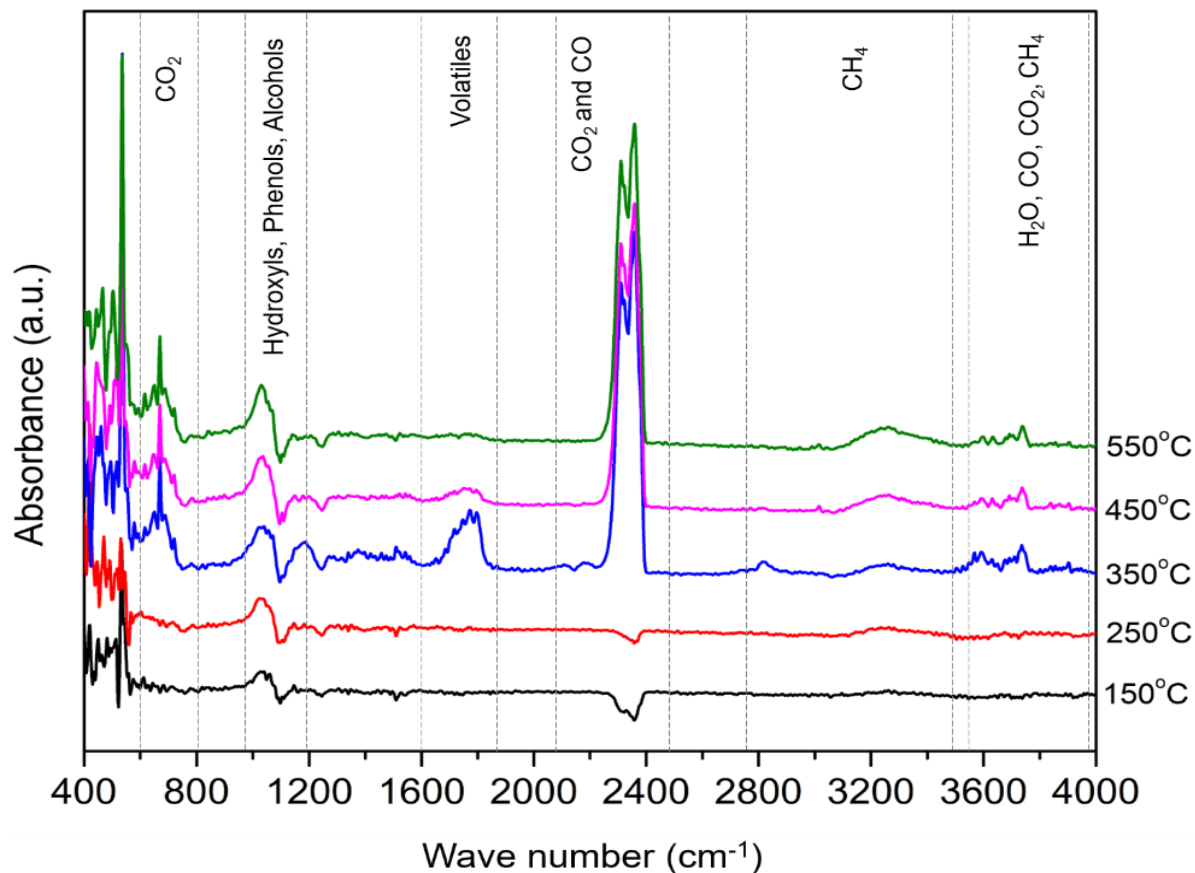


Fig. 4-3: Evolved gas analysis of *Miscanthus* using TG-IR analysis

4.4 Thermogravimetric analysis

The TGA analysis of *Miscanthus* and its biochars produced at 400-500°C was performed to observe the behavior of thermal degradation and the kinetic pattern of biomass devolatilization with temperature. *Miscanthus* started to degrade at 100°C until 250°C with only 5% weight (Fig. 4-4a). This initial weight loss was mainly due to the release of moisture and volatile matter. A sharp drop in the spectra indicating maximum weight loss of nearly 70 wt% was noticed in *Miscanthus* at 250-350°C. This weight loss was mainly due to the release of heavy volatiles and the degradation of cellulose and hemicellulose (Nanda et al., 2017a). A gradual decrease in the weight loss took place from 350°C to 700°C revealing a final weight loss of about 80%. This slower weight loss in the biomass indicated char production, which has a slower devolatilization pattern.

Heo et al. (2010) suggested the peak temperature for *Miscanthus* degradation is 350°C as evident from the TGA pattern, thus suggesting 400-500°C as the optimal temperature range for higher bio-oil production. The initial degradation temperatures for BC-400, BC-450 and BC-500 were approximately 300, 350 and 370°C in contrast to *Miscanthus* biomass, which started to degrade at 100°C (**Fig. 4-4a**). Similarly, the approximate residual weight at 700°C in BC-400, BC-450 and BC-500 were 60%, 35% and 25%. The lowest weight loss in BC-500 indicates its thermal stability due to the maximum loss of organic compounds and volatiles due to dehydration, decarboxylation and decarbonylation (Azargohar et al., 2014).

The DTA curves for *Miscanthus* represent the degradation of cellulose, hemicellulose and lignin content at different temperature zones (**Fig. 4-4b**). The peak below 100°C observed in the DTA spectra of *Miscanthus* indicated the loss of moisture. The shoulder peak at 250-280°C indicated the thermal decomposition of hemicellulose while the intense peak centering at 300-350°C was due to the degradation of cellulose (Correa et al., 2010). It is difficult to represent a peak for lignin decomposition unlike cellulose and hemicellulose, because lignin degradation occurs at a much wider range of 200-500°C (Jeguirim and Trouve, 2009). Kim et al. (2014) also explained the DTA pattern of raw *Miscanthus* indicating the degradation of hemicellulose at 300°C and cellulose at 350-400°C. The intensity of the peak centering at 350°C in the biochars decreased in the biochars produced at higher pyrolysis temperatures. This peak in BC-400 represents residual cellulose and lignin that were retained from the precursor *Miscanthus* biomass. In the DTA spectra of BC-500, the lowering intensity of the peak at 350°C indicates extreme carbonization and aromatization of the biochar (Nanda et al., 2017a).

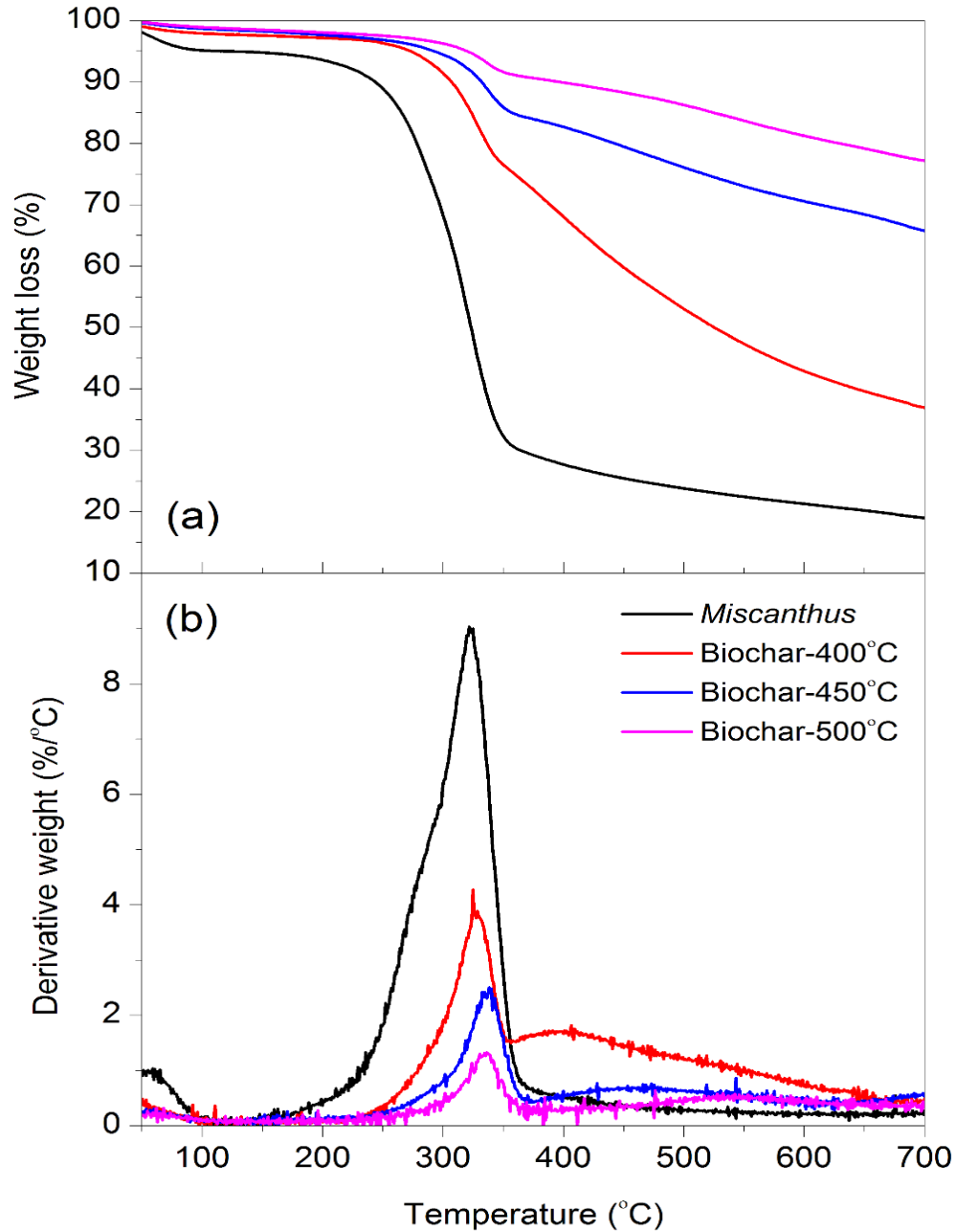


Fig. 4-4: (a) TGA and (b) DTA of *Miscanthus* and its bio-chars generated from pyrolysis at 400-500°C with 2.7 s of vapor residence time for 1 h of run time

The TGA analysis of activated biochar reveals maximum thermal stability with the lowest weight losses (**Fig. 4-5**). AB-500 exhibited the lowest weight loss of 7%, whereas AB-400 had slightly higher weight loss of 27%. Regardless, activated biochars showed lower weight

losses (7-27%) when compared to that of biochars (25-60%) (Fig. 4-4a). Moreover, AB-400 started to devolatilize at a much higher temperature of 350°C, while the pattern of devolatilization in AB-450 and AB-500 can barely be differentiated due to the formation of stable and aromatic carbon crystallites. Because of CO₂ activation at 900°C for 1.5 h, the activated biochar demonstrated the extreme thermal stability due to maximum devolatilization and removal of residual organics, carbohydrates, hydrocarbons and volatile components.

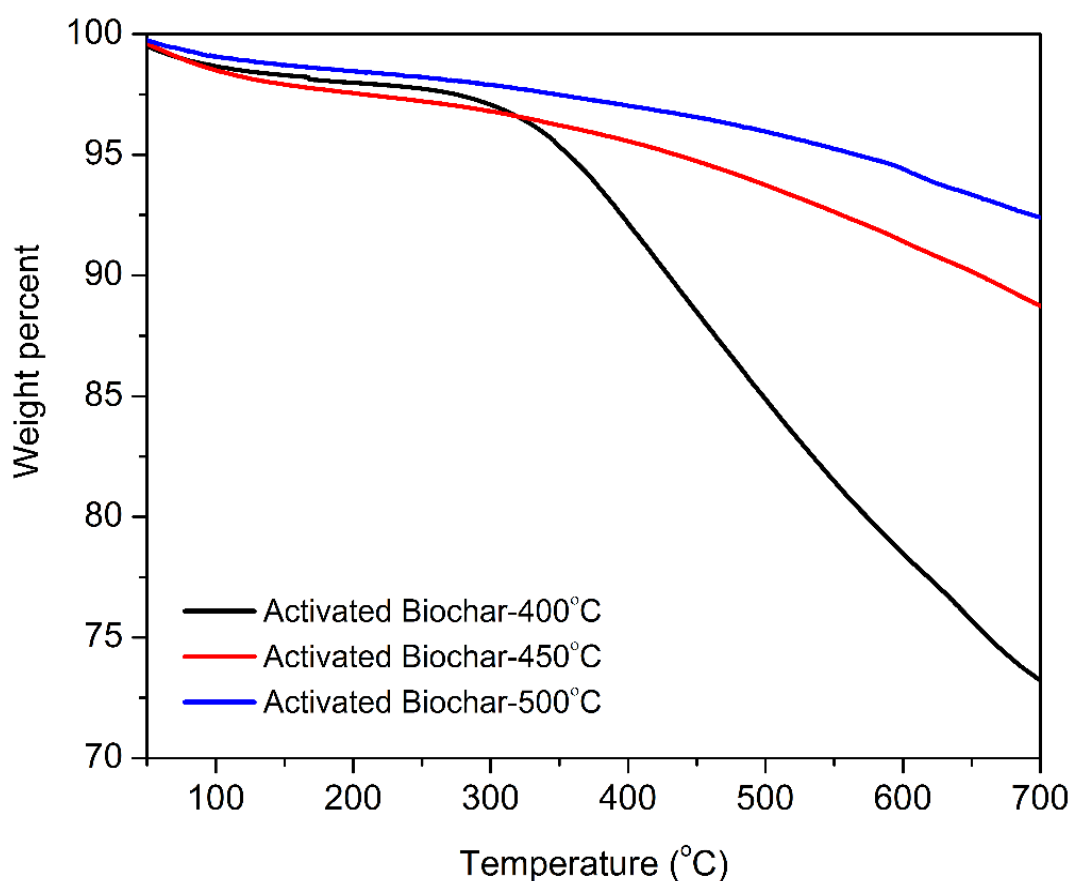


Fig. 4-5: TGA of *Miscanthus*-derived activated biochar generated from CO₂ activation at 900°C

In the case of biomass, maximum devolatilization takes place at 200-400°C leading to the formation of biochar, a phase called as primary pyrolysis (Fisher et al., 2002). With gradual increase in the temperature above 400°C, the organic matter in the biomass continues to crack with the release of smaller amounts of volatile matter as the biochar undergoes many physical and chemical transformations, which are characteristic to secondary pyrolysis. Owing to the release of volatiles from the degrading carbohydrates, the fixation of carbon under the inert atmosphere and high temperatures occur (Antal Jr. et al., 2003). Therefore, a negative correlation is found between volatile matter and fixed carbon in the proximate analysis of biomass and biochars.

4.5 FT-IR analysis

The FT-IR spectra of bio-oils, biochar and activated biochar were collected in the infra-red region of 600-3600 cm^{-1} wave number (**Fig. 4-6**). **Table 4-5** summarizes the assignments for different groups of organic components identified in the biomass, bio-oil, biochar and activated carbon samples. FTIR is an analytical technique used to characterize the surface organic functional groups in organic compounds.

In the FT-IR spectra of bio-oils, the broad bands at 3000-3600 cm^{-1} represent hydroxyl ($-\text{OH}$) functional groups originating from alcohols, phenols and carboxylic acids (**Fig. 4-6a**). The vibrations observed at 1364, 1456, 2853, 2953 and 2968 cm^{-1} represent the presence of C-H alkanes (Nanda et al., 2013). An intense band observed at the 1710 cm^{-1} with highest intensity in BL-400 indicated the presence of C=O functional group from aldehydes and ketones. With the rise in temperature, the relative intensity of this band lowered in BL-450 and BL-500 indicating their reduced concentration. The bands presented at 1515 and 1614 cm^{-1} are due to the formation of C=C aromatic phenyl rings originating from lignin. The bands at 1111 and 1208 cm^{-1} are ascribed to C-O alcohols, ethers, carboxylic acids and ethers (Mohanty et al., 2013). The presence of C-H alkene groups was observed at 926 and 1034 cm^{-1} while the phenyl components were also detected at 753 and 834 cm^{-1} .

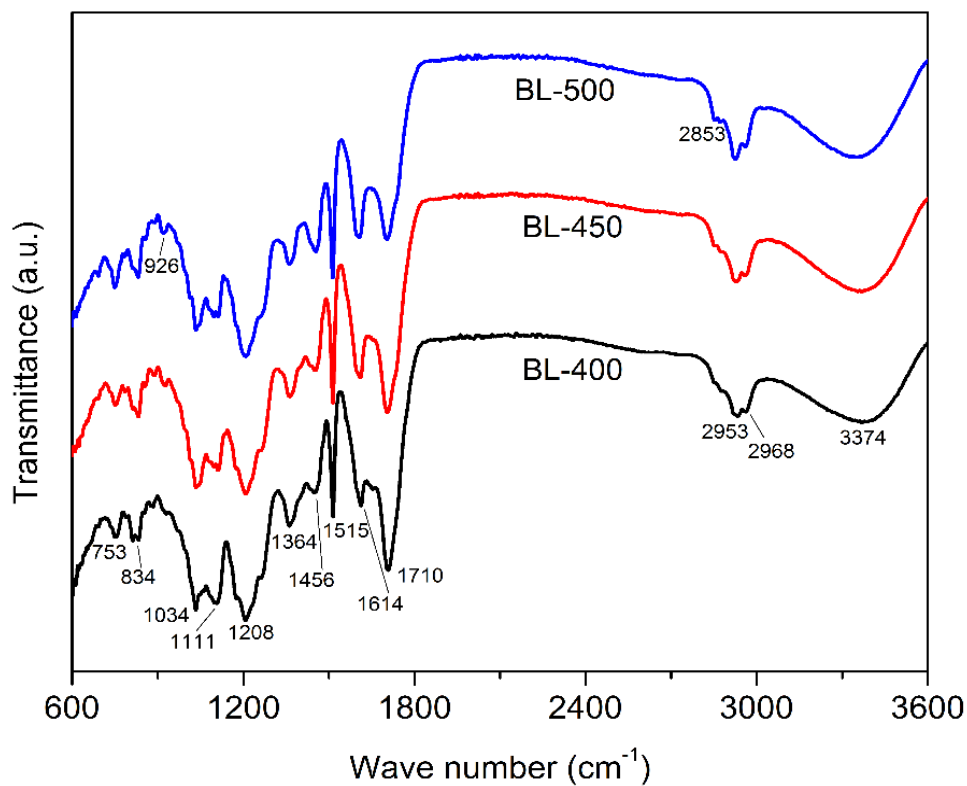
Table 4-5: FT-IR assignment of bands identified in bio-oil, biochar and activated biochar generated from pyrolysis at 400-500°C for 2.7 s of vapor residence time and 1 h and 1.5 h of run times and subsequent activation at 900°C for 1.5 h

Wave number (cm ⁻¹)	Functional group
Bio-oil	
753, 834	(C–H) Phenyl ring
926, 1034	(C–H) Alkenes
1111, 1208	(C–O) Alcohols, ethers, esters and carboxylic acids
1364, 1456, 2853, 2953, 2968	(C–H) Alkanes
1515, 1614	(C=C) Aromatic and phenyl rings
1710	(C=O) Aldehyde and ketones
3374	(–OH) Alcohols, phenols and carboxylic acids
Biomass, biochar and activated biochar	
739	(C–H) Alkenes
872, 898	(C–H) Phenyls and aromatic rings
1034, 1161, 1203, 1231	(C–O) Alcohols, ethers, esters and carboxylic acids
1366, 1367, 1429, 2969, 2918	(C–H) Alkanes
1531, 1602	(C=C) Aromatic rings
1737, 1739	(C=O) Esters, ketones and aliphatic acids
3350	(–OH) Alcohols, phenols and carboxylic acids

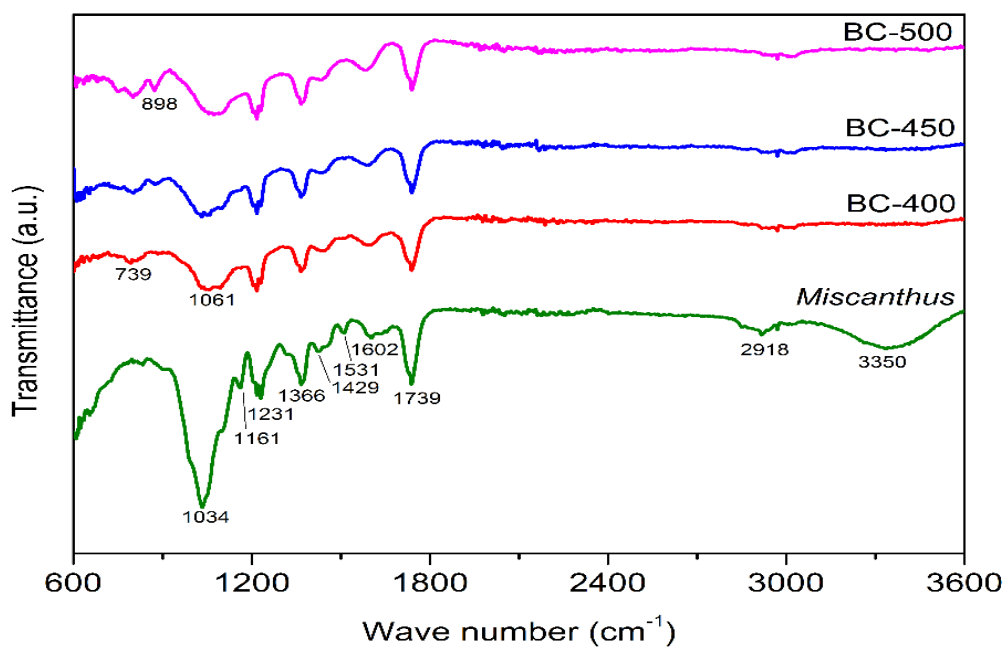
The FT-IR spectra for *Miscanthus* and its biochars are shown in **Fig. 4-6b**. The intense vibrations at 1034, 1161 and 1231 cm⁻¹ represent the presence of oxygenated (C–O) functional groups such as alcohols, ethers, esters and carboxylic acids. The reduction in the relative intensities of these bands in the biochars indicate their transformation to liquid or gas phase during pyrolysis via dehydration, decarboxylation and cracking (Kim et al., 2011). The bands at 1366, 1367, 1429, 2969 and 2918 cm⁻¹ were ascribed to C–H functional group of alkanes, which originated from the biopolymers of cellulose and hemicellulose and fatty acids present in the biomass. The vibrations occurring at 1531 and 1602 cm⁻¹ were due to the characteristic bands of C=C aromatic rings attributed to lignin (Nanda et al., 2015b). The presence of the dense vibration at 1739 cm⁻¹ was due to the carbonyls originating from hemicellulose (Kristensen et al., 2008).

The vibration stretching at 3350 cm^{-1} was assigned to the alcohols, phenols and carboxylic acids owing to the hydroxyl and carboxyl group of lignin and carbohydrates in biomass (Budai et al., 2017). These components were also not noticed in the biochars due to dehydration and decarboxylation reactions during pyrolysis. The vibrations representing aromatic rings were observed at 898 cm^{-1} in the case of biochar produced at 500°C (BC-500) due to the formation of thermally stable carbon, which was also discussed earlier in thermogravimetric and ultimate analyses. Peng et al. (2011) reported a reduction in the C–H, –OH and C–O functional groups and the intensification of C=C structures in the biochars produced from rice husk as the temperatures increased from 250 to 450°C during pyrolysis.

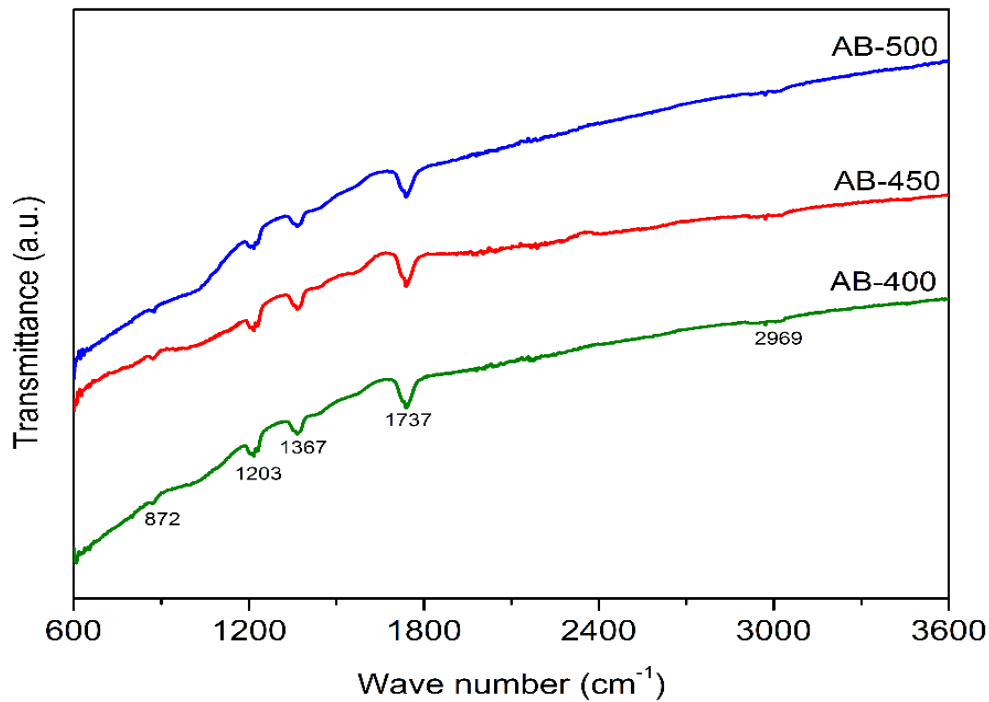
Comparing the spectra of activated biochars with that of the original biomass and precursor biochars, it can be clearly seen that most of the functional groups were lost due to CO_2 activation at 900°C for 1.5 h or holding time. Only a few vibrations at 872 cm^{-1} (aromatic carbon), 1737 cm^{-1} (esters, ketones and aliphatic acids), 1203 cm^{-1} (carboxyl groups) as well as 1367 and 2969 cm^{-1} (alkanes) were seen in the case of activated biochars (Demiral and Güngör, 2016) (**Fig. 4-6c**). It can be suggested that in the case of activated biochars, the carbon became aromatic and thermally stable with the extreme loss of organic components.



(a)



(b)



(c)

Fig. 4-6: FT-IR analysis of *Miscanthus*-derived (a) bio-oil, (b) biochar, and (c) activated biochar generated from pyrolysis at 400-500°C for 1 h of run time with 2.7 s of vapor residence time and subsequent CO₂ activation at 900°C

In summary, the FTIR of raw *Miscanthus* shows that the biomass contains functional groups belonging to hydroxyl, carboxyl, carbonyl, aldehydes, ketones, esters and aliphatic compounds. Moreover, the FTIR spectrum of the bio-oil exhibits more phenolic, alcohols and acidic groups, as confirmed also through the GC-MS analyses of bio-oils. In contrast, the FTIR of biochar and activated biochar produced at higher temperatures shows significant removal of the above-mentioned compounds and intensification of aromatic carbon.

4.6 Scanning electron microscopy

SEM was used to study the morphology of biomass, biochars and activated biochars. From the SEM images obtained from this technique, it was easy to understand the porosity of the materials and the structural change occurring during the thermal treatment. SEM is a microscopy technique used to study the surface morphology of organic and inorganic materials at micro- and nano-scale.

With the rise in temperature during pyrolysis process, the biochars were found to be more porous and fragmented with maximum deterioration and porosity visually being obtained in BC-500 (Fig. 4-7). Biochar produce at 500°C showed significant destruction of inner morphology of raw material (*Miscanthus*) with numerous fine pores being developed on its surface. This could be attributed to the release of volatile components and organics during thermal cracking.

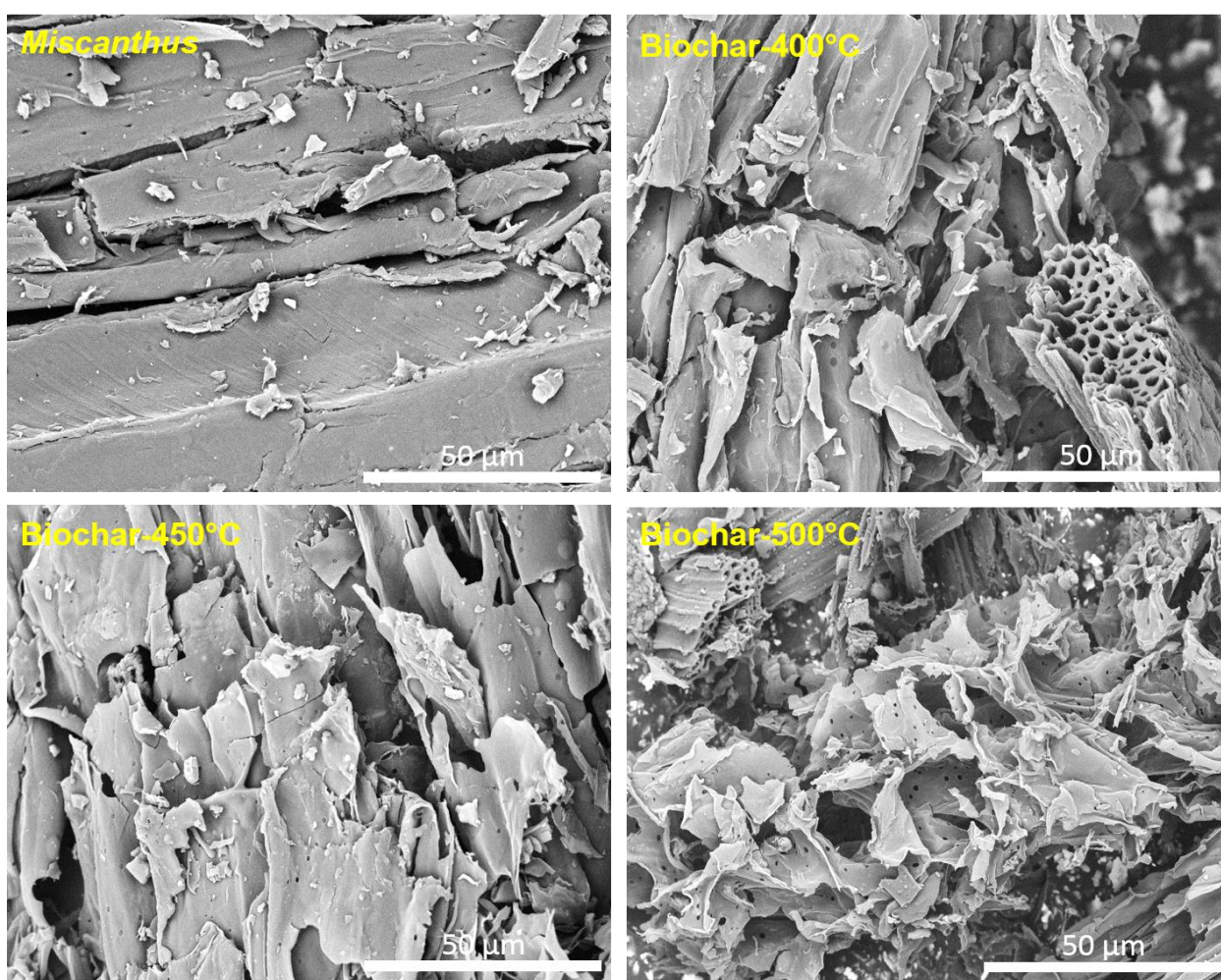


Fig. 4-7: SEM analysis of *Miscanthus* and its biochars generated from pyrolysis at 400-500°C for 1 h of run time with 2.7 s of vapor residence time

The EDX spectra of *Miscanthus* as well as its biochars and activated carbon showed the presence of major elements such as C, O, Mg, K, Ca and Si (Fig. 4-8 and Fig. 4-9). The presence of Au was due to the gold coating of the samples prior to SEM imaging to prevent sample fluorescence and charring under high electron beam during microscopy. It can be clearly seen that with the increase in the pyrolysis temperature, the carbon content was found to rise with 62 wt% in *Miscanthus* to 89% in BC-500 (Fig. 4-8). The carbon content of activated biochars as determined through EDX spectroscopy was in the range of 79-95 wt% with superior levels found in AB-500 (Fig. 4-9). As mentioned earlier, biochar from lignocellulosic feedstocks usually contain substantial amounts of alkali metals like Na, Ca, Mg and K, which are inherited from the original biomass (Yin et al., 2013; Mohanty et al., 2013). The presence of such alkali metals in the biochars and activated biochars re responsible for their alkaline pH (Table 4-2).

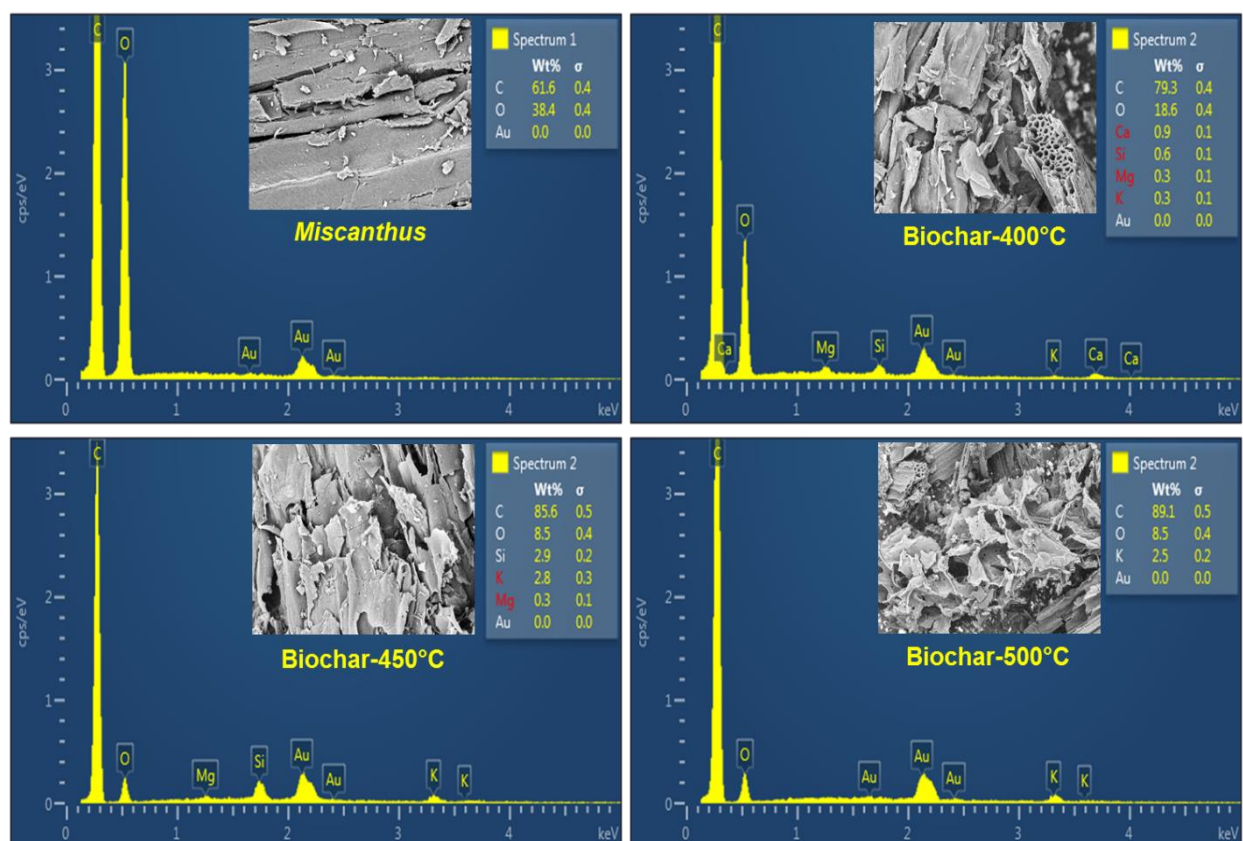


Fig. 4-8: SEM-EDX analysis of *Miscanthus* and its biochars generated from pyrolysis at 400-500°C for 1 h of run time with 2.7 s of vapor residence time

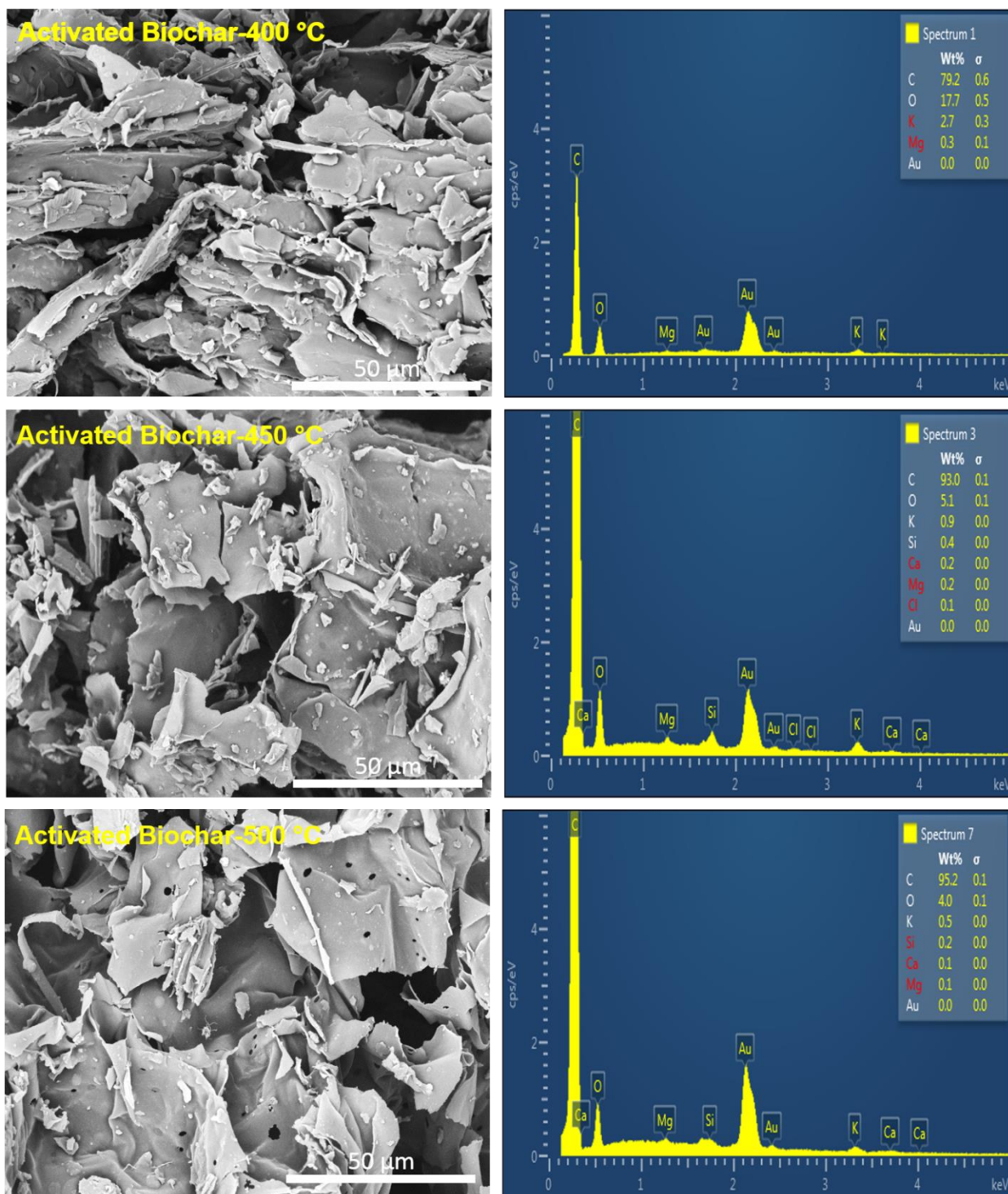


Fig. 4-9: SEM-EDX analysis of activated biochars generated from *Miscanthus* biochars at 900°C for 1.5 h of run time with CO₂ flow rate of 60 mL/min

The activated biochars revealed significant deterioration of their surface structure with significant pore formation in AB-500. For activated biochars, the developed pores are responsible for increasing their surface area, which determines the absorption capacity. Highly porous and thermally stable activated biochars produced from *Miscanthus* suggest their application in the adsorption of environmental pollutants from industrial exhaust gases, wastewater or contaminated lands. Moreover, the pores in the biochar can act as a niche to accommodate beneficial soil bacteria and fungi to form biofilms and hyphal networks, respectively and release the plant-growth promoting hormones when applied into the soil (Nanda et al., 2016a; Jaafar et al., 2015). Not only these porous structure in the biochar are responsible for colonizing fungi and bacteria, but also, they help in water retention, adsorption of environmental pollutants and releasing essential elements in the soil (Yin et al., 2013; Oginni et al., 2017).

4.7 Porosity analysis

For measuring the adsorption capacity of a material, it is necessary to physical characterize its porosity, specific surface area, pore size distribution and pore volume. The BET surface area of *Miscanthus*-derived biochars produced at 400-500°C was in the range of 0.27-3.98 m²/g (**Table 4-5**). Oginni et al. (2017) reported the BET surface areas of *Miscanthus* and switchgrass biochars produced at the pyrolysis temperature of 500°C were 0.24 and 0.981 m²/g, respectively. The lower porosity in certain low-temperature biochars is due to particle conglomeration and deposition of tar vapors or heavy molecular volatiles on char surface during pyrolysis at lower temperatures, which cause blocking of the pores (Oginni et al., 2017). Sintering effect can also promote low surface area, which results in the shrinkage of the biochar as well as realignment of the structure and decrease of the porosity (Trazzi et al., 2016).

On the other hand, physical activation of biochar conducted at 900°C with 60 mL/min of CO₂ flow rate for a holding time of 1.5 h (once the target temperature was reached) resulted in opening of the blocked pores, cracking the residual volatiles and organic compounds, thereby increasing the surface area. A remarkable increase in the specific surface area was found in the case of activated biochars, especially with AC-500 demonstrating the largest

BET surface area of 332.8 m²/g (**Table 4-6**). The total pore volume also augmented from 0.007 cm³/g in BC-500 to 0.213 cm³/g in AB-500. Trazzi et al. (2016) showed that the specific surface area of biochar produced from *Miscanthus* at 700°C for a holding time of 60 min to be much higher (228 m²/g) than the biochar produced at 300°C for a holding time of 20 min (6.17 m²/g). Madej et al. (2016) reported the specific surface area of 212.4 m²/g for the biochar produced from slow pyrolysis of *Miscanthus* under a medium of N₂ mixed with O₂ (2%) at 700°C for 4 h of holding time. Liang et al. (2011) performed the activation of sugarcane bagasse at 900°C for 100 min to have a surface area > 350 m²/g. Biochar and activated carbon with larger surface area can be used in multifarious applications such as an adsorbent, catalyst, catalyst support, fuel cells, graphitic materials and templated porous carbon (Nanda et al., 2016a). Therefore, mesoporous materials have drawn great attention due to their high surface area, large pore volume and tunable pore size (Guayaquil-Sosa et al., 2017).

Table 4-6: BET porosity analysis of *Miscanthus*-derived biochars and activated carbon generated from pyrolysis at 400-500°C for 2.7 s of vapor residence time and 1 h of run time and subsequent activation at 900°C for 1.5 h

Sample	BET specific surface area (m ² /g)	Total pore volume (cm ³ /g)	Average pore size diameter (nm)
BC-400	0.27		
BC-450	1.02		
BC-500	3.98	0.007	7.4
AB-400	121.2	0.079	2.6
AB-450	277.8	0.158	2.3
AB-500	332.8	0.213	2.6

Mainly surface area of the biochar depends upon the reaction temperature, which when increased leads to structural deformations and pore developments. Typically, an increase in the pyrolysis, gasification or carbonization temperature results in increasing the fixed carbon content, ash content, alkalinity and porosity of the biochar, while reducing its yield and volatile matter (Nanda et al., 2016a). Lua et al. (2004) studied the effects of pyrolysis temperature, heating rate, holding time and N₂ flow rate on the properties of biochar. They

concluded that temperature has the most significant effect upon the biochar yield and properties followed by heating rate, which aid to increase the surface area.

4.8 Methylene blue adsorption

For measuring the adsorption performance of the biochars and activated biochars in comparison to the performance of commercial activated carbon (CAC), a series of experiments have been performed using methylene blue as a model compound. Methylene blue is a cationic dye used as a model compound representing a relatively large molecule and its adsorption is an index of mesoporosity of different materials (Foo et al., 2011; Lei et al. 2006) In the literature, Methylene blue has been shown to be useful to assess the adsorption capability of activated biochar (Colomba, 2015; Foo et al., 2011; Delgado et al; 2019; Altenor et al; 2009; Hirata et al. 2002).

Fig. 4-10 shows the methylene blue adsorption per gram of *Miscanthus*-derived biochar and activated biochars synthesized in this study. It is evident that the adsorption increases with the physical activation given that CO₂ modifies the nature of the available functional active sites in the activated biochars synthesized at 900°C as reported in **Table 4-3**. Thus, for AB-500, full adsorption of methylene blue reached within the first 30 min, whereas for the commercial activated carbon this occurred at 1 h even though the later material has 3 times larger specific surface area (900 m²/g) than the former (332.8 m²/g) as reported in Table 5. The full adsorption of methylene blue for AB-450 was observed at 3 h.

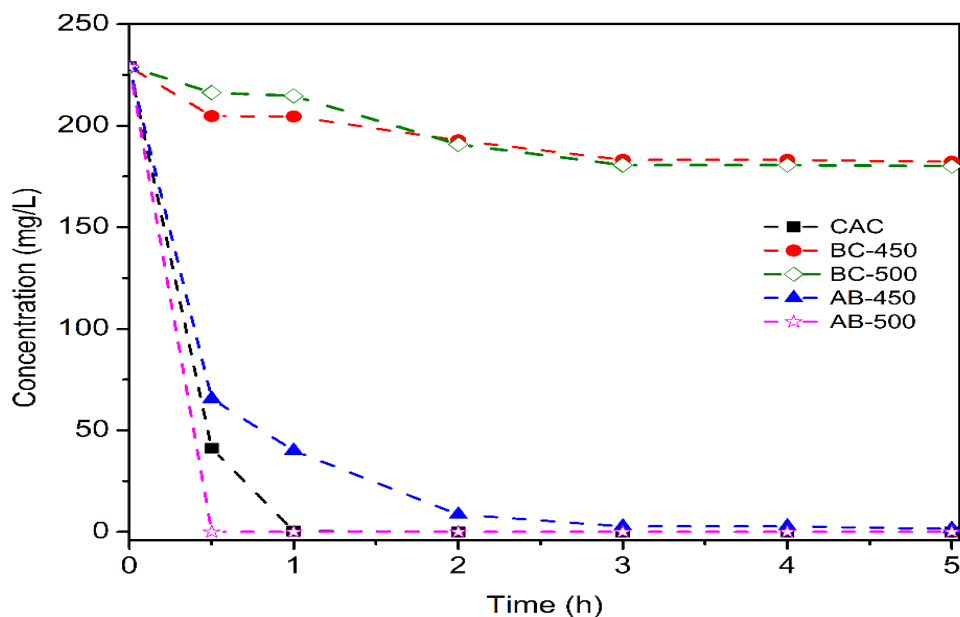


Fig. 4-10: Methylene blue (MB) adsorption profiles for the reference commercial activated carbon (CAC) as well as *Miscanthus*-derived biochar and activated biochars generated from pyrolysis at 450-500°C and subsequent CO₂ activation at 900°C. (Adsorption profiles of different biochars at 1 g adsorbent loading, C₀ [MB] of 250 mg/L and volume of 100 mL)

The poor adsorption performance by the non-activated biochars (BC-450 and BC-500) may be because some of the adsorption sites remain unsaturated during the adsorption process. It is noted that the total adsorptive capability of methylene blue improves faster as the number of both surface area and available active sites in the biochars increases. Although the commercial activated carbon had a maximum surface area of 900 m²/g its adsorption performance was inferior when compared to AB-500, which could be related to the pH of both materials. The pH of the commercial activated carbon was reported to be 6-7 (acidic) because of acid washing as reported by the manufacturer (General Carbon Corporation, 2019). In contrast, the pH level of *Miscanthus*-derived activated biochars (AB-400, AB-450 and AB-500) were found to be 7.9 to 9.7 (alkaline). It should also be noted that the pH of the biochar/activated biochar impacts the physisorption and chemisorption. Chemisorption results from electrostatic interactions between the ions of the adsorbate with an opposite charge and the surface-charged adsorbent material (biochar and activated biochar). This mechanism largely depends on the pH value and point of zero charge of the (activated) biochar (Inyang et al., 2016). Moreover, activated biochars generated at elevated

temperatures tend to develop graphene-like carbon crystallite structures, which promote chemisorption (Keiluweit and Kleber, 2009).

Pathania et al. (2017) reported that the study of adsorption of methylene blue with activated carbon produced from *Ficus carica* bast. The authors reported the maximum removal of methylene blue at the pH value of 8. He reported that the basic dye releases the positively charged ions after dissolution in water. Therefore, the positively charged surface of the sorbent opposed the adsorption of the cationic adsorbate in the acidic medium. When the pH of the dye solution was increased, the surface of the activated biochar acquired a negative charge. This resulted in a greater adsorption of methylene blue because of the higher electrostatic attraction between positively charged dye and negatively charged adsorbent material (Pathania et al., 2017).

4.9 GC-MS of bio-oil

As discussed earlier, bio-oil obtained from biomass pyrolysis is a complex mixture of two phases, i.e. aqueous phase and organic phase. More specifically, bio-oil is the complex mixture of water, carboxylic acids, organic acids, ketones, aldehydes, alcohols, esters, ethers, sugars, furanic and phenolic compounds. Bio-oil mostly contains hydroxyaldehydes, furancarboxaldehydes, hydroxyketones, phenolics and sugars such as guaiacols, catechols, vanillins, syringols and isoeugenol (Kelkar et al., 2014). Due to the large diversity of compounds identified in bio-oils, the components can be classified under five major groups such as monoaromatics, polyaromatics, aliphatic, oxygenated and nitrogenates (Nanda et al. 2014a).

Table 4-7 and Table 4-8 summarizes the list of compounds identified in the aqueous and organic phases of *Miscanthus*-derived bio-oil at 450°C for 1.4 s of vapor residence time and 1.5 h of run time. Since the yield of bio-oil was highest (59 wt%) at these optimal conditions, the sample was chosen for GC-MS analysis. Based on quantitative occurrence, the aqueous phase of bio-oil showed higher amounts of acetic acid; catechol; cyclopentenone; butyrolactone; 1-hydroxy-2-butanone; phenolics; 3-methyl-butanal;

levoglucosan; propanoic acid; 2-furanmethanol; 2,3-dihydro-benzofuran; benzenediol; cyclotene; vanillin; etc. (**Table 4-7**). On the other hand, the organic phase predominantly contained heavier phenolics and its derivatives such as 2-methyl-phenol; 3-methyl-phenol; 2-methoxy-phenol; 2,6-dimethyl-phenol; 3,4,5-trimethyl-phenol; 2-ethyl-phenol and 2,4-dimethyl-phenol. In addition, acetic acid, furfural, hydroxyacetone, butanedial, cyclopentanone, 2-furanmethanol, methyl levulinate were also obtained.

A majority of compounds identified in the GC-MS of the aqueous phase of bio-oils is produced from the thermal cracking of cellulose and hemicellulose present in *Miscanthus* during pyrolysis. The compounds produced from the decomposition of the cellulose and hemicellulose were mainly consist of acids, esters, alcohols, ketones, aldehydes, sugars, furans and oxygenates (Nanda et al. 2014b; Nanda et al., 2014c). However, the phenols and its derivatives including guaiacols, syringols, catechols are the pyrolysis product of lignin (Joshi and Lawal, 2012). Potassium, which is present as an inherent alkali metal in the biomass can act as a catalyst during pyrolysis of cellulose and levoglucosan to produce cyclopentenone and phenol derivatives (Kelkar et al. 2014). The organic acids are the products of deacetylation of hemicellulose and ring-opening reactions of cellulose.

Park et al. (2012) also showed the same results in the GC-MS characterization of *Miscanthus* bio-oil derived through pyrolysis. They showed that the bio-oil contained acids, carbonyls, carboxyls, phenolics and levoglucosan as the main products. Moreover, Wang and Lee (2018), in their study on fast pyrolysis of *Miscanthus* concluded that the bio-oil contained majority of phenolic compounds in addition to ketones, aldehydes, alcohols and acids as the degradation products of cellulose, hemicellulose and lignin, which is in accordance to this study. The amount of cellulose, hemicellulose and lignin in the biomass is one of the most prominent factors determining the chemical composition and properties of resulting bio-oil due to depolymerization, fragmentation, cracking and repolymerization among many primary and secondary reactions during pyrolysis.

Table 4-7: Major components identified through GC-MS of the aqueous phase of *Miscanthus*-derived bio-oil at 450°C for 1.4 s of vapor residence time and 1.5 h of run time

Retention time (min)	Area (%)	Compound
2.473	1.68	(S)-2-Hydroxypropanoic acid
2.958	29.32	Acetic acid
3.769	0.56	3-Hydroxy-2-butanone
5.088	2.37	1-Hydroxy-2-butanone
5.559	1.22	(2-Methyloxiranyl)methanol
7.406	1.35	4,5-Dimethyl-1H-imidazole
7.523	1.08	2-Cyclopenten-1-one
8.883	0.55	3-(Acetylthio)-2-methyl-propanoic acid
9.007	1.67	2-Furanmethanol
10.047	1.37	1-(Acetyloxy)-2-propanone
11.737	0.91	2-Methyl-2-cyclopenten-1-one
12.198	2.44	Butyrolactone
12.752	0.93	2-Hydroxy-2-cyclopenten-1-one
13.979	0.93	3-methyl-2-cyclopenten-1-one
14.589	1.74	Phenol
15.749	2.76	2-Hydroxy-3-methyl-2-cyclopenten-1-one
16.327	1.46	N-[(Phenylmethoxy)carbonyl]-DL-norvaline
16.783	2.28	3-Methyl-phenol
16.964	1.19	2-Methoxy-phenol
17.208	1.97	3-Methyl-butanal
17.392	0.61	8-Acetyl-8-methyl-7-oxatetracyclo[4.2.0.0(2,4).0(3,5)]octane
17.58	0.81	3-Ethyl-2-hydroxy-2-cyclopenten-1-one
18.451	1.95	4-Ethyl-phenol
18.851	0.54	2-Methoxy-4-methyl-phenol
18.963	3.87	Catechol
19.317	1.66	2,3-Dihydro-benzofuran
19.554	0.85	2,3-Anhydro-d-mannosan
19.932	1.94	4-Methyl-1,2-benzenediol
20.264	1.32	Hydroquinone
20.409	1.54	4-Methyl-1,2-benzenediol
20.746	1.01	2-Methoxy-4-vinylphenol
21.158	0.60	1,2,4-Cyclopentanetriol
21.258	1.77	2,6-dimethoxy-phenol
21.712	1.03	4-Ethylcatechol
21.978	0.72	Vanillin
22.534	0.59	4-Methoxy-3-(methoxymethyl)-phenol
23.522	1.61	5- <i>tert</i> -Butylpyrogallol

23.623	1.62	1-Methyl-N-vanillyl-(+)-s-2-phenethanamine
23.748	1.96	1,6-Anhydro- β -D-glucopyranose (levoglucosan)
23.897	0.92	Idosan triacetate

Table 4-8: Major components identified through GC-MS of the organic phase of *Miscanthus*-derived bio-oil at 450°C for 1.4 s of vapor residence time and 1.5 h of run time

Retention time (min)	Area (%)	Compound
2.225	0.99	Methyl 2-methoxypropenoate
2.492	1.84	(S)-2-Hydroxypropanoic acid
2.858	7.48	Acetic acid
2.946	0.28	1-Hydroxy-2-propanone
3.003	1.81	1-Hydroxy-2-propanone
3.54	0.17	3-Hydroxy-2-butanone
4.882	0.67	1-Hydroxy-2-butanone
5.317	0.41	Butanedial
5.57	0.2	Cyclopentanone
7.488	2.8	Furfural
8.973	1.18	2-Furanmethanol
11.734	1.14	2-Methyl-2-cyclopenten-1-one
11.973	0.28	1-(2-Furanyl)-ethanone
12.818	0.25	3-Hydroxy-cyclohexanone
13.06	0.17	2,3-Dimethyl-2,4-hexadiene
13.924	0.58	5-Methyl-2-furancarboxaldehyde
13.972	0.18	3-Methyl-2-cyclopenten-1-one
14.05	0.24	3,3-Dimethyl-2-butanone
14.14	0.19	1-(Scetyloxy)-2-butanone
14.406	0.11	3-Methyl-2(5H)-furanone
14.745	4.16	Phenol
14.867	0.18	4-Oxo-pentanoic acid methyl ester (methyl levulinate)
14.965	0.27	3,4-Dimethyl-2-cyclopenten-1-one
15.007	0.19	2,3-Dimethyl-2-cyclopenten-1-one
15.063	0.31	2,5-dihydro-3,5-dimethyl-2-furanone
15.2	0.3	Tetrahydro-2-furanmethanol
15.8	0.62	[4aS-(4 α ,5 β ,8a β)]-Hexahydro-5-methyl-4H-1,3-benzodioxin-4-one
15.923	1.57	2-Hydroxy-3-methyl-2-cyclopenten-1-one
16.402	1.54	2-Methyl-phenol
16.551	0.51	2-Methyl-3-methylene-cyclopentanecarboxaldehyde
16.884	3.46	3-Methyl-phenol
17.024	3.25	2-Methoxy-phenol

17.108	0.42	Trifluoroacetate trans-2-dodecen-1-ol
17.177	0.22	4,5-Dimethyl-4-hexen-3-one
17.285	0.44	Bicyclo[3.3.1]nonane
17.425	0.45	2,6-Dimethyl-phenol
17.513	0.2	3,4,5-Trimethyl-phenol
17.622	0.1	2-Methylene-cyclohexaneethanol
17.958	0.25	2-Ethyl-phenol
18.182	1.06	2,4-Dimethyl-phenol

Chapter 5

5. Conclusion and recommendation

5.1. Conclusions.

Continuous fast pyrolysis of *Miscanthus* was performed at different temperatures (400, 450 and 500°C) and vapor residence times (1.4-5.2 s) for 1 h of run time. Pyrolysis temperature was found to be one of the most significant process parameters determining the product yield and quality. Among the temperatures tested, 450 °C concluded as the adequate temperature for getting higher bio-oil yield during 1 h run time. Due to poorer material balance because of the product losses occur during collection run time extended to 1.5 h. When the run time was prolonged to 1.5 h at a constant temperature of 450°C, the bio-oil yield increased to 59 wt% at 1.4 s of vapor residence time as well as biochar and gas yield increased with increase in vapor residence time.

The biochar obtained at 400-500°C were physically activated under inert CO₂ atmosphere at 900°C for 1.5 h CO₂ activation led to the increase in the surface area for activated biochar (121.2-332.8 m²/g) compared to raw biochar (0.27-3.98 m²/g). Activated biochar produced from its precursor biochar originally generated at 500°C showed better adsorption potentials for methylene blue, which enhances the scope of *Miscanthus* to produce biofuels and biomaterials for industrial applications. The development of pores in the activated biochars at higher temperatures were also confirmed through SEM analysis. Both biochars and activated biochars were found to contain alkaline metals as detected in the SEM-EDX spectroscopy. The alkalinity of biochars (pH 7.2-7.9) and activated biochars (pH 8.4-9.7) suggest their application to acidic soil for neutralization.

Compared to raw *Miscanthus* (17.4 MJ/kg), the heating values of biochars (24-28.2 MJ/kg) and activated biochars (27.4-28.8 MJ/kg) were also found to increase with temperature. Due to the loss of moisture, volatiles and organic components from *Miscanthus*, the biochars and activated biochars were found to be thermally stable with the development of aromatic carbon structures, which was evident from TGA and FTIR analysis. The carbon composition

of activated biochars (72.9-83.4 wt%) was much higher than that of biochars (68.4-77.5 wt%) due to carbonization and aromatization. Similarly, the bio-oils obtained using 1 h of run time for 2.7 s of residence time at 500°C (54.8 wt%) had higher carbon contents in contrast to the bio-oil at 400°C (47.6 wt%). In contrast, bio-oil obtained at 450°C for 1.5 h of run time demonstrated maximum contents of carbon (63.2 wt%) and hydrogen (9.6 wt%) as well as HHV (27.6 MJ/kg). Moreover, the bio-oils revealed the presence of functional groups for ketones, aldehyde, alcohols, aromatics, carboxylic acids, esters and ethers, which suggests the potential for recovery of biochemicals. Nevertheless, the evolved gas analysis using TG-IR demonstrated the release of different gas species (i.e. CO, CO₂, CH₄, H₂ and volatiles) from *Miscanthus*. Overall findings suggest that *Miscanthus* is an outstanding energy crop for pyrolysis and physical activation to generate products that can have value-added market applications in energy, environment and multifarious industries.

5.2 Recommendations for future study

During the period of experimentation, there were some technical difficulties. One of the major problems was the leakage of hot pyrolysis vapors at the various places of the reactor system. Leakage of non-condensable vapors can create significant issues in the mass balance and carbon balance of the entire process. One of the possible solutions is to check the reactor assembly for any loose connections.

Moreover, filtration of gases and condensable vapors from fine particles of biochar is another major issue, which has to be taken care. For this, the surface area of the filter and mesh size of the screen used for filtration are important factors. More surface area according to the size of the reactor can be made and temperature of this filter should be same as the reactor temperature to prevent any condensation of bio-oil vapors at the surface of filter. Thus, it is necessary that filter should be inside the reactor.

Other problems like the maintenance of a uniform temperature gradient inside the reactor, condensing systems, nitrogen flow rates and feeding rates also required proper care for making the process smooth and accurate. Agitation of the biochar inside the reactor for making sure that fluidization is taking place is also important to ensure near-complete

decomposition of biomass particles. Uniform fluidization by hot biochar particles inside the reactor also ensures proper heat distribution and homogeneity of thermal cracking of biomass.

Miscanthus biochar and activated biochar have emerging scope for industrial applications. During activation, different flow rates of CO₂ at variable temperatures can be studied to understand their effects on the pore volume, BET surface area other features of biochar. More properties of biochar for industrial use can be explored as already shows potential for being a good absorbing agent.

Bio-oil produced in this process could be studied for catalytic upgradation and hydrotreating, which can increase the environmental and economic values of *Miscanthus* as industrially relevant energy crop.

Appendices

- Appendix A: All data for pyrolysis experiments

Table A1: Yields (wt%) of products (bio-oil, biochar and gases) produced at 400°C with variable vapor residence time (1.4 s, 2.7 s and 5.2 s) at 1 h of run time

Residence time (s)	Bio-oil (wt%)	Bio-char (wt%)	Gas(wt%)
5.2	27	37	36
5.2	31	37	32
2.7	33	38	29
2.7	34	37	29
1.4	33	38	29
1.4	35	36	29

Table A2: Yield (wt%) of products (bio-oil, bio-char and gas) produced at 450°C with variable vapor residence time (1.4 s, 2.7 s and 5.2 s) at 1 h of run time

Residence time (s)	Bio-oil (wt%)	Bio-char (wt%)	Gas (wt%)
5.2	37	27	36
5.2	36	29	35
2.7	46	25	29
2.7	45	25	30
1.4	40	23	37
1.4	42	25	33

Table A3: Yield (wt%) of products (bio-oil, bio-char and gas) produced at 500°C with variable vapor residence time (1.4 s, 2.7 s and 5.2 s) at 1 h of run time

Residence time (s)	Bio-oil (wt%)	Bio-char (wt%)	Gas (wt%)
5.2	33	22	45
5.2	36	21	43
2.7	38	21	41
2.7	37	21	42
1.4	40	18	42
1.4	42	20	38

Table A4: Yield (wt%) of products (bio-oil, bio-char and gas) produced at 450°C with variable vapor residence time (1.4 s, 2.7s and 5.2 s) at 1.5 h of run time

Res. Time (s)	Bio-oil (wt %)	Bio-char (wt%)	Gas (wt %)
1.4	60	25	15
1.4	58	25	17
2.7	53	26	21
2.7	50	28	22
5.2	40	30	30
5.2	40	32	28

- Appendix B: Calculated Nitrogen gas flow rates

Used formula

$$V_1/T_1 = V_2/T_2$$

V₁: Flow rate of the Nitrogen gas before entering to the reactor

T₁: Temperature of the Nitrogen gas before entering to the reactor

V₂: Flow rate of the gas after leaving the reactor

T₂: Temperature of the gas after leaving the reactor

Assumption:

1. Reactor volume is constant during the experiment (No building of char)
2. Negligible gas production during the experiment
3. Pressure is constant.

Volume of the reactor: 2.66 L

Volume of reactor covered by stirrer: 0.15 L

Volume of the reactor used for calculation of nitrogen flow rates: 2.51 L

Table B1: Calculated flow rate of nitrogen at three vapor residence time (1.4 s, 2.7 s and 5.2 s) and three temperatures (400, 450 and 500°C)

Vapour residence time: 5.2 s	
Temperature (°C)	N ₂ flow rate (L/min)
400°C	14
450°C	13
500°C	12
Vapor residence time: 2.7 s	
400°C	27
450°C	25
500°C	24
Vapor residence time- 1.4 s	
400°C	55
450°C	52
500°C	48

REFERENCES

1. Ail S.S., Dasappa S., Biomass to liquid transportation fuel via Fischer Tropsch synthesis – Technology review and current scenario. *Renewable and Sustainable Energy Reviews* 58, 2016, 267-286.
2. Altenor S., Carene B., Emmanuel E., Lambert J., Ehrhardt J. J., Gaspard S. Adsorption studies of methylene blue and phenol onto vetiver roots activated carbon prepared by chemical activation. *Journal of Hazardous Materials* 165, 2009, 1029-1039.
3. Antal Jr. M.J., Gronil M. The art, science, and technology of charcoal production. *Industrial & Engineering Chemistry Research*. 42, 2003, 1619-1640.
4. Arnavat M. P., Bruno J. C., Coronas A. Review and analysis of biomass gasification models. *Renewable and Sustainable Energy Reviews* 14, 2010, 2841-2851.
5. Arnoult S., Hulmel M. B. A Review on *Miscanthus* Biomass Production and Composition for Bioenergy Use: Genotypic and Environmental Variability and Implications for Breeding. *Bio-Energy Research* 8, 2015, 502–526.
6. ASTM D3175-11 (2011) Standard method for volatile matter in the analysis sample of coal and coke. ASTM International, Pennsylvania, USA.
7. ASTM D95-13 (2018) Standard Test Method for Water in Petroleum Products and Bituminous Materials by Distillation. ASTM International, Washington, DC, USA.
8. ASTM E1755-01 (2007) Standard test method for ash in biomass. ASTM International, Pennsylvania, USA.
9. Azargohar R., Dalai A.K. Biochar as a precursor of activated carbon. *Applied Biochemistry Biotechnology* 129-132, 2006, 762–773.
10. Azargohar R., Nanda S., Kozinski J.A., Dalai A.K., Sutarto R. Effects of temperature on the physicochemical characteristics of fast pyrolysis bio-chars derived from Canadian waste biomass. *Fuel* 125, 2014, 90-100.
11. Azargohar R., Nanda S., Rao B.V.S.K., Dalai A.K. Slow pyrolysis of deoiled Canola meal: Product yields and characterization. *Energy and Fuels* 27, 2013, 5268-5279.

12. Balat M. Mechanisms of thermochemical biomass conversion processes. *Energy Sources, Part A: Recovery, Utilization, and Environmental Effects* 30, 2008, 620-635.
13. Behrendt F., Neubauer Y., Oevermann M., Wilmes B., Zobel N. Direct liquefaction of biomass. *Chemical Engineering & Technology* 31, 2008, 667-677.
14. Berndes G., Hoogwijk M., Broek R.V. D. The contribution of biomass in the future global energy supply: a review of 17 studies. *Biomass and Bioenergy* 25, 2003, 1-28.
15. Biagini E., Barontini F., Tognotti L. Devolatilization of Biomass Fuels and Biomass Components Studied by TG/FTIR Technique. *Industrial Engineering Chemistry Res.* 45, 2006, 4486–4493.
16. Bousiosa S., Worrell E. Towards a Multiple Input-Multiple Output paper mill: Opportunities for alternative raw materials and sidestream valorisation in the paper and board. *Resources, Conservation and Recycling* 125, 2017, 218-232
17. Bridgwater A.V. Principles and practice of biomass fast pyrolysis processes for liquids. *Journal of Analytical and Applied Pyrolysis* 51, 1999, 3–22.
18. Bridgwater A.V. Review of fast pyrolysis of biomass and product upgrading. *Biomass and Bioenergy* 38, 2012, 68-94.
19. Brosse N., Dufour A., Meng X., Sun Q., Ragauskas A. *Miscanthus*: a fast- growing crop for biofuels and chemicals production. *Biofuels, Bioproducts and Biorefining* 6, 2012, 580-598.
20. Brosse N., Sannigra P., Ragauskas A. Pre-treatment of *Miscanthus* × *giganteus* using the ethanol organosolv process for ethanol production. *Industrial Engineering. Chemistry Resources*, 48 (18), 2009, 8328–8334.
21. Budaeva V.V., Makarova E. I., Gismatulina Y. A. Integrated Flowsheet for Conversion of Non-woody Biomass into Polyfunctional Materials. *Key Engineering Materials* 670, 2015, 202-206.
22. Budai A., Calucci L., Rasse D. P., Strand L.T., Pengerud A., Wiedemeier D., Abiven S., Forte C. Effects of pyrolysis conditions on *Miscanthus* and corncob chars: Characterization by IR, solid state NMR and BPCA analysis. *Journal of Analytical and Applied Pyrolysis* 128, 2017, 335-345.

23. Cao X., Harris W. Properties of dairy-manure-derived biochar pertinent to its potential use in remediation. *Bioresource Technology*. 101, 2010, 5222-5228.
24. Cappelletto P., Mongardini F., Barberi B., Sannibale M., Brizzi M., Pignatelli V. Papermaking pulps from the fibrous fraction of *Miscanthus x giganteus*. *Industrial Crops and Products* 11, 2000, 205-210.
25. Chandel A. K., Singh O. V. Weedy lignocellulosic feedstock and microbial metabolic engineering: advancing the generation of 'Biofuel'. *Applied Microbiology and Biotechnology* 89, 2011, 1289–1303.
26. Chen D., Chen X., Sun J., Zheng Z., Fu K., Pyrolysis polygeneration of pine nut shell: Quality of pyrolysis products and study on the preparation of activated carbon from biochar. *Bioresource Technology* 216, 2016, 629–636.
27. Cheng S., D'cruz I., Wang M., Leitch M., Xu C. (Charles). Highly efficient liquefaction of woody biomass in hot-compressed alcohol-water co-solvents. *Energy Fuels* 24 (9), 2010, 4659–4667.
28. Choi S. K., Choi Y. S., Han S. Y., Kim S. J., Rahman T., Jeong Y. W., Nguyen V. Q., Cha Y. R. Bio-crude oil production from a new genotype of *Miscanthus sacchariflorus* Geodae-Uksae 1. *Renewable Energy* 144, 2019, 153-158.
29. Clark L.V., Brummer J. E., Głowacka K., Hall M. C., Heo K., Peng J., Yamada T., Yoo J. H., Yu C. Y., Zhao H., Long S. P., Sacks E.J. A footprint of past climate change on the diversity and population structure of *Miscanthus sinensis*. *Annals of Botany* 114, 2014, 97–107.
30. Colomba, A. Production Of Activated Carbons From Pyrolytic Char For Environmental Applications, MESC Thesis, University of Western Ontario, 2015.
31. Correa A.C., de Morais Teixeira E., Pessan L.A., Mattoso LHC. Cellulose nanofibers from curaua fibers. *Cellulose* 17, 2010, 1183–1192.
32. Czernik S., Bridgwater A. V. Overview of applications of biomass fast pyrolysis oil. *Energy and Fuels* 18 (2), 2004, 590–598.
33. Dauber J., Jones M. B., Stout J. C. The impact of biomass crop cultivation on temperate biodiversity. *Global change biology Bioenergy* 2, 2010, 289-309.

34. Demiral H., Güngör C. Adsorption of copper (II) from aqueous solutions on activated carbon prepared from grape bagasse. *Journal of Cleaner Production* 124, 2016, 103-113.
35. Delgado C. N., Gutierrez D. P., Mendez J. R. R. Preparation of activated carbon cloths from renewable natural fabrics and their performance during the adsorption of model organic and inorganic pollutants in water. *Journal of Cleaner Production* 213, 2019, 650-658.
36. Dohleman F. G., Long S. P. More Productive Than Maize in the Midwest: How Does *Miscanthus* Do it? *Plant physiology* 150, 2009, 2104-2115.
37. Du S., Y. Sun, Gamliel D. P., Valla J. A., Bollas G. M. Catalytic pyrolysis of *Miscanthus × giganteus* in a spouted bed reactor. *Bioresource Technology* 169, 2014, 188-197.
38. Fisher T., Hajaligol M., Waymack B., Kellogg D. Pyrolysis behaviour and kinetics of biomass derived materials. *Journal of Analytical and Applied Pyrolysis*. 62, 2002, 331-349.
39. Fontoura C.F., Brandão L.E., Gomes L.L. Elephant grass biorefineries: Towards a cleaner Brazilian energy matrix? *Journal of Cleaner Production* 96, 2015, 85-93.
40. Foo K. Y., Hameed B.H. Microwave assisted preparation of activated carbon from pomelo skin for the removal of anionic and cationic dyes. *Chemical Engineering Journal* 173, 2011, 385-390.
41. Ge X., Xu F., Vasco-Correa J., Li Y. Giant reed: A competitive energy crop in comparison with *Miscanthus*. *Renewable and Sustainable Energy Reviews* 54, 2016, 350-362.
42. General Carbon Corporation. 2019. GC 12x40AW Activated Carbon. <http://generalcarbon.com/activated-carbon/gc-12x40aw/> (Accessed on June 6, 2019)
43. Greenhalf C., Nowakowski D., Yates N., Shield I., Bridgwater A. The influence of harvest and storage on the properties of and fast pyrolysis products from *Miscanthus x giganteus*. *Biomass Bioenergy* 56, 2013, 247-59.
44. Gronwald, Marco, Vos, Cora, Helfrich, Mirjam, Don, Axel. Stability of pyrochar and hydrochar in agricultural soil - a new field incubation method. *Geoderma* 284, 2016, 85-92.

45. Gu X., Ma X., li L., Liu C., Cheng K., Li Z. Pyrolysis of poplar wood sawdust by TG-FTIR and Py-GC/MS. *Journal of Analytical and Applied Pyrolysis*. 102, 2013, 16-23.
46. Guayaquil-Sosa F., Serrano-Rosales B., Valades-Pelayo P. J., de Lasa H., Photocatalytic hydrogen production using mesoporous TiO₂ doped with Pt. *Applied Catalyst*, 211, 2017, 337–348.
47. Guo B., Zhang Y., Suk-jin Ha, Young-su Jin, Morgenroth E. Combined biomimetic and inorganic acids hydrolysis of hemicellulose in *Miscanthus* for bioethanol production. *Bioresource Technology* 110, 2012, 278-287.
48. Guo G. L., Chen W. H., Chen W. H., Men L. C., Hwang W. S. Characterization of dilute acid pre-treatment of silver grass for ethanol production. *Bioresource Technology* 99, 2008, 6046-6053.
49. Hafez I., Hassan E. B. Rapid liquefaction of giant *Miscanthus* feedstock in ethanol–water system for production of biofuels. *Energy Conversion and Management* 91, 2015, 219-224.
50. Hale S.E., Lehmann J., Rutherford D., Zimmerman A.R., Bachmann R.T., Shitumbanuma V., O'Toole A., Sundqvist K.L., Arp H.P.H., Cornelissen G. Quantifying the total and bioavailable polycyclic aromatic hydrocarbons and dioxins in biochars. *Environment Science Technology* 46, 2012, 2830-2838.
51. Han M., Kim Y., Koo B., Choi G. Bioethanol production by *Miscanthus* as a lignocellulosic biomass: focus on high efficiency conversion to glucose and ethanol. *Bioresource* 6, 2011.
52. Heo H. S., Park H. J., Sohn J. M., Park J., Kim S. S., Ryu C., Jeon J. K., Park Y. K. Influence of operation variables on fast pyrolysis of *Miscanthus sinensis* var. *purpurascens*. *Bioresource Technology* 101, 2010, 3672-3677.
53. Heo H. S., Park H. J., Yim J. H., Sohn J. M., Park J., Kim S. S., Ryu C., Jeon J., Park Y. K. Influence of operation variables on fast pyrolysis of *Miscanthus sinensis* var. *purpurascens*. *Bioresource Technology* 101, 2010, 3672-3677.
54. Hirata M., Kawasaki N., Nakamura T., Matsumoto K., Kabayama M., Tamura T., Tanada S. Adsorption of dyes onto carbonaceous materials produced from coffee

- grounds by microwave treatment. *Journal of Colloid and Interface Science* 254, 2002, 17-22.
55. Hodgson E. M., Lister S. J., Bridgwater A. V., Clifton Brown J., Donnison I. S. Genotypic and environmentally derived variation in the cell wall composition of *Miscanthus* in relation to its use as a biomass feedstock. *Biomass and Bioenergy* 34,2010, 652-660.
 56. Hodgson E., James A. L., Ravella S.R., Jones S.T., Perkins W., Gallagher J. Optimisation of slow-pyrolysis process conditions to maximise char yield and heavy metal adsorption of biochar produced from different feedstocks. *Bioresource Technology* 214, 2016, 574-581.
 57. Hodgson E.M., Nowakowski D. J, Shield I., Riche A., Bridgwater A. V., Clifton Brown J. C., Donnison I. S. Variation in *Miscanthus* chemical composition and implications for conversion by pyrolysis and thermo-chemical bio-refining for fuels and chemicals. *Bioresource Technology* 102, 2011, 3411-3418.
 58. Howaniec N., Smoliński A. Steam gasification of energy crops of high cultivation potential in Poland to hydrogen-rich gas. *International Journal of Hydrogen Energy* 36, 2011, 2038-2043.
 59. Inyang M. I., Gao B., Yao Y., Xue Y., Zimmerman A., Mosa A., Pullammanappallil P., Ok Y. S., Cao X. A review of biochar as a low-cost adsorbent for aqueous heavy metal removal. *Critical Reviews in Environmental Science and Technology* 46, 2016, 406–33.
 60. Jaafar N.M., Clode P.L., Abbott L.K. Soil Microbial Responses to Biochars Varying in Particle Size, Surface and Pore Properties. *Pedosphere* 25, 2015, 770-780.
 61. Janus A., Pelfrène A., Sahmer K., Heymans S., Deboffe C., Douay F., Waterlot C. Value of biochars from *Miscanthus x giganteus* cultivated on contaminated soils to decrease the availability of metals in multicontinental aqueous solutions. *Environmental Science and Pollution Research* 24, 2017, 18204–18217.
 62. Jayaraman K., Gökalp I. Pyrolysis, combustion and gasification characteristics of *Miscanthus* and sewage sludge. *Energy Conversion and Management* 89, 2015, 83-91.

63. Jeguirim M., Trouve G., Pyrolysis characteristics and kinetics of *Arundo donax* using thermogravimetric analysis, *Bioresource Technology* 100, 2009, 4026–4031.
64. Jenkins B. M., Baxter L. L., Miles Jr. T. R., Miles T. R. Combustion properties of biomass Fuel Processing Technology. *Fuel Processing Technology* 54, 1998, 17-46.
65. Johnson E. Goodbye to carbon neutral: getting biomass footprints right. *Environmental Impact Assessment Review.*, 29, 2009, 165-168.
66. Johnson M., Tucker N., Barnes S., Kirwan K. Improvement of the impact performance of a starch-based biopolymer via the incorporation of *Miscanthus giganteus* fibres. *Industrial Crops and Products* 22, 2005, 175-186.
67. Joshi J., Lawal A. Hydrodeoxygenation of pyrolysis oil in a microreactor. *Chemical Engineering Science* 74, 2012, 1-8.
68. Kamio E., Takahashi S., Noda H., Fukuhara C., Okamura T. Liquefaction of cellulose in hot compressed water under variable temperatures. *Industrial Engineering. Chemistry Resources.* 45 (14), 2006, 4944–4953.
69. Karampinis E., Vamvuka D., Sfakiotakis S., Grammelis P., Itkos G., Kakaras E. Comparative study of combustion properties of five energy crops and Greek lignite. *Energy Fuels* 26 (2), 2012, 869–878.
70. Keiluweit M., Kleber M. Molecular-level interactions in soils and sediments: The role of aromatic pi-systems. *Environmental Science and Technology* 43, 2009, 3421–9.
71. Kelkar S, Li Z, Bovee J, Thelen KD, Kriegel RM, Saffron CM. Pyrolysis of North-American grass species: Effect of feedstock composition and taxonomy on pyrolysis products. *Biomass and Bioenergy* 64, 2014, 152-161.
72. Kennes D., Abubackar H.N., Diaz M., Veiga M.C., Kennes C. Bioethanol production from biomass: carbohydrate vs syngas fermentation. *Journal of Chemical Technology and Biotechnology* 91, 2016, 304-317.
73. Kenneth B.H. Finch, Richards R. M., Richel A., Medvedovici A. V., Gheorghe N. G., Verziu M., Coman S. M., Parvulescu V. I. Catalytic hydro processing of lignin under thermal and ultrasound conditions. *Catalysis Today* 196, 2012, 3-10.
74. Kim H., Kim J., Kim M., Hyun S., Moon D. H. Sorption of sulfathiazole in the soil treated with giant *Miscanthus*-derived biochar: effect of biochar pyrolysis

- temperature, soil pH, and aging period. *Environmental Science and Pollution Research* 25, 2018, 25681–25689.
75. Kim J. Y., Oh S., Hwang H., Moon Y. H., Choi J. W. Assessment of miscanthus biomass (*Miscanthus sacchariflorus*) for conversion and utilization of bio-oil by fluidized bed type fast pyrolysis. *Energy* 76, 2014, 284-291.
 76. Kim P., Johnsonv A., Edmunds C.W., Radosevich M., Vogt F., Rials T.G., Labbé N., Surface functionality and carbon structures in lignocellulosic-derived biochars produced by fast pyrolysis. *Energy and Fuel*. 25, 2011, 4693–4703.
 77. Kristensen J.B., Thygesen L.G., Felby C., Jorgensen H., Elder T. Cell-wall structural changes in wheat straw pretreated for bioethanol production, *Biotechnol. Biofuel*. 1:5 2008.
 78. Kwapinski W., Byrne C. M. P., Kryachko E., Wolfram P., Adley C., Leahy J. J., Novotny E. H., Hayes M. H. B. Biochar from Biomass and Waste. *Waste and Biomass Valorization* 1, 2010, 177–189.
 79. Lee W. C., Kuan W. C. *Miscanthus* as cellulosic biomass for bioethanol production. *Biotechnology Journal* 10, 2015, 840-854.
 80. Lehmann J., Rillig M.C., Thies J., Masiello C.A., Hockaday W.C., Crowley D. Biochar effects on soil biota – A review. *Soil Biology and Biochemistry* 43, 2011, 1812-1836.
 81. Lei S., Miyamoto J., Kanoh H., Nakahigashi Y., Kaneko K. Enhancement of the methylene blue adsorption rate for ultramicroporous carbon fiber by addition of mesopores. *Carbon* 44, 2006, 1884-1890.
 82. Lewandowski I., Scurlock J. M. O., Lindvall E., Christou M. The development and current status of perennial rhizomatous grasses as energy crops in the US and Europe. *Biomass and Bioenergy* 25, 2003, 335-361.
 83. Li H. Q., Li C. L., Sang T., Xu J. Pretreatment on *Miscanthus lutarioriparius* by liquid hot water for efficient ethanol production. *Biotechnology for Biofuels*. 6:76 2013.
 84. Liang et al., H. Z. (2011). *Environmental Biotechnology and Materials Engineering*, Pts 1–3, in: Y.G. Shi, J.L. Zuo (Eds.), Trans Tech Publications Ltd., Stafa-Zurich, 2011, 1046.

85. Liu C., Xiao L., Jiang J., Wang W., Gu F., Song D., Yi Z., Jin Y., Li L. Biomass properties from different *Miscanthus* species. *Food and Energy Security* 2, 2013, 12-19.
86. Low T., Booth C., Sheppard A. Weedy biofuels: what can be done? *Current Opinion in Environmental Sustainability* 3, 2011, 55-59.
87. Lua A.C., Yang T., Guo J. Effects of pyrolysis conditions on the properties of activated carbons prepared from pistachio-nut shells. *Journal of Analytical and Applied Pyrolysis* .72, 2004, 279-287.
88. Luo H., Klein I. M, Jiang Y., Zhu H., Liu B., Kenttämaa H. I., Abu-Omar M. M. Total Utilization of *Miscanthus* Biomass, Lignin and Carbohydrates. *ACS Sustainable Chemical Engineering* 4 (4), 2016, 2316–2322.
89. Luo Y., Jennifer A. J. Dungait, Zhao X., Brookes P. C., Durenkamp M., G. Li, Q. Lin. pyrolysis temperature during biochar production alters its subsequent utilisation by microorganisms in an acid arable soil. *Land Degradation & Development* 29, 2017, 2183-2188.
90. Mabee W.E., Saddler J. Bioethanol from lignocellulosic: Status and perspective in Canada. *Bioresource Technology*. 101, 2010, 4806-13.
91. Madej J., Hilber I., Bucheli T. D., Oleszczuk P. Biochars with low polycyclic aromatic hydrocarbon concentrations achievable by pyrolysis under high carrier gas flows irrespective of oxygen content or feedstock. *Journal of Analytical and Applied Pyrolysis* 122, 2016, 365-369.
92. Maschio G., Koufopoulos C., Lucchesi A. Pyrolysis, a promising route for biomass utilization. *Bioresources Technology* 42, 2009, 219–231.
93. Mayer P., Hilber I., Gouliarmou V., Hale S.E., Cornelissen G., Bucheli T.D. How to determine the environmental exposure of PAHs originating from biochar. *Environment Science and Technology* 50, 2016, 1941-1948.
94. McKendry P. Energy production from biomass (part 2): conversion technologies. *Bioresource Technology* 83, 2002, 47-54.
95. Melligan F., Aucaille R., Novotny E.H., Leahy J.J., Hayes M.H.B., Kwapinski W. Pressurised pyrolysis of *Miscanthus* using a fixed bed reactor. *Bioresource Technology* 102, 2011, 3466–3470

96. Menon V., Rao M. Trends in bioconversion of lignocellulose: Biofuels platform chemicals & biorefinery concept. *Progress in Energy and Combustion Science* 38, 2012, 522-550.
97. Meyer F., Wagner M., Lewandowski I. Optimizing GHG emission and energy-saving performance. *Biomass Conversion and Biorefinery* 7, 2017, 139–152.
98. Mimmo T., Panzacchi P., Baratieri M., Davies C. A., Tonon G. Effect of pyrolysis temperature on miscanthus (*Miscanthus × giganteus*) biochar physical, chemical and functional properties. *Biomass and Bioenergy* 62, 2014, 149-157.
99. Mohan D., Pittman, C.U., Steele, P.H., Pyrolysis of wood/biomass for bio-oil: a critical review. *Energy Fuels* 20, 2006, 848–889.
100. Mohanty P., Nanda S., Pant K.K., Naik S., Kozinski J. A., Dalai A. K. Evaluation of the physiochemical development of bio-chars obtained from pyrolysis of wheat straw, timothy grass and pinewood: Effects of heating rate. *Journal of Analytical and Applied Pyrolysis* 104, 2013, 485-493.
101. Mohammad M.H., Scott I. M., McGarvey B. D., Conn K., Ferrante L., Berruti F., Briens C. Insecticidal and anti-microbial activity of bio-oil derived from fast pyrolysis of lignin, cellulose, and hemicellulose. *Journal of Pest Science* 88, 2015, 171–179.
102. Murnen H. K., Balan V., Chundawat S. P. S., Bals B., da Costa Sousa L., Dale B. E. Optimization of Ammonia Fiber Expansion (AFEX) Pre-treatment and Enzymatic Hydrolysis of *Miscanthus x giganteus* to Fermentable Sugars. *Biotechnology Progress* 23, 2008, 846-850.
103. Naik S.N., Goud V.V., Rout P.K., Dalai A.K. Production of first- and second-generation biofuels: A comprehensive review. *Renewable and Sustainable Energy Reviews* 14, 2010, 578-597.
104. Nanda S., Azargohar R., Dalai A.K., Kozinski J.A. An assessment on the sustainability of lignocellulosic biomass for biorefining. *Renewable and Sustainable Energy Reviews* 50, 2015a, 925-941.
105. Nanda S., Azargohar R., Kozinski J.A., Dalai A.K. Characteristic studies on the pyrolysis products from hydrolyzed Canadian lignocellulosic feedstocks. *Bioenergy Research* 7, 2014a, 174-191.

106. Nanda S., Dalai A.K., Berruti F., Kozinski J.A. Biochar as an exceptional bioresource for energy, agronomy, carbon sequestration, activated carbon and specialty materials. *Waste and Biomass Valorization* 7, 2016a, 201-235.
107. Nanda S., Dalai A.K., Kozinski J.A. Butanol and ethanol production from lignocellulosic feedstock: biomass pre-treatment and bioconversion. *Energy Science and Engineering* 2, 2014b, 138-148.
108. Nanda S., Dalai A.K., Kozinski J.A. Supercritical water gasification of timothy grass as an energy crop in the presence of alkali carbonate and hydroxide catalysts. *Biomass and Bioenergy* 95, 2016b, 378-387.
109. Nanda S., Gong M., Hunter H.N., Dalai A.K., Gökalp I., Kozinski J.A. An assessment of pinecone gasification in subcritical, near-critical and supercritical water. *Fuel Processing Technology* 168, 2017a, 84–96.
110. Nanda S., Maley J., Kozinski J.A., Dalai A.K. Physio-chemical evolution in lignocellulosic feedstocks during hydrothermal pre-treatment and delignification. *Journal of Bio-based Materials and Bioenergy* 9, 2015b, 295-308.
111. Nanda S., Mohammad J., Reddy S.N., Kozinski J.A., Dalai A.K. Pathways of lignocellulosic biomass conversion to renewable fuels. *Biomass Conversion and Biorefinery* 4, 2014c, 157-191.
112. Nanda S., Mohanty P., Pant K.K., Naik S., Kozinski J.A., Dalai A.K. Characterization of North American lignocellulosic biomass and biochars in terms of their candidacy for alternate renewable fuels. *Bioenergy Research* 6, 2013, 663-677.
113. Nanda S., Rana R., Zheng Y., Kozinski J.A., Dalai A.K. Insights on pathways for hydrogen generation from ethanol. *Sustainable Energy & Fuels* 1, 2017b, 1232–1245.
114. Niu Y., Tan H, Hui S. Ash-related issues during biomass combustion: Alkali-induced slagging, silicate melt-induced slagging (ash fusion), agglomeration, corrosion, ash utilization, and related countermeasures. *Progress in Energy and Combustion Science* 52, 2016, 1-61.
115. Novaes E., Kirst M., Chiang V., Winter-Sederoff H., Sederoff R. Lignin and biomass: A negative correlation for wood formation and lignin content in trees. *Plant Physiology* 154, 2010, 555–561.

- 116.Nsanganwimana F., Pourrut B., Mench M., Douay F. Suitability of *Miscanthus* species for managing inorganic and organic contaminated land and restoring ecosystem services. A review. *Journal of Environmental Management* 143, 2014,123-134.
- 117.Oginnia O., Singh K., Zondlo J. W. Pyrolysis of dedicated bioenergy crops grown on reclaimed mine land in West Virginia. *Journal of Analytical and Applied Pyrolysis* 123, 2017, 319-329.
- 118.Ontario's Invading Species Awareness Program (2019). *Miscanthus*.
<http://www.invadingspecies.com/miscanthus/>
- 119.Osman A.I., Abdelkader A., Johnston C. R., Morgan K., Rooney D. W. Thermal Investigation and Kinetic Modeling of Lignocellulosic Biomass Combustion for Energy Production and Other Applications. *Industrial Engineering Chemistry Resources* 56, 2017, 12119–12130.
120. Park H.J., Park K.H., Jeon J.K., Kim J., Ryoo R., Jeong K.E., Park S.H., Park Y.K. Production of phenolics and aromatics by pyrolysis of *Miscanthus*. *Fuel* 97, 2012, 379–384.
- 121.Pang J., Zheng M., Wang A., Sun R., Wang H., Jiang Y., Zhang T. Catalytic Conversion of Concentrated *Miscanthus* in Water for Ethylene Glycol Production. *American Institute of Chemical Engineers Journal* 60, 2014, 2254-2262.
- 122.Peng X., Ye L.L., Wang C.H., Zhou H., Sun B. Temperature- and duration-dependent rice straw-derived biochar: Characteristics and its effects on soil properties of an Ultisol in southern China, *soil & tillage research* 112, 2011, 159–166.
- 123.Petrou E. C., Pappis C. P. Biofuels: a survey on pros and cons. *Energy and Fuels*.23, 2009, 1055–1066.
- 124.Pathania D., Sharma S., Singh P. Removal of methylene blue by adsorption onto activated carbon developed from *Ficus carica* bast. *Arabian Journal of Chemistry* 10, 2017, S1445-S1451.
- 125.Robbins M. P., Evans G., Valentine J., Donnison I. S., Allison G. G. New opportunities for the exploitation of energy crops by thermochemical conversion in

- Northern Europe and the UK. *Progress in Energy and Combustion Science* 38, 2012, 138-155.
126. Ruddy D. A., Schaidle J. A., Ferrell J. R., Wang J., Moens L., Hensley J. E. Recent advancement in heterogeneous catalysts for biooil upgrading via ex situ catalytic fast pyrolysis: catalyst development through the study of model compound. *Green Chemistry* 2014, 454-490.
 127. Sattar A., Leeke G. A., Hornung A., Wood J. Steam gasification of rapeseed, wood, sewage sludge and *Miscanthus* biochars for the production of a hydrogen-rich syngas. *Biomass and Bioenergy* 69, 2014, 276-286.
 128. Shoosharian S., Anderson J.A., Armstrong G.W., Luckert M.K.M. Growing hybrid poplar in western Canada for use as a biofuel feedstock: A financial analysis of coppice and single-stem management. *Biomass and Bioenergy* 113, 2018, 45-54.
 129. Simmons B. A., Loque D., Blanch H. W. Next-generation biomass feedstocks for biofuel production. *Genome Biology* 9:242, 2008.
 130. Sims R. E. H., Hastings A., Schlamadinger B., Taylor G., Smith P. Energy crops: current status and future prospects. *Global Change Biology* 12, 2006, 2054-2076.
 131. Sluiter A., Hames B., Ruiz R., Scarlata C., Sluiter J., Templeton D. Determination of sugars, byproducts, and degradation products in liquid fraction process samples. Technical report NREL/TP-510-42623. National Renewable Energy Laboratory (NREL), Colorado, USA, 2008.
 132. Song W., Guo M. Quality variations of poultry litter biochar generated at different pyrolysis temperatures. *Journal of Analytical Applied Pyrolysis* 94, 2012, 138-145.
 133. Su Y., Song K., Zhang P., Su Y., Cheng J., Chen X. Progress of microalgae biofuel's commercialization. *Renewable and Sustainable Energy Reviews* 74, 2017, 402-411.
 134. Thapa S., Johnson D. B., Liu P. P., Canam T. Algal Biomass as a Binding Agent for the Densification. *Waste and Biomass Valorization*, 6, 2015, 91-95.
 135. Thu Lan T., Nguyen, J. E. Hermansen. Life cycle environmental performance of *Miscanthus* gasification versus other technologies for electricity production. *Sustainable Energy Technologies and Assessments* 9, 2015, 81-94.

136. Trazzi P.A., Leahy J. J., Hayes M. H. B., Kwapinski W. Adsorption and desorption of phosphate on biochars. *Journal of Environmental Chemical Engineering* 4, 2016, 37-46.
137. Vassilev S. V., Baxter D., Andersen L.K., Vassileva C.G. An overview of the chemical composition of biomass. *Fuel*, 89, 2010, 913-933.
138. Villaverde J. J., Ligeró P, de Vega A. *Miscanthus x giganteus* as a Source of Bio based Products Through Organosolv Fractionation: A Mini Review. *The Open Agriculture Journal*, 4, 2010, 102-110.
139. Wafiq A, Reichel D., Hanafy M. Pressure influence on pyrolysis product properties of raw and torrefied *Miscanthus*: Role of particle structure. *Fuel* 179, 2016, 156-167.
140. Wang W. C., Lee A. C. Thermochemical Processing of *Miscanthus* through Fluidized-Bed Fast Pyrolysis: A Parametric Study. *Chemical Engineering & Technology*. 41, 2018, 1737-1745.
141. Weijde T. V. D., KieseL A., Iqbal Y., Muylle H., Dolstra O., Visser R. G. F., Lewandowski I., Trindade L. M. Evaluation of *Miscanthus sinensis* biomass quality as feedstock for conversion into different bioenergy products. *Global change biology Bioenergy* 9, 2016, 176-190.
142. Wilk M., Margdziaz A. Hydrothermal carbonization, Torrefaction and slow pyrolysis of *Miscanthus giganteus*. *Energy* 140, 2017, 1292-1304.
143. Wu X., McLaren J., Madl R., Wang D. Biofuels from lignocellulosic biomass. In: *Sustainable Biotechnology* 2009, 19-41.
144. Xue G., Kwapinska M., Horvat A., Li Z., Dooley S., Kwapinski W., Leahy J. J. Gasification of *Miscanthus x giganteus* in an Air-Blown Bubbling Fluidized Bed: A Preliminary Study of Performance and Agglomeration. *Energy Fuels* 28 (2), 2014, 1121–1131.
145. Xue G., Kwapinska M., Kwapinski W., Czajka K. M., Kennedy J., Leahy J. J. Impact of torrefaction on properties of *Miscanthus giganteus* relevant. *Fuel* 121, 2014, 189-197
146. Yang K., Peng J., Xia H., Zhang L., Srinivasakannan C., Guo S. Textural characteristics of activated carbon by single step CO₂ activation from coconut shells. *Journal of the Taiwan Institute of Chemical Engineers* 41, 2010, 367–372.

147. Yang X., Wang H., Strong P. J., Xu S., Liu S., Lu K., Sheng K., Guo J., Che L., He L., Ok Y. S., Yuan G., Shen Y., Chen X. Thermal Properties of Biochars Derived from Waste Biomass Generated by Agricultural and Forestry Sectors. *Energies* 10(4), 2017, 469.
148. Yi Y. B., lee J. W., Chung C. H. Conversion of plant materials into Hydroxymethylfurfural using ionic liquids. *Environmental Chemistry Letters* 13, 2015, 173–190.
149. Yin R., Liu R., Mei Y., Fei W., Sun X. Characterization of bio-oil and bio-char obtained from sweet sorghum bagasse fast pyrolysis with fractional condensers. *Fuel* 112, 2013, 96-104.
150. Yorgun S., Şimşek Y. E. Catalytic pyrolysis of *Miscanthus × giganteus* over activated alumina. *Bioresource Technology* 99, 2008, 8095-8100.
151. Yu G., Afzal W., Yang F., Padmanabhan S., Liu Z., Xie H., Shafy M. A., Bell A. T., Prausnitz J. M. Pre-treatment of *Miscanthus × giganteus* using aqueous ammonia with hydrogen peroxide to increase enzymatic hydrolysis to sugars. *Journal of Chemical Technology & Biotechnology* 89, 2013, 698-706.
152. Yu T.E., English B.C., He L., Larson J.A., Calcagno J., Fu J.S., Wilson B. Analyzing economic and environmental performance of switchgrass biofuel supply chains. *Bio-Energy Research* 9, 2016, 566–577.
153. Zacher A.H., Olarte M.V., Santosa D.M., Elliott D.C., Jones S.B. A review and perspective of recent bio-oil hydrotreating research. *Green Chemistry* 16, 2014, 491-515.
154. Zaines G. G., Soratana K., Harden C. L., Landis A. E., Khanna V. Biofuels via Fast Pyrolysis of Perennial Grasses: A Life Cycle Evaluation of Energy Consumption and Greenhouse Gas Emissions. *Environment Science and Technology* 49, 2015, 10007–10018.

Curriculum Vitae

Name: Arshdeep Singh

Post-secondary Education and Degrees: Guru Nanak Dev University
Amritsar, Punjab, India
2012-2016 Bachelor of Technology (B. Tech) in Food science and technology

The University of Western Ontario
London, Ontario, Canada
2017-2019 MEdSc in Chemical and Biochemical Engineering

Honors and Awards: Western Graduate Scholarship
2017-2019

Related Work Experience Graduate Research Scholar
ICFAR, The University of Western Ontario
London, Ontario, Canada
2017-2019